

# Short-term forecasting of individual household electrical consumption

Ir. Stijn Staring

Thesis submitted for the degree of  
Master of Science in Artificial  
Intelligence, eg

**Thesis supervisor:**

Prof. dr. ir. Bart De Moor

**Assessors:**

Ir. Konstantinos Theodorakos

Ir. Jonas Soenen

Dr. ir. Aras Yurtman

**Mentor:**

Ir. Lola Botman

© Copyright KU Leuven

Without written permission of the thesis supervisor and the author it is forbidden to reproduce or adapt in any form or by any means any part of this publication. Requests for obtaining the right to reproduce or utilize parts of this publication should be addressed to the Departement Computerwetenschappen, Celestijnenlaan 200A bus 2402, B-3001 Heverlee, +32-16-327700 or by email [info@cs.kuleuven.be](mailto:info@cs.kuleuven.be).

A written permission of the thesis supervisor is also required to use the methods, products, schematics and programmes described in this work for industrial or commercial use, and for submitting this publication in scientific contests.

# Preface

I am very pleased to present my master thesis to complete my study in Artificial Intelligence. Conducting this research was an informative process in which I was able to apply the knowledge and skills that I gained during my studies. Writing my thesis and thus completing my studies would not have been possible without the support of my mentor Lola Botman, PhD student at the KU Leuven. Thank you for the interesting meetings and brainstorm sessions we had. Also, I would like to thank my family for their ongoing support during all phases of my studies. They have always been my biggest fans and I could not have done this without the opportunities they have given me. As lastly, I want to thank everybody that reads this text. Sit back, relax and enjoy.

*Ir. Stijn Staring*

# Contents

<b>Preface</b>	i
<b>Abstract</b>	iv
<b>List of Figures and Tables</b>	v
<b>1 Introduction</b>	1
1.1 Importance of topic . . . . .	3
1.2 Problem formulation and link with previous studies . . . . .	4
1.3 Thesis objective and structure . . . . .	4
<b>2 Exploratory Data Analysis</b>	7
2.1 Data description . . . . .	7
2.2 Preprocessing . . . . .	9
2.3 Data Analysis . . . . .	13
2.4 Conclusion . . . . .	21
<b>3 Short-term residential load forecasting : state of the art</b>	23
3.1 Introduction to neural networks . . . . .	23
3.2 Short-Term residential electrical load forecasting . . . . .	30
3.3 Conclusion . . . . .	35
<b>4 Forecasting the electricity consumption of individual households</b>	37
4.1 Preprocessing . . . . .	37
4.2 Error metrics . . . . .	39
4.3 Microsoft Azure cloud . . . . .	39
4.4 Baseline models . . . . .	40
4.5 Implementation deep LSTM neural network . . . . .	45
4.6 Conclusion . . . . .	61
<b>5 Model evaluation</b>	63
5.1 Model selection . . . . .	63
5.2 Performance on the test set . . . . .	64
5.3 Conclusion . . . . .	67
<b>6 Conclusion</b>	71
<b>A Different household attributes</b>	77
<b>B Forecasting the electricity consumption of individual households - extra</b>	79

## CONTENTS

---

B.1 Baseline models . . . . .	79
B.2 Parameter Search . . . . .	80
<b>C Model evaluation - extra</b>	<b>87</b>
C.1 Results on the testset . . . . .	87
<b>Bibliography</b>	<b>91</b>

# Abstract

Every year 40000 new solar panel installations take place in Flanders and the amount of electrical vehicles on the roads in Belgium is on the rise [15]. Fluvius, which is a Belgian distribution grid operator, faces a challenge to deal with the increasing burden on the low voltage grid. It needs to carry out maintenance work to make sure that it can cope with the future demands of electricity. Expenses can be saved when implementing customized updates of the grid which are possible when the electrical consumption of individual households can be accurately forecasted. On top of that, forecasts have to be made without intruding the privacy of the residents.

Therefore, the objective of this thesis is to implement short-term load forecasting for individual households, when using only a limited amount of information. LSTM neural networks are implemented to predict a load signal of 24 hours ahead with time steps of 30 minutes. Information used about the household consists out of past load values, calendar information and the average temperature of tomorrow. Real-life data from households in the UK is used which originates from the IEEE-CIS technical challenge dataset. From this dataset three households are selected with the least amount of missing data and their data will be used to train and test the neural networks. Forecasting the electrical consumption of an individual household is a very complex task due to the high amount of uncertainty and volatility of the electrical load signal.

First, an exploratory data analysis is elaborated followed by a literature study that explains why the LSTM neural networks are specialized in handling time series data. A summary is made of state of the art papers discussing short-term residential load forecasting. There are LSTM neural networks developed from which two of the three are stateless with Model 2 having an additional flattening layer in comparison to Model 1. Model 3 is a stateful model, which makes use of seeding before it makes predictions. Additionally, a parameter search is conducted, to retrieve the best parameter values for the different models. The LSTM models developed are evaluated on a test set consisting out of 30 days. The two baseline models used are “mean forecast” and “MAPE forecast”. The three LSTM models convincingly outperform both baseline models for two of the three series, based on the MAE metric. It is shown that all three LSTM models are able to predict peaks with a higher precision than the baseline models.

# List of Figures and Tables

## List of Figures

1.1	Electricity grid (Source: KU Leuven thesis proposal).	2
2.1	The amount of NaN values in all the 3248 load signals.	8
2.2	Resulting time serie of the month March after imputation of the missing data.	9
2.3	Resulting month of March after substitution of the missing values by the mean value of the measurements.	10
2.4	Comparison of series with and without zero load days.	11
2.5	The maximum differences between the maximum and minimum weekly rolling mean for all the 261 different load signals.	12
2.6	Removed load signal with a shift in the rolling mean.	12
2.7	The seasonality of the electrical load during the year 2017. The blue line indicates the average load signal.	14
2.8	Error between different pairs of weekdays.	15
2.9	Comparison between bank holiday and business day electrical consumption.	16
2.10	Error between a bank holiday and other days of the week.	16
2.11	Relation between normalized daily consumption and daily temperature.	18
2.12	Influence of the dwelling type (sample size: 1702) and number of bedrooms (sample size: 1859).	20
3.1	Figure of a MLP (source [24]).	24
3.2	Vanilla RNN,(source: [24]).	25
3.3	Exponential decrease of the gradient size of a simple RNN (red) or a LSTM (blue) (source: [23]).	27
3.4	A LSTM cell that is repeated over time (source: [18]).	27
3.5	A GRU cell that is repeated over time (source: [18]).	28
3.6	Comparing different methods in [20].	31
3.7	Influence of the number of layers and the pooling method(Source: [20]).	32
3.8	Different approaches tried in [13] and their performance in making 29,808 predictions.	33
3.9	Comparison between LSTM and CNN-LSTM. (source: [12])	34

---

3.10	The importance of the different inputs based on the average class activation score. (source: [12]) . . . . .	35
4.1	The electrical consumption in 2017 for the three selected series. . . . .	38
4.2	Daily predictions of two baseline models. (Blue: True / Orange: Prediction) . . . . .	44
4.3	The generation of inputs for a stateless model (Source: [6]). . . . .	48
4.4	The generation of inputs for a stateful model (Source: [6]). . . . .	48
4.5	The flow of functions that are executed in order during the prediction process with LSTM models. . . . .	50
4.6	Model 1 - stateless model with as input a subserie of N time steps and $C_i \in \mathbb{R}^m$ , $H_j \in \mathbb{R}^n$ , $X_k \in \mathbb{R}^{59}$ , $\hat{y} \in \mathbb{R}^1$ . . . . .	51
4.7	Model 2 - stateless model with as input a serie of N time steps and $C_i \in \mathbb{R}^m$ , $H_j \in \mathbb{R}^n$ , $X_k \in \mathbb{R}^{59}$ , $\hat{y} \in \mathbb{R}^1$ . . . . .	51
4.8	Model 3 - stateful model that connects single LSTM blocks and $C_i \in \mathbb{R}^m$ , $H_j \in \mathbb{R}^n$ , $X_k \in \mathbb{R}^{59}$ , $\hat{y} \in \mathbb{R}^1$ . . . . .	52
4.9	Results of the sensitivity analysis on the size of the regularization parameter and the dropout rate according to MAE. (Legend: $r_D$ : regularization size of weights of DENSE layer, $r_{rL}$ : regularization size of recurrent weight of LSTM, $r_L$ : regularization size of input weights of LSTM, $d_L$ : dropout rate of inputs LSTM, $r_{dL}$ : dropout rate of hidden states LSTM, $d_D$ : dropout rate of DENSE layer, or: best performing serie from phase one) . . . . .	57
4.10	The MAE on the validation set in function of the learning rate size. . . . .	58
5.1	The evolution of the MSE on the training and validation sets. . . . .	64
5.2	The MAE performance on all the days of the test set for Serie 1. . . . .	65
5.3	The MAE performance on all the days of the test set for Serie 2. . . . .	65
5.4	The MAE performance on all the days of the test set for Serie 3. . . . .	66
5.5	The prediction results of the different models on 7th December. (True values: blue/ Prediction: orange) . . . . .	69
B.1	An example histogram of the consumption in [kWh] versus count [-] used during MAPE forecast. . . . .	79
B.2	Results of the sensitivity analysis on the size of the regularization parameter and the dropout rate according to MAE.(Legend: $r_D$ : regularization size of weights of DENSE layer, $r_{rL}$ : regularization size of recurrent weight of LSTM, $r_L$ : regularization size of input weights of LSTM, $d_L$ : dropout rate of inputs LSTM, $r_{dL}$ : dropout rate of hidden states LSTM, $d_D$ : dropout rate of DENSE layer, or: best performing serie from phase one) . . . . .	81
B.3	The evaluation of the error on the validation set in function of the learning rate size. . . . .	82

---

B.4	Results of the sensitivity analysis on the size of regulation parameter and the dropout rate with respect to the mean absolute error.(Legend: $r\_r\_L$ : regularization size of recurrent weight of LSTM, $r\_L$ : regularization size of input weights of LSTM and $or$ : best performing serie from phase one) . . . . .	84
B.5	The evaluation of the error on the validation set in function of the learning rate size. . . . .	85
C.1	The MAE performance for the different days in the test set for Serie 1. .	87
C.2	The MAE performance for the different days in the test set for Serie 2. .	88
C.3	The MAE performance for the different days in the test set for Serie 3. .	89

## List of Tables

1.1	Prediction types [16]. . . . .	2
2.1	Summary of the available csv files form the IEEE-CIS technical challenge.	8
4.1	Summarizing characteristics about the selected series. . . . .	38
4.2	Specifications of different CPU's and GPU used. . . . .	40
4.3	Baseline results for Serie 1 tested on 31 days of December. . . . .	43
4.4	Baseline results for Serie 2 tested on 12 days of December. . . . .	43
4.5	Baseline results for Serie 3 tested on 12 days of December. . . . .	43
4.6	Relative performance over all the 261 time series with a full year of measurements. . . . .	45
4.7	Parameters used during phase 1 for the two stateless models. . . . .	53
4.8	Different regularization added during phase 2. . . . .	53
4.9	Each value in this table shows the average error when the corresponding parameter value is used, normalized by the largest error of the possible values of one parameter and finally subtracted by one. Therefore, each value shows a percentage of improvement with respect to the worst value for one parameter for each serie during phase 1 of the parameter search.	55
4.10	The values of the parameters with the lowest average MAE on the validation set over three runs. . . . .	56
4.11	Final values found after the parameter search for model 1. . . . .	58
4.12	Final values found after the parameter search for model 2. . . . .	59
4.13	Final values found after the parameter search for model 3. . . . .	61
5.1	The amount of training epochs for each selected model. . . . .	64
5.2	The MAPE for each Model and serie. . . . .	66
A.1	Amount of response on the voluntary questionnaires. . . . .	77

---

LIST OF FIGURES AND TABLES

---

B.1	Each value in this table shows the average error when the corresponding parameter value is used, normalized by the biggest error of the possible values of one parameter and finally subtracted by one. Therefore, each value shows a percentage of improvement with respect to the worst value for one parameter for each serie during phase 1 of the parameter search.	80
B.2	The values of the parameters with the lowest average MAE on the validation set over three runs. . . . .	80
B.3	Each value in this table shows the average error when the corresponding parameter value is used, normalized by the biggest error of the possible values of one parameter and finally subtracted by one. Therefore, each value shows a percentage of improvement with respect to the worst value for one parameter for each serie during phase 1 of the parameter search.	83
B.4	The values of the parameters with the lowest average MAE on the validation set over three runs. . . . .	83

# Chapter 1

## Introduction

There is an increasing awareness of the potential benefits of intelligent energy control. Indeed, intelligent control of the balance between the distributed energy resources and the demand requirements has many advantages. It leads to efficient planning, more satisfied customers and can even help national electricity markets in saving considerable operating and maintenance costs [16]. Having accurate forecasting models is one of the key conditions to realize intelligent energy control. When electricity consumption forecasting is improved, energy suppliers can build a better trust with their customers by sending reliable bills. Furthermore, the electricity supplier can better estimate the energy demand of the whole customer population. The optimization of the energy production planning is possible, which will lead to cheaper electricity production and increased profit margins. More substantiated decisions can be taken with regard to investments and there will be less need of the more flexible, but more expensive electricity installations e.g. diesel engines, to catch the deficiencies in electricity production.

With the invention of the smart meter in 1974 by **Paraskevakos**, it became possible to measure the electricity consumption with a higher accuracy and communicate this with the electricity consumer and producer. Electricity consumption is nearly recorded real time and a smart meter allows for two-way communication between the smart meter and the supplier. As explained in [4]: “By introducing smart meters as a new component of their smart grid system, an avalanche of immensely useful energy usage information became available to the energy markets.” From the availability of more detailed datasets comes the explosion of research in the area of electrical forecasting techniques and the applicability of more complex models. To tackle the electrical consumption forecasting problem neural networks are applied. These models allow for learning non-linear relations between the inputs and outputs.

Depending on the forecasting horizon, different applications are considered, as is summarized in Table 1.1 [16]. The forecast horizon is chosen in consultation with the uncertainty that is contained in the signal. If the signal doesn’t show clear patterns, forecasting will be more difficult which means that the forecasting horizon should

## 1. INTRODUCTION

---

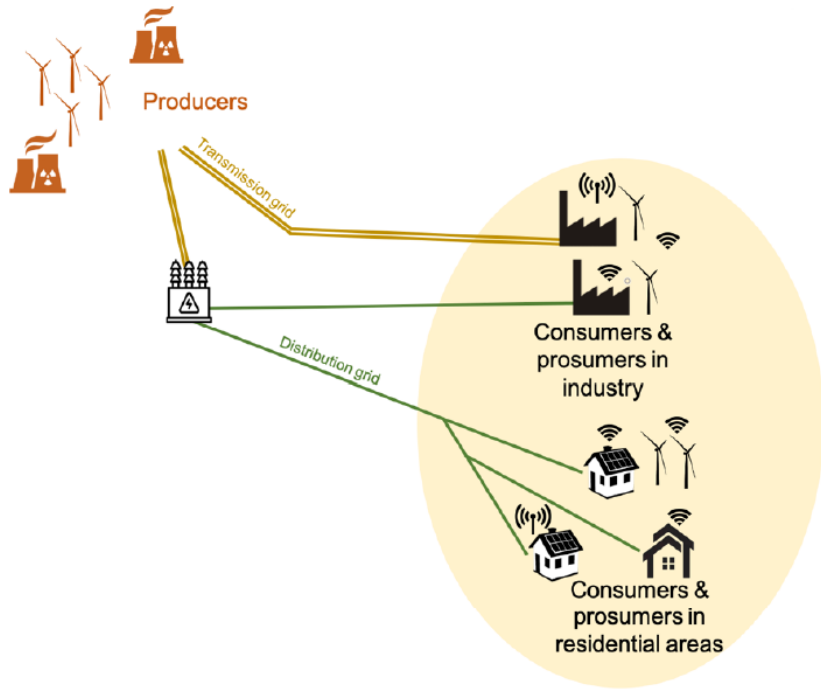


FIGURE 1.1: Electricity grid (Source: KU Leuven thesis proposal).

Acronym	Prediction type	Time span	Application
VSTLF	Very short Term Load Forecasting	One minute to an hour	Operational and maintenance scheduling and Demand side management (decision making for load control and voltage reduction)
STLF	Short Term Load Forecasting	Daily or weekly	Distribution and transmission planning and Demand side management (decision making for load control and voltage reduction)
MTLF	Medium Term Load Forecasting	A month to a few years	Finance or power supply planning
LTLF	Long Term Load Forecasting	A year to a few decades	Finance or power supply planning

TABLE 1.1: Prediction types [16].

be shorter. In this thesis the forecasting horizon falls in the category of “VSTLF” and “STLF” because the consumption is predicted with time steps of 30 minutes and 24 hours ahead. The practical application of the developed models in this thesis

have as goal to monitor the demand side of the low voltage distribution grid. Figure 1.1 shows in green where the distribution grid is located in the whole electricity grid. The low voltage distribution grid is also called the secondary network and is the part of the distribution grid that carries electric energy from distribution transformers to the electrical appliances located in a house. Typical inputs that are used in literature for electrical load forecasting are past values of the load, weather information, calendar information and error-correction terms [5]. Often used inputs for electrical load forecasting are summarized here.

- Historical data e.g. [13]
- Weather information
  - Temperature e.g. [13]
  - Cloudiness e.g. [3]
  - Humidity e.g. [3]
  - Wind e.g. [1]
- Day of the week e.g. [13]
- Time of the day e.g. [13]
- Holiday e.g. [13]
- Anthropological data : Social aspects of the community, general behaviour of house occupants e.g. [11]
- Structural data : physical properties of the house e.g. [11]

## 1.1 Importance of topic

This research on short term load forecasting is done in the context of an increased adoption of solar panels and electric vehicles by the general public. Every year 40000 new solar panel installations take place in Flanders [15]. Fluvius, which is one of the Belgian distribution grid operators, has carried out, together with Deloitte in 2019, an unique stress test on the low voltage distribution grid to analyse how the current grid would react on an increased amount of charging points for electrical vehicles and solar panels. It was found that on the short term, which means up to 2025, the grid will be able to cope with the estimated increase of the burden on the low voltage grid. However, now is the time of anticipation and to strengthen the weak spots in the network. To carry out the maintenance work, detailed forecasting of the load signals of only a small amount of households is needed. Detailed forecasts of individual households is now possible thanks to the use of smart meters. If detailed predictions can be achieved for individual households, expenses are saved because customized updates of the network can be done. With forecasts on the household level, a plan can be made where only certain parts of the grid have to be replaced.

## 1. INTRODUCTION

---

Replacing everything is avoided. Individual household predictions can be used as part of a congestion prediction, which means predicting when the low voltage grid can't handle the demand anymore. In that case, a precise prediction of the size and time of peaks is crucial. If an accurate congestion prediction can be done, the reliability of the network increases and the risk for blackouts and brownouts is decreased.

### 1.2 Problem formulation and link with previous studies

As discussed in [20], the complexity of the household forecasting lies in the significant uncertainty and volatility of the load signal. Uncertainty comprises the aperiodic part influenced by external factors e.g. customer behaviour and weather. In order to attain accurate forecasting results, it is found in literature that aggregated load signals are considered [5]. Aggregation cancels out the individual uncertainty, and the signal will show a higher periodicity, which is easier to model. However, this doesn't help for individual household forecasting. Papers about load forecasting of an individual household often use a lot of information about the household situation and submeters to measure the consumption of different appliances or parts of the house [12]. This will in practise not be scalable due to privacy concerns, among other things. This thesis investigates state of the art time series short term forecasting techniques based on LSTM neural networks that have as goal to directly learn the uncertainties on the load signals, given only limited information.

The data used in this thesis was made available for the [IEEE-CIS technical challenge on energy prediction from smart data](#) and is very similar to smart meter data from the Belgian Energy supplier Fluvius. This dataset consists out of 3248 smart meter time series from the UK during the year 2017.

### 1.3 Thesis objective and structure

The goal of this thesis is to implement short-term load forecasting for individual households when using only a limited amount of information. Firstly, the following question will be answered : "How much electricity will a individual household consume in the next 24 hours?" LSTM neural networks are investigated to predict a load signal of 24 hours ahead with time steps of 30 minutes. The information used to make the predictions consists of past load values, calendar information and the daily average temperature of tomorrow. These inputs can easily be obtained in practice without intruding the privacy of the residents. The three households considered, originate form the IEEE-CIS technical challenge dataset. The results of this research are interesting, because real-life data is used. However, the development of the models is more challenging due to the anomalies and missing values that are present in the data. The second part of the thesis objective is to evaluate the forecasting performance of the different developed models. To be able to develop the

models I had to get familiar with: scikit-learn, Jupyter Notebook, Tensorflow, Keras, Pandas, Anaconda and Microsoft Azure. Therefore, completing this thesis was an educational experience that improved my software skills.

This report is divided in 4 chapters, followed by the conclusion and the appendix. First, an exploratory data analysis conducted on the dataset from the IEEE-CIS technical challenge is presented in Chapter 2. The goal is to determine the general characteristics of the data. 261 load series, with a full year of measurements are assessed. In section 2.2 the missing values, zero days, normalization and shifts in the rolling mean loads are discussed. In Section 2.3 the selected load series with a full year of smart meter measurements are aggregated to identify general characteristics of the data. In this section seasonality, comparison between weekdays and weekends, impact of an holiday on the load signal, influence of the temperature and the identification of the influence of properties of the household e.g. dwelling type is analysed. The additional household properties considered in the last analysis were available through a voluntary questionnaire.

In Chapter 3 the literature study is explained. First, an introduction is given about neural networks. The challenges and solutions are discussed in Section 3.1.3. The advanced LSTM and GRU neural networks are detailed in Section 3.1.4 and 3.1.5 respectively. These networks are specialized in the handling of time series. The introduction to neural networks ends with an explanation concerning the performance of different parameter settings and different LSTM architectures in Section 3.1.6. The second part of the literature study covers the use of LSTM models for short-term residential electrical load forecasting in Section 3.2.

In Chapter 4, three households are selected from the IEEE-CIS technical challenge dataset. The corresponding load signals are used for individual household forecasting. In section 4.1, the raw data is introduced and the preprocessing is detailed. Section 4.2 discusses the error metrics used to evaluate the prediction performance of the models. Section 4.3 clarifies how Microsoft Azure is used for cloud computing. Section 4.4 describes the development of baseline models that serve as a benchmark for the advanced Deep LSTM models which are explained in Section 4.5.2. In Section 4.5 the developed Deep LSTM models are discussed and a parameter search is conducted. Chapter 5 shows the results of the LSTM models on the test set with respect to the baseline models. The conclusion of this work is presented in Chapter 6.



## Chapter 2

# Exploratory Data Analysis

This chapter starts by describing the dataset were the exploratory data analysis will be performed on in Section 2.1. Next, the preprocessing steps done before the data analysis are explained in Section 2.2. The preprocessing steps consists out of handling missing data, identifying zero days, normalization and removing time series with a big shift in its rolling mean for all the 261 load series with a full year of smart meter measurements. In Section 2.3 follows a data analysis on the preprocessed data. For this all the 261 load series with a full year of smart meter measurements are aggregated to identify general characteristics of the data. Things of the aggregated load serie that are assessed are seasonality, comparing electrical consumption between weekdays and weekends, impact of an holiday, the influence of the temperature and the identification of the influence of properties of the household e.g. dwelling type. This last part was possible due to the availability of extra information through a voluntary questionnaire.

### 2.1 Data description

The data used in this thesis was made available for the [IEEE-CIS technical challenge on energy prediction from smart data](#). The dataset consists of load signals with time steps of 30 minutes of 3248 households located in the UK during the year 2017. Only households are considered and no The definition of an household are all the people who occupy a single housing unit, regardless of their relationship to one another. Each smart meter is property of E.ON UK and can collect a maximum of 17520 measurements during the year 2017. Not all the 3248 smart meters consist out of full data as can be seen in Figure 2.1. It can be clearly seen that there are 12 jumps in the amount of missing values. This is because the available data ranges from one month (only December) to a full year of data. This acknowledges that customers may have joined the measuring campaign at different times during the year. There are additional missing values in the time series due to sending or receiving errors of the smart meter.

Besides of the electricity consumption of the different households, also information is available about the average, minimum and maximum temperatures on a daily

## 2. EXPLORATORY DATA ANALYSIS

---

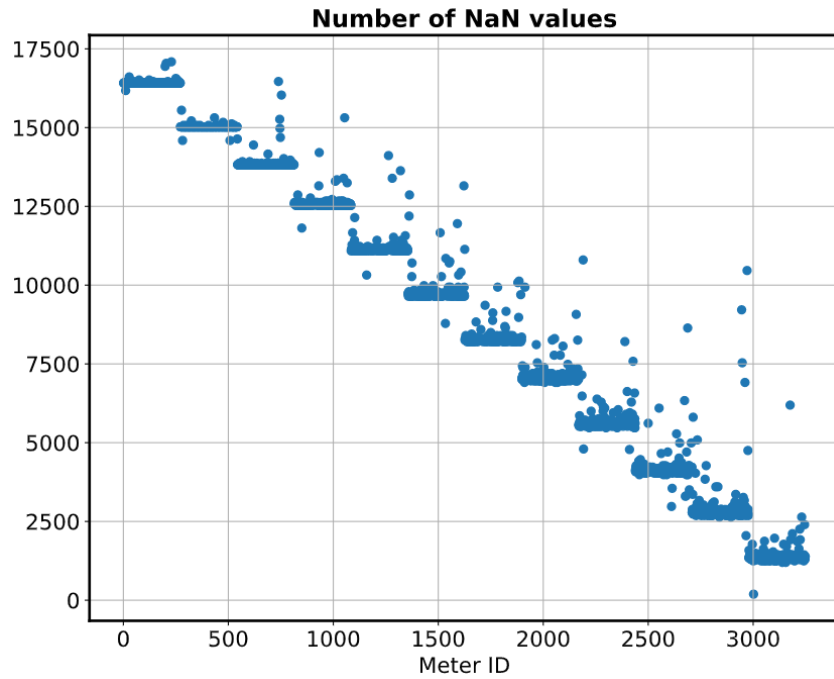


FIGURE 2.1: The amount of NaN values in all the 3248 load signals.

resolution. Finally, extra household information has been partially collected about 2143 households through voluntary surveys. This concerns the dwelling type, number of occupants, number of bedrooms etc. as further detailed in Table A.1. From the questionnaire it can be derived that the maximum amount of residents is 4 and there is a maximum amount of bedrooms of 5. The kind of house units are: flat, bungalow, detached house, semi detached house and terraced house. Industrial loads or small businesses e.g. a bakery is not considered. The available datasets and their features are summarized by Table 2.1.

<b>Consumption.csv</b>		<b>Weather.csv</b>	
# households	3248	Information	Average temperature
Information	Electric load		Max temperature
Max measurements/serie	17520		Min temperature
Granularity	1/2 hour	Granularity	daily
Timespan	year 2017		
Location	UK	# households	2143

TABLE 2.1: Summary of the available csv files form the IEEE-CIS technical challenge.

## 2.2 Preprocessing

Following sections describe the preprocessing applied on the 261 load series containing measurements for the entire year. The preprocessing done here is in preparation of the data analysis of Section 2.3. It shouldn't be confused with the preprocessing done for the three considered load series in Chapter 4.

### 2.2.1 Missing data

As discussed in Section 2.1, there exists two types of missing data in the Consumption csv file as was stated in the data description of the competition: fully missing months, due to the later participation in the measuring campaigns and missing values due to sending or receiving errors of the smart meter. When a smart meter fails, always all the measurements of that day are lost. In this Section two methods to impute the missing values are compared. Method Average Neighbours: replaces a missing value by the mean of the consumption values at the same moment on the next and previous days. Method Mean: substitutes the missing values of a time serie by the mean of all the measurements done by the meter. If the next or previous day is also missing in the serie, two days forward or back in time are used to replace the unknown day and so on. The resulting imputed signals can be seen in Figure 2.2.

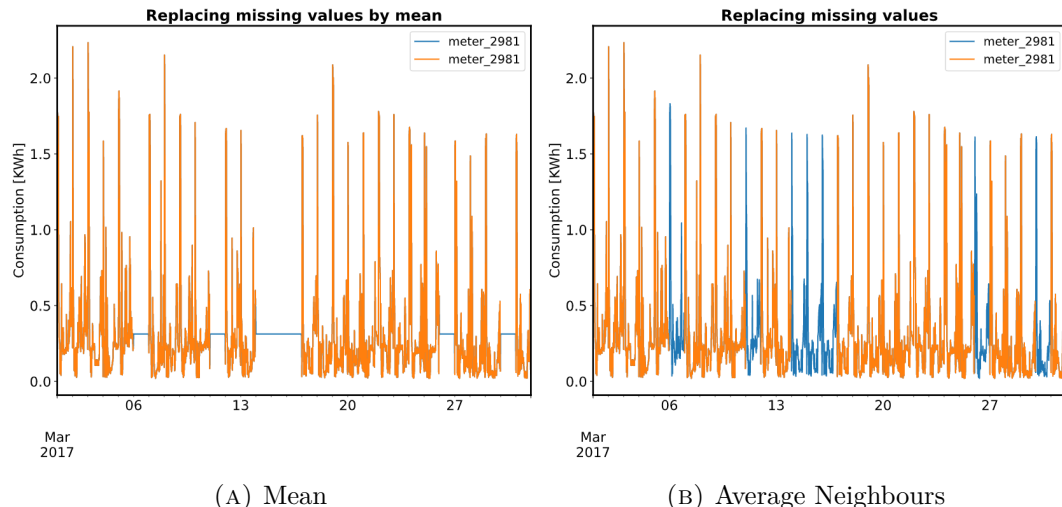


FIGURE 2.2: Resulting time serie of the month March after imputation of the missing data.

In order to compare how accurate both methods impute missing values, 181 months of March without any missing values were used and in each month randomly 7 days were removed. After applying both imputation methods, the resulting estimated signal was compared with the original one and an error value between both signals is calculated, using the mean squared error metric. Normalization is done by dividing the calculated MSE's by the MSE of the worst performing method to calculate the

## 2. EXPLORATORY DATA ANALYSIS

---

percentage of improvement of one method in comparison to the other. Figure 2.3 shows that on average, a reduction of the MSE of more than 20% is achieved when the average neighbours method is used in comparison to the mean method. Therefore, the average neighbours method will be applied to impute the missing values of the 261 time series with a full year of smart meter measurements. The only exception is made when the first of January and thirty-one December are imputed. Because not both neighbouring days can be known, the mean method is used.

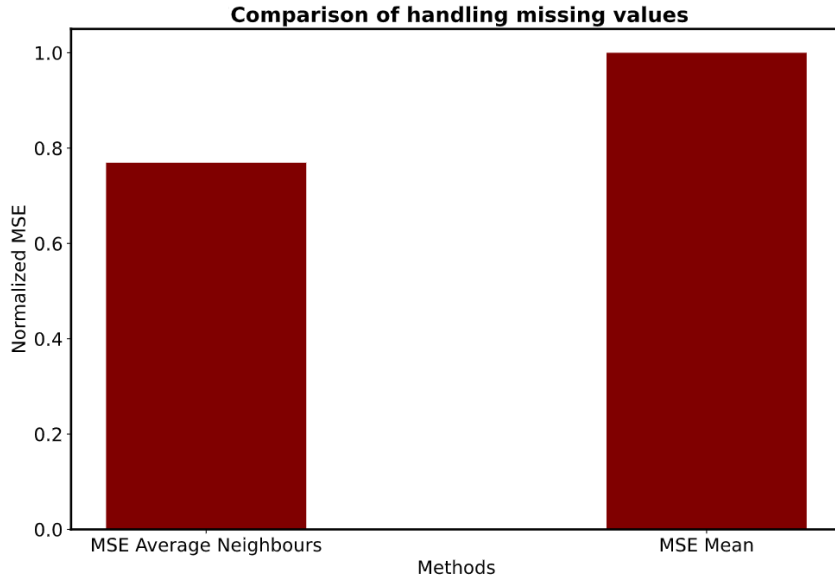


FIGURE 2.3: Resulting month of March after substitution of the missing values by the mean value of the measurements.

### 2.2.2 Zero days

When inspecting the load series, some untraditional meter measurements were identified. There were 9 meters of the 261 that had more than one day with a total electrical consumption of zero. Because it is unlikely that a household produces exactly zero kWh on an entire day all these 9 meters were removed. One of 9 load series is compared in Figure 2.4 with a load serie with zero days and it is clear that the horizontal lines are not part of a normal household load signal.

### 2.2.3 Normalization of the data

Normalization is necessary because while absolute consumption differs, relative patterns of human behaviour can be more similar according to [14]. The goal of a forecasting model applied on an individual household is to extract the human behaviour and normalization contributes to this by avoiding the disturbance of different magnitudes in which this human pattern may occur. Every load serie is normalized based on its yearly consumption as was done by [14]. The advantage

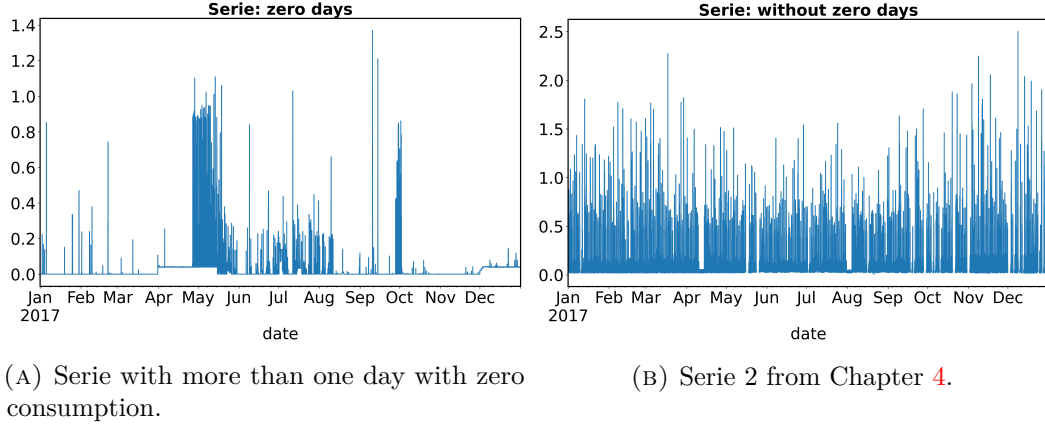


FIGURE 2.4: Comparison of series with and without zero load days.

of using the yearly consumption for normalization in comparison to the min-max method often used in literature, is the robustness against measurement outliers. This is important because in Section 2.3 all the 261 time series will be aggregated, which means that when a serie has only one very large outlier, the rest of its consumption values will be observed as small values in comparison with other series without a very large outlier. This is avoided when using the yearly consumption normalization where every load serie will be one at the end of the year as shown by Eq. 2.1. This allows for better comparison among the different series. The min-max normalization method is however used in Chapter 4, but here the series are always assessed individually

$$\text{normalized consumption}_i = \frac{\text{consumption}_i}{\sum_{k=1}^{17520} \text{consumption}_k}. \quad (2.1)$$

#### 2.2.4 Shifts in rolling mean of load signal

In this Section the normalized time series are assessed on fundamental changes in the load signal which can't be explained by normal human behaviour in the current household setting. A fundamental change of the load signal can be caused by an extra inhabitant or when systems are installed during the year that use a lot of electricity e.g. air-conditioning. A fundamental change is identified by looking at the maximum difference of the maximum and minimum rolling mean consumption over 7 days. Figure 2.5 shows all the maximum differences between the maximum and minimum weekly rolling averages for the 261 load series. Outliers in the maximum difference are detected as is done in a boxplot, namely from the third quartile a distance of one and a half times the interquartile range is added and values higher are considered as outliers. The red line in Figure 2.5 shows when a maximum difference is considered as an outlier. Finally, the outliers which corresponds to 5 load series above the red line, are removed because they are seen as a disturbance when the load signals are aggregated in Section 2.3. Figure 2.6 shows one of the

## 2. EXPLORATORY DATA ANALYSIS

---

removed load signals.

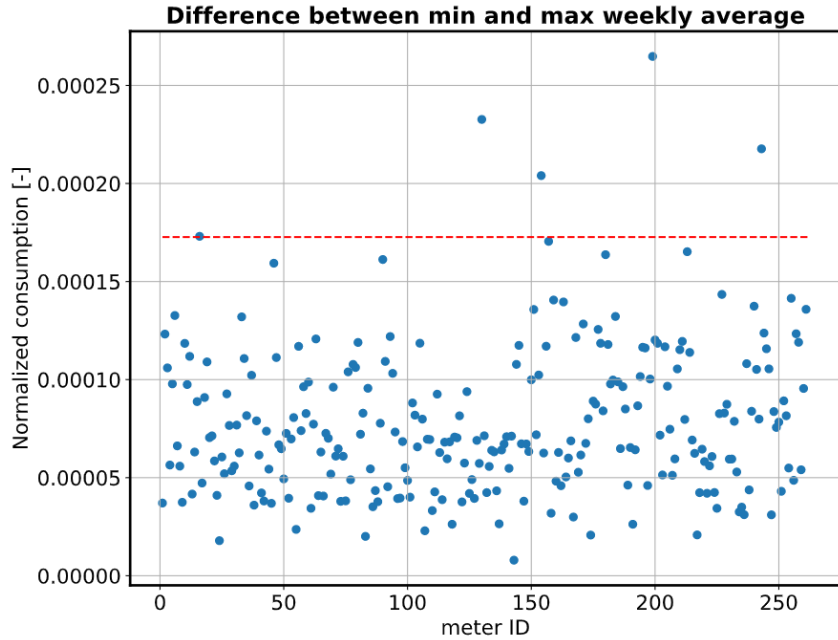


FIGURE 2.5: The maximum differences between the maximum and minimum weekly rolling mean for all the 261 different load signals.

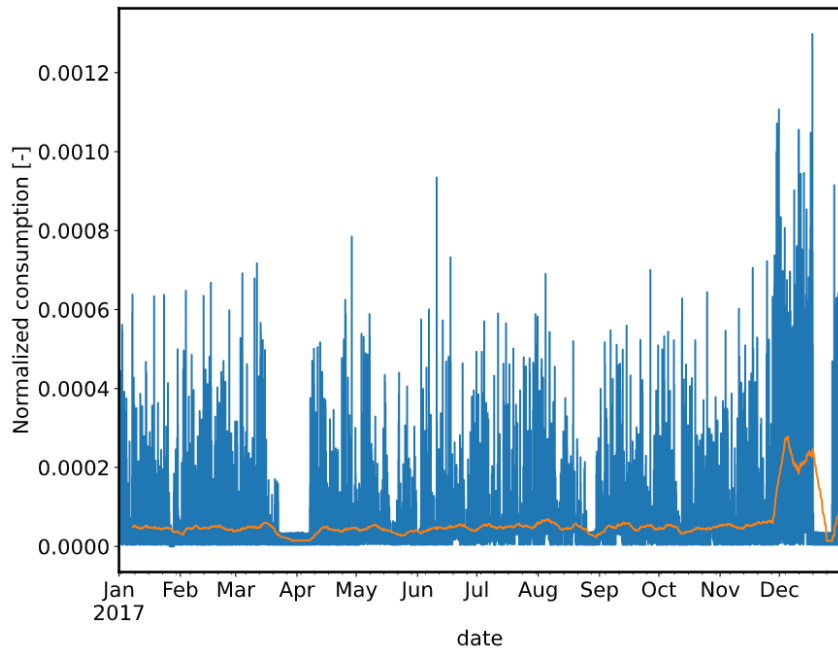


FIGURE 2.6: Removed load signal with a shift in the rolling mean.

## 2.3 Data Analysis

In this section the remaining 256 time series are converted to a single load serie by taking the mean. The single load serie is further referenced as the mean signal. This is done to identify general characteristics of the data. Things that are going to be assessed are: seasonality, comparing electrical consumption between weekdays and weekends, impact of an holiday, the influence of the temperature and the influence of properties of the household e.g. dwelling type.

### 2.3.1 Seasonality

In [9] it is concluded that all the forecasting algorithms that were considered, produced more accurate forecasts when they were combined with a preprocessing stage that extracted the seasonality before forecasting, compared to applying the same algorithms directly on raw data. The forecasting model is left with the task of modelling the deviation from the template consumption instead of performing a forecast out of the blue. However in [9] they made forecasts of an aggregated signal which had a reasonable amount of regularity which is not the case for electrical consumption forecasting of individual households. That it is not useful to extract a regular pattern is in accordance to [20], where it is explained that the use of a spectral analysis such as a wavelet analysis, that aims at separating the regular pattern from the uncertainty and the noise, is not applicable during load forecasting of individual households due to the low amount of regularity. However, the analyses of the seasonality of the mean signal is still informative to get a feeling of the general human behaviour.

These day and week templates are extracted from the mean signal by the use of equations 2.2 and 2.3 that calculate respectively the average day and week indicated by a thick blue line in Figure 2.7.

$$\bar{y}_i = \frac{1}{D} \sum_{d=1}^D y_{d,i}, \quad i \in [1, 48], \quad (2.2)$$

$$\bar{y}_j = \frac{1}{W} \sum_{w=1}^W y_{w,j}, \quad j \in [1, 336]. \quad (2.3)$$

$D$  and  $W$  give respectively the amount of days and weeks in the year 2017.  $\bar{y}_i$  and  $\bar{y}_j$  give the consumption of half an hour, averaged over respectively all days and weeks. In Figure 2.7 a clear consumption peak can be seen after midnight. This is due to heat storage systems that use electricity in the hours of low tariff and that release heat during high electricity tariffs. The daily seasonality shows a small peak in the load around 7 am and a bigger one around 6 pm. In the weekly seasonality it can be seen that all the peaks at 6 pm are of the same height but the smaller peak is different depending if it is a weekday or weekend as will be further explained in Section 2.3.2.

## 2. EXPLORATORY DATA ANALYSIS

---

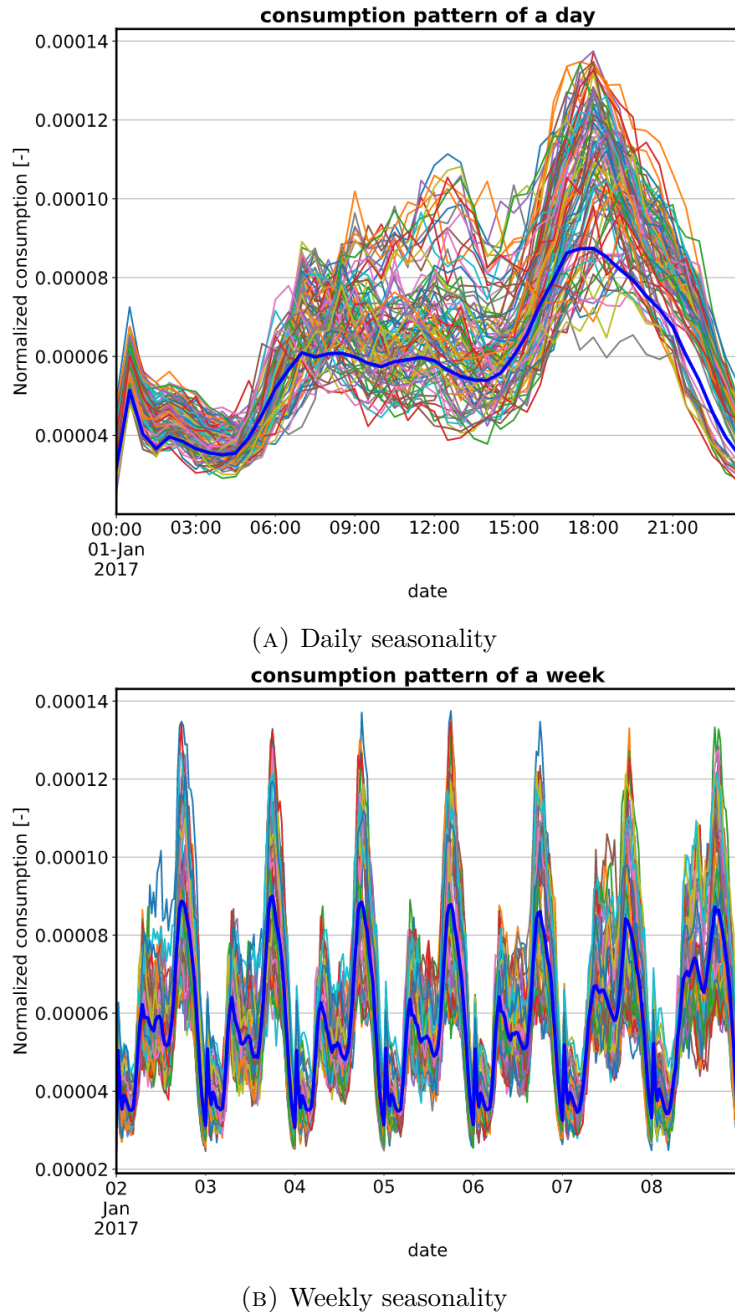


FIGURE 2.7: The seasonality of the electrical load during the year 2017. The blue line indicates the average load signal.

### 2.3.2 Comparing weekdays with weekends

Weekdays and weekends are compared with the help of Figure 2.7. It is clear that the consumption of the average business day is similar to a weekend day considering the

time of three two peaks each day. There is a morning peak around 7 am, an evening peak around 6pm and a peak after midnight. However, in the weekends, the morning peaks seems to be a little higher and decreases less. The effect can be seen during both weekend days, but is most visible on Sundays. To prove previous statements, the similarity is assessed by calculating the normalized MAE is calculated for the hourly difference of each combination of 2 days of the week. Normalization is done by dividing the different MAE's by the biggest MAE calculated. Figure 2.8 shows in blue and orange the error of combinations between business days or weekend days and in green the error of combinations between a business day and weekend day. It can be clearly seen that when a business day and weekend day are combined (green) the error is larger and thus more dissimilar. The left cluster of dots corresponds to a Saturday that is combined with a weekday and the right cluster corresponds to a Sunday combined with a weekday. It can be noticed that Saturdays are more similar to a business day than Sundays.

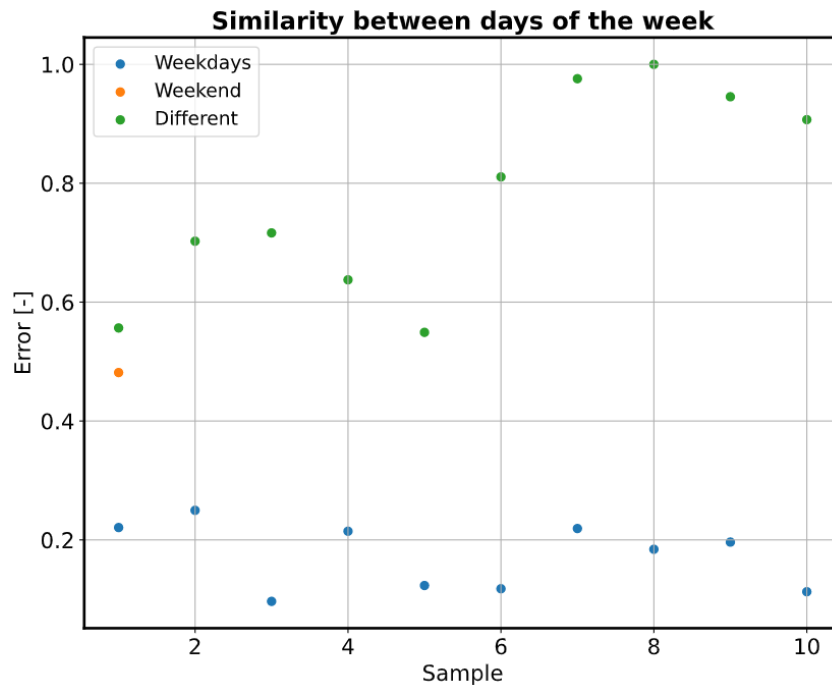


FIGURE 2.8: Error between different pairs of weekdays.

### 2.3.3 Impact of bank holidays

In order to look at the impact of a bank holiday, all the holidays of the English and Welsh calendar are identified for the year 2017. For each of the 8 bank holidays a corresponding business day is selected with an in euclidean distance as close as possible average temperature of the day. Therefore, mitigating the temperature influence. Note that each of the 8 holidays or business days are from the mean signal

## 2. EXPLORATORY DATA ANALYSIS

---

and they therefore are already averaged over 256 load signals. The 8 bank holidays and business days are averaged to obtain Figure 2.9. It is observed that a bank holiday behaves similarly to a weekend day which means a higher morning peak that decreases less. Figure 2.10 illustrates the similarity between a holiday and the days of the week. The error is calculated as the MAE of the hourly difference between the average day of the week and holiday. It can be seen that a bank holiday behaves most similarly to a Sunday.

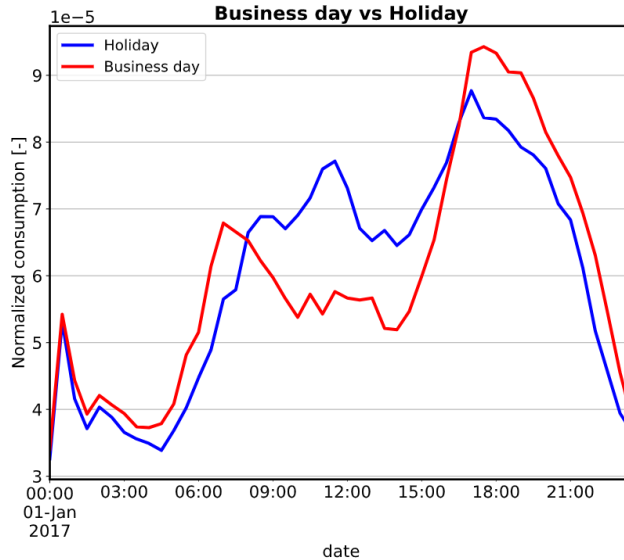


FIGURE 2.9: Comparison between bank holiday and business day electrical consumption.

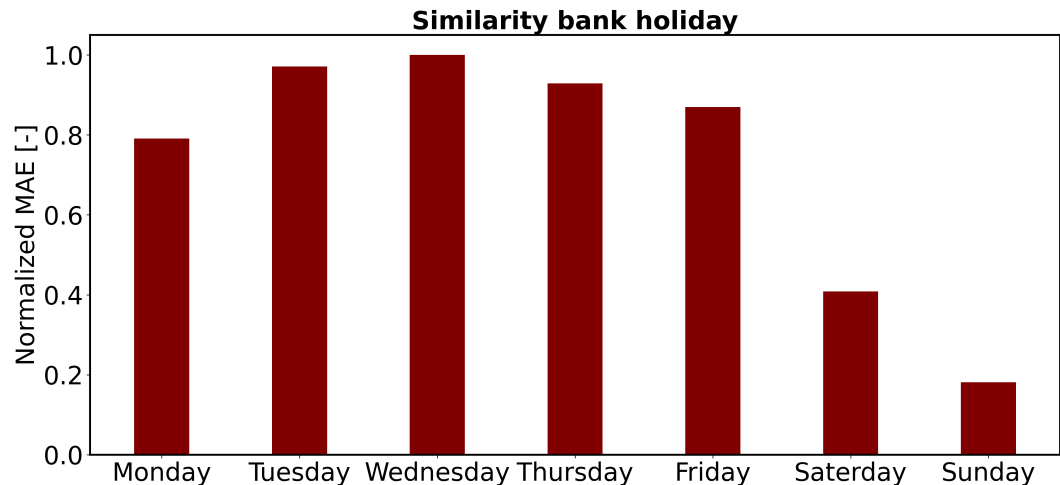


FIGURE 2.10: Error between a bank holiday and other days of the week.

### 2.3.4 Influence of temperature

In this section the correlation between the temperature and the electricity consumption is discussed.

#### Pearson correlation

The Pearson correlation is a measure of the linear dependency between two variables, based on the covariance. A Pearson correlation value gives information concerning the magnitude of the association and the corresponding direction of it. A Pearson value of 1 and  $-1$  gives respectively a perfect positive and negative linear relation between the variables. A value of zero, corresponds to independent behaviour. The following formula gives the Pearson correlation

$$\rho_{X,Y} = \frac{\text{cov}(X, Y)}{\sigma_x \sigma_y}. \quad (2.4)$$

Assumptions concerning the Pearson correlation are that samples used for the correlation should be independently drawn, coming in pairs, following homoscedasticity and there are no outliers. Outliers are especially undesirable when there are not a lot of samples. The variables should be normally distributed, linearly related to each other and be continuous. A normal distribution is necessary otherwise the assumption that a distribution can be described by a mean and variance is violated. The samples used for the correlation are generated by calculating the daily consumptions matched with the daily average temperature of the mean signal. Homoscedasticity is important because Eq. 2.4 assumes that  $\sigma_x$  and  $\sigma_y$  are constant values. The homoscedasticity assumption is validated by making use of Figure 2.11.

This figure shows the classic cone-shaped pattern of heteroscedasticity. On days when it is warm there is more similar human behaviour in lowering the electricity consumption. However, on colder days the variation in consumption is higher, which means that homoscedasticity is not perfectly fulfilled. This is a logical result because when it is cold there can be a lot of variation in what extent electricity is used for heating, while when it is warm everybody is likely to turn off the heating. Because the assumptions of the Pearson correlation are not all met, care should be taken with the output. Applying the Pearson correlation on Figure 2.11 gives a correlation value of  $-0.87$ . This means there is a strong linear, decreasing relation.

#### Spearman correlation

The Spearman correlation is a rank correlation. A sample consists out of a daily consumption value with a corresponding average temperature value. The consumption and temperature values belonging to a sample are each compared with respect to all the consumption and temperature values and an ordering is retrieved for both values. When the ordering of both variables in a sample is similar, correlation is strong and positive. If the ordering is reversed, correlation is strong and negative. There is a perfect positive ordering if a larger consumption always corresponds to a higher temperature. Notice that for a perfect ordering, no linear relation of the variables is necessary. The Spearman correlation coefficient is calculated using Eq.

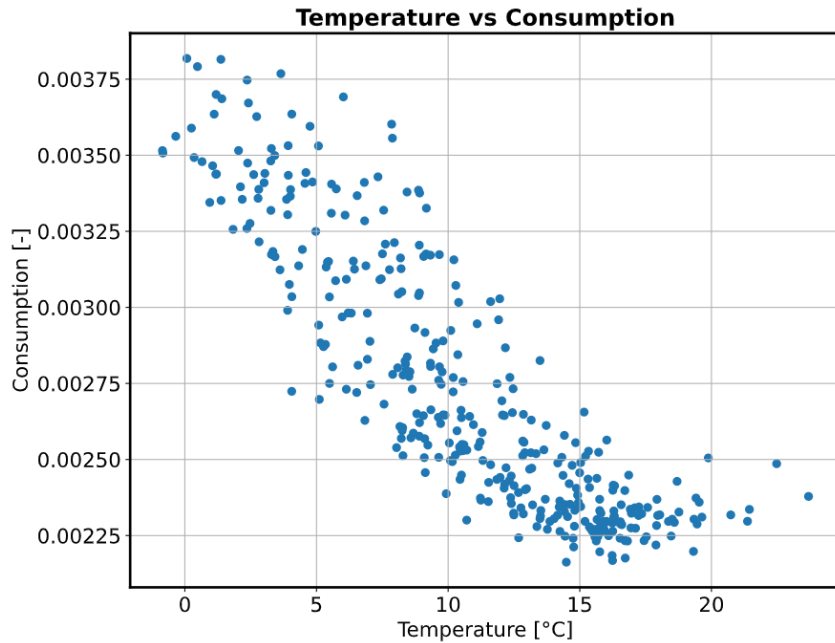


FIGURE 2.11: Relation between normalized daily consumption and daily temperature.

[2.4](#), but replaces the values of the variables by the rank of the variables in the a sample.

In order to use the Spearman correlation data has to be ordinal, which means that it can be ordered. The Spearman correlation gives information about the monotonicity relation between the variables.  $\rho = 1$  corresponds to a monotonically increasing relation.

Applying the Spearman correlation gives a correlation value of  $-0.89$ , which means there is a large negative monotone relation. This means if the temperature is higher, consumption is likely to be lower. Identically, if the temperature is lower it is likely that the consumption will be higher and vice versa. This confirms the conclusions from the Pearson correlation.

### Kendal correlation

The Kendal correlation is also a rank correlation. It is looked how many samples are concordant, discordant or neither when each combination of 2 samples are compared with each other. A concordant pair means that when the consumption value of sample 1 is higher than the consumption value of sample 2, this must also be the case for the temperature values. A discordant pair means that when the consumption value of sample 1 is higher than the consumption value of sample 2, this should be not the case for the temperature. Neither can occur when consumption values or temperature values are equal for the 2 samples. When a Kendal correlation of 1 is

retrieved, this means that all samples are concordant and only  $n^+$  differs from zero. This automatically imposes monotonicity which means that when a consumption value is increased, also the temperature value must be increased. Equation 2.5 gives the equation to calculate the Kendal correlation coefficient. Applying the Kendal correlation gives a correlation value of  $-0.67$ , which again confirms the conclusions from the Pearson correlation

$$\tau = \frac{n^+ - n^-}{\sqrt{(n^+ + n^- + n^x)(n^+ + n^- + n^y)}}. \quad (2.5)$$

- $n^+$  is the number of concordant pairs
- $n^-$  is the number of discordant pairs
- $n^x$  is the number of ties only in x
- $n^y$  is the number of ties only in y
- concordant  $\rightarrow (x_i > x_j)$  and  $(y_i > y_j)$  or  $(x_i < x_j)$  and  $(y_i < y_j)$
- discordant  $\rightarrow (x_i > x_j)$  and  $(y_i < y_j)$  or  $(x_i < x_j)$  and  $(y_i > y_j)$
- neither  $\rightarrow (x_i = x_j)$  or  $(y_i = y_j)$
- if both  $(x_i = x_j)$  and  $(y_i = y_j) \rightarrow$  not included in either  $n^x$  or  $n^y$

### 2.3.5 Influence of household attributes

In this section the influence of different attributes of the households on the load signals is investigated. Instead of the mean signal, every smart meter of the total of 3248 meters with additional information, is used during the analysis. This means that also load series are included that don't have measurements for the full year as was discussed in Section 2.2.1. Because all load signals have measurements for the month December, the total consumption during December is used in the analysis. This leads to a bias because it is winter time. Missing values during December are imputed according to the Average neighbours method.

It is observed that only for the dwelling type and the amount of bedrooms, there is a higher response in the questionnaire. Respectively, 1702 and 1859 answers are obtained in comparison to the rest of the questions were the amount of collected answers varies between 69 and 78. Sometimes the answers are evenly distributed over the different options, for example when assessing heating fuel there are only three answers registered for using electricity in comparison to 69 answers that are registered for using gas. An overview of the amount of answers per household attribute, can be seen in Table A.1. Because of the low sample sizes of the attributes different from dwelling type and number of bedrooms, care should be taken with the results of the stochastic analysis.

Figure 2.12 shows boxplots of the collected data concerning the dwelling type and

## 2. EXPLORATORY DATA ANALYSIS

---

the amount of bedrooms. According to the mean and median values of the different dwelling types, the order in monthly consumption is: Flat < Bungalow < Semi detached < Terraced < Detached. It was noted that there were a lot of outliers in the consumption values of a detached house. A “real” house also tends to have a higher monthly consumptions than a flat or bungalow. Next, it is observed that when a housing unit has more bedrooms, also the monthly consumption is larger. This is a logical result, because it is likely that when the number of bedrooms is larger, the house is larger which means that it requires more electrical heating when used and it can store more electrical appliances. Conclusions drawn for the other attributes are summarized below.

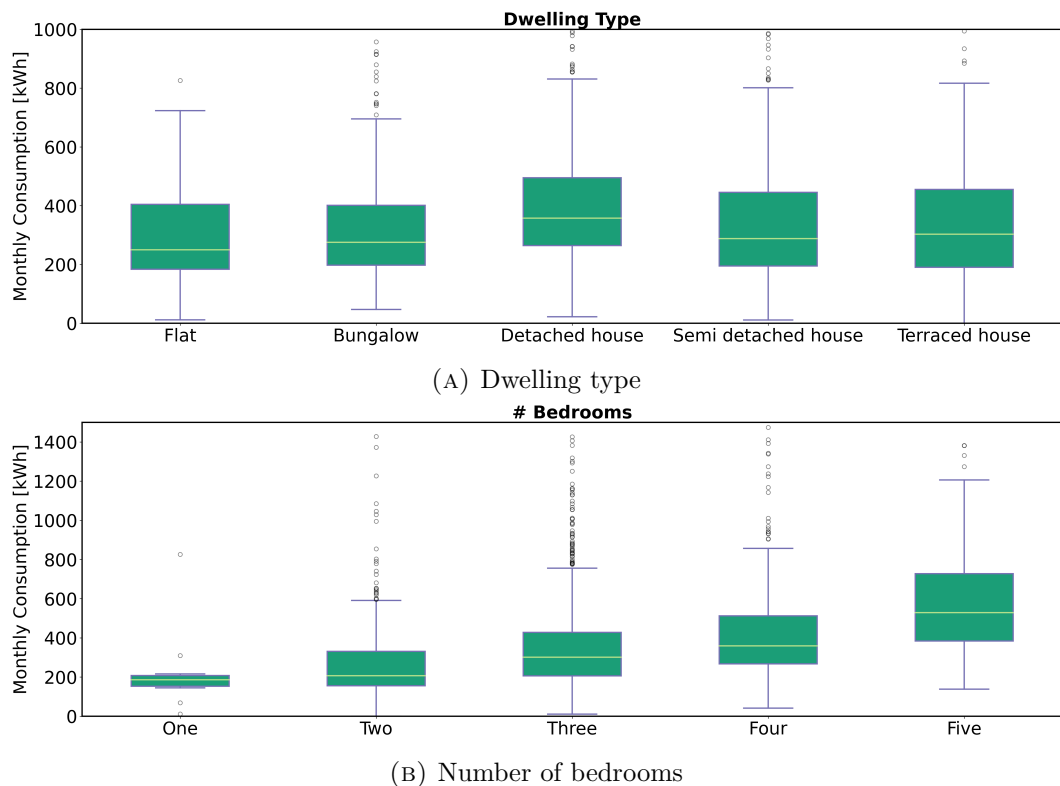


FIGURE 2.12: Influence of the dwelling type (sample size: 1702) and number of bedrooms (sample size: 1859).

- More inhabitants leads to higher monthly consumption
- 88% of the households use gas as heating fuel
- 81% of all houses use gas as hot water fuel
- When the boiler age is categorized as old, the median of the monthly consumption is 30% higher with respect to the median of a new boiler

- 91% of the lofts are insulated
- 72% of the walls are insulated
- 76% heats up to a temperature between 18 and 20 degrees
- 66% has an efficient lighting percentage between 75% and 100%

## 2.4 Conclusion

During this chapter the exploratory data analysis of the data retrieved from the IEEE-CIS technical challenge on energy prediction from smart data, is conducted. First, the data was described by giving its most important features and displaying the amount of NaN values. It was found that there are 261 load signals with a full year of measurements. Next, preprocessing of the data was done by discussing the imputation of the missing values, the identification of zero days, normalization and shifts in the rolling mean of the load signal. Thereafter, the data analysis followed were an aggregated load signal was assessed and seasonality, weekdays versus weekend days, impact of bank holidays and the influence of the temperature were explained. Finally, the influence of household attributes was discussed.



# Chapter 3

## Short-term residential load forecasting : state of the art

As discussed in the introduction, forecasting an individual household is a complex task due to the high uncertainty and volatility of the load signal. To tackle the electrical consumption forecasting, problem neural networks are applied. These models allow for learning very non-linear relations between the inputs and output. Learning is done by updating the model every time such that the observations in the training set are better explained. In this chapter first, an introduction is given about neural networks and the difficulties and solutions are discussed in Section 3.1.3. Next follows the explanation of the more advanced LSTM and GRU neural networks in respectively Section 3.1.4 and 3.1.5, which are specialized in handling time series data. Finally, the introduction to neural networks ends with the explanation of what was found in literature concerning the performance of different parameter settings and different LSTM neural networks in Section 3.1.6. The second part of the literature study covers the use of LSTM models for short-term residential electrical load forecasting in Section 3.2.

### 3.1 Introduction to neural networks

#### 3.1.1 MLP

The simplest configuration of neural networks are multilayer perceptrons and they are made up out of multiple fully connected layers of neurons. Figure 3.1 shows a MLP with one hidden layer.

All layers are connected to the next layer by the means of an affine function together with a non-linear activation function represented by sigma as shown by equation 3.1 with  $\mathbf{L}^{(N)}$  the vector with outputs of the Nth layer,  $\mathbf{W}^{(N)}$  the Nth weight matrix and  $\mathbf{b}^{(N)}$  the Nth bias

$$\mathbf{L}^{N+1} = \sigma(\mathbf{W}^{(N)}\mathbf{L}^N + \mathbf{b}^{(N)}). \quad (3.1)$$

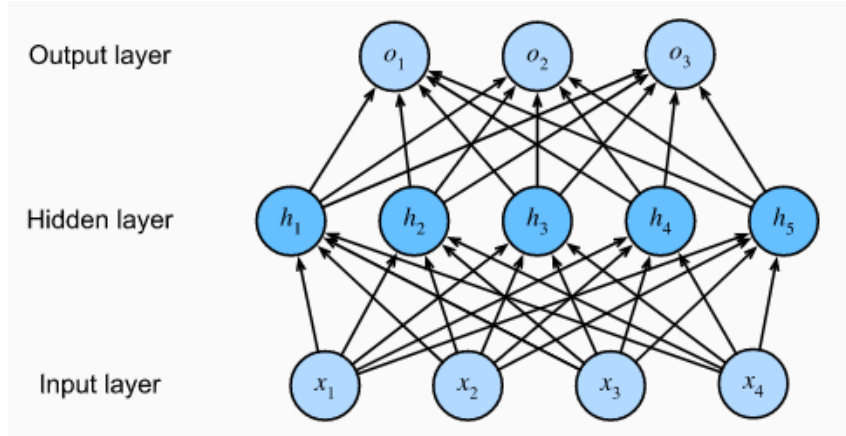


FIGURE 3.1: Figure of a MLP (source [24]).

A standard multilayer feedforward neural network with locally bounded piecewise continuous activation function can approximate any continuous function to any degree of accuracy if and only if the network's activation function is not a polynomial, as stated by **Leshno et al** in 1993. This theorem proves that a “universal approximator” exists for continuous functions, but it lacks the recipe to construct it. In [17] it is shown that a feedforward network with a single layer is enough to approximate any function by a specified accuracy if the hidden layer has the possibility to add an unlimited amount of hidden neurons in its layer. It is discussed that when a function is discontinuous, which means that it makes sudden, sharps jumps, it is not possible to approximate the function by any prescribed accuracy. However, in practise a continuous approximation is often good enough.

Neural networks are suitable of learning very non-linear mappings between inputs and outputs. The difference between “Deep neural networks” and “Shallow neural networks” is the amount of layers of neurons that are used inside the network. The layers of neurons, that are not inputs or outputs are called “hidden neurons”. Because a “Deep neural network” has a hierarchical layout of the different hidden layers, it not only learning features from the non-linear combinations of inputs, but uses other layers to learn features of combinations of features learned in lower hidden layers. This is possible because higher hidden layers get the outputs of lower hidden layers as input. However, because of the higher expressiveness, a “Deep neural network” with respect to a “Shallow neural network”, suffers more of overfitting as is discussed in section 3.1.3.

### 3.1.2 RNN

A recurrent neural network is a specialized neural network to deal with sequential information. The output of recurrent neural networks depend on the prior elements within the sequence. In order to take past information from previous inputs into account, a hidden variable  $\mathbf{H}^t$  is used. By making use of this variable which makes a

### 3.1. Introduction to neural networks

summary of the previous seen information, a large increase in the number of model parameters is avoided. Cited from [?]: “Hidden states are technically speaking inputs to whatever we do at a given step, and they can only be computed by looking at data of previous time steps”. Equation 3.2 shows how the previous hidden state and the current information are merged in the next hidden state with  $\mathbf{X}^t \in \mathbb{R}^d$ ,  $\mathbf{H}^t \in \mathbb{R}^h$ ,  $\mathbf{W}_1 \in \mathbb{R}^{h \times d}$ ,  $\mathbf{W}_2 \in \mathbb{R}^{h \times h}$  and  $\mathbf{b} \in \mathbb{R}^h$

$$\mathbf{H}^{t+1} = \tanh(\mathbf{W}_1 \mathbf{X}^t + \mathbf{W}_2 \mathbf{H}^t + \mathbf{b}). \quad (3.2)$$

The equation  $\mathbf{X}^t$  corresponds to one input at time step  $t$  with dimensionality  $d$ . Also a deep RNN is possible, where multiple layers and hidden states are used per time step.

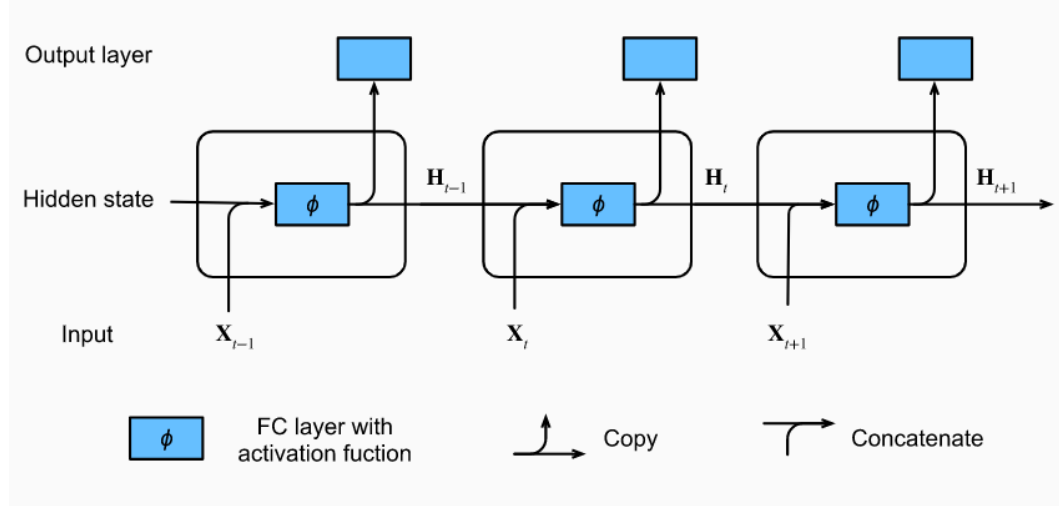


FIGURE 3.2: Vanilla RNN,(source: [24]).

As was discussed in the beginning of this section a standard neural network can act as a “universal approximator” when given enough hidden states. A similar result exist for a recurrent neural network which states that it is capable to approximate a sequence-to-sequence mapping to an arbitrary accuracy as discussed in [8]. However, as discussed in [23] even if expressiveness of the simple model is very powerful in theory, this doesn’t indicate that such a representation can be learn in a reasonably amount of time from a dataset. As will be discussed in Section 3.1.3, the main drawback of the vanilla recurrent neural network is that it forgets fast important information in function of the amount of time steps. When using “backpropagation through time” for updating the weights, the gradients that corresponds to inputs seen a lot of time steps ago will become very small due to the multiplication of small gradients over the time steps. Therefore, their contribution of updating the weights of the recurrent neural network will be very small and thus this information will be “forgotten”.

### 3.1.3 Difficulties & Solutions of neural networks

Neural networks have a high expressiveness but this comes at the cost of overfitting and a vanishing gradient. When the neural network is learning from training data, every epoch the error between the input and output of the training examples is reduced. In the beginning the validation error reduces simultaneously with the training error. The validation error is the error that the model makes on data that is not seen during training. On a certain point during the training the validation error increases while the training error still decreases. This means that the model is no longer learning intelligent general rules and patterns in the data, but it starts remembering the training data and therefore the model will not perform well in general. This is often the case in a model with an high expressiveness because the model is less pushed to make generalizations and has the ability to just remember the training data. Solutions to overfitting can be regularization which includes the weight sizes as a cost in the objective function. Typical choices for resembling the size of the weights are the  $L_1$  and the  $L_2$  norms. Other methods that can be used are: early stopping, dropout and pruning.

It should be noted that the gradient can increase very much over the different time steps, which in literature is called gradient explosion. The solution strategy for this is applying gradient clipping by norm or by value. Gradient clipping by norm means that when the 2-norm of the gradient  $\xi$  exceeds a threshold value  $\theta$ , the 2-norm of the gradient is scaled to equal the threshold value. The mathematical formulation is given by equation 3.3:

$$\xi = \min(1, \frac{\theta}{\|\xi\|}) \times \xi. \quad (3.3)$$

An alternative method to avoid gradient explosion is using gradient value clipping. The second problem is the vanishing gradient which in a RNN setting corresponds to having a short term memory which means that initial inputs that were presented to the neural network are being forgotten. This can be mitigated using a LSTM or GRU. Both techniques have in common that they can learn which data in the sequence is important and should be retained and which information can be thrown away. It is important to state that LSTM and GRU are not solving the vanishing gradient problem as explained in [23]. The gradient is still exponentially decreasing, but the effect is less pronounced as can be seen for LSTM in Figure 3.3. When the forget gate, that sits inside a LSTM cell outputs a value that is close to one, the exponential decay will have also a base close to one.  $\tau$  gives the number of epochs. As discussed in [23], the amount of memory and calculation effort needed to do a gradient update increases linearly with the amount of time steps. Memory and calculation load can be mitigated by making use of truncated backpropagation through time.

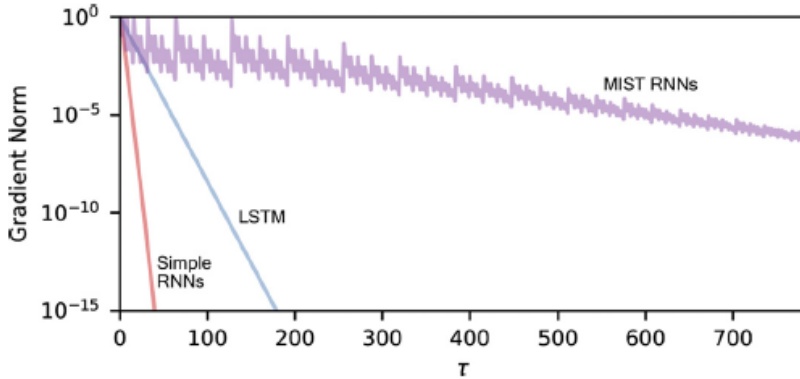


FIGURE 3.3: Exponential decrease of the gradient size of a simple RNN (red) or a LSTM (blue) (source: [23]).

### 3.1.4 LSTM

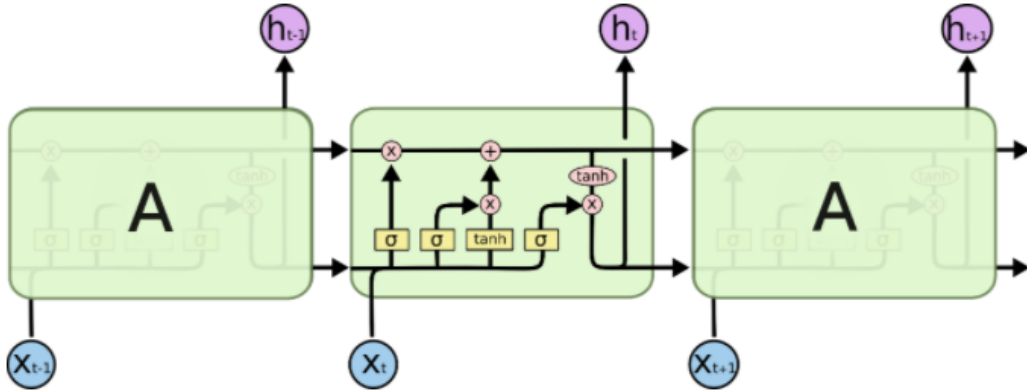


FIGURE 3.4: A LSTM cell that is repeated over time (source: [18]).

As discussed in Section 3.1.3, the LSTM is an updated version of the conventional RNN first proposed by **Hochreiter & Schmidhuber** in 1997 to deal with the short term memory a RNN suffers from. A LSTM can longer take important aspects of the presented time series into account which can be used during prediction. To do this a LSTM makes use of three gates: forget gate  $f_t$ , input gate  $i_t$  and an output gate  $o_t$ . When comparing the three gates with Eq. 3.2, it is clear that every gate is by itself a recurrent neural network, with the only difference that a sigmoid function is used instead of a hyperbolic tangent. The core concept of the LSTM is that it makes use of a memory cell that is passed on through the different time steps. The memory cell contains important information that is seen before in the data and should be taken into account at the current new output. The three gates can delete, write and read information from this memory cell. It can also be noted that Eq. 3.7 is exactly equal to the conventional RNN described by Eq. 3.2. Eq. 3.7

processes the hidden states  $\mathbf{H}_t$  and the new input  $\mathbf{X}_t$  to propose an update  $\tilde{\mathbf{c}}_t$  to the previous memory cell. The input gate Eq. 3.5 decides what will be preserved of the proposal and actually updated. The forget gate Eq. 3.4 decides what will be preserved from the original memory cell  $\mathbf{c}_t$ . When both the old memory cell and the proposal are pruned, they are combined to one new memory cell. This new memory cell is together with the output gate Eq. 3.6 used to output new hidden states.

In order to train a LSTM neural network there are considerably more parameters that have to be learned than a conventional RNN. An LSTM has four different weight matrices for both the hidden states and the inputs. Because by this increase of weights also the expressiveness of the model has increased with respect to the vanilla recurrent neural network of Section 3.1.2. Therefore, overfitting of the data should be extra monitored. The LSTM equations are given as follows as they were found in [23]:

$$\mathbf{f}_t = \sigma(\mathbf{W}_{fH}\mathbf{H}_{t-1} + \mathbf{W}_{fX}\mathbf{X}_{t-1} + \mathbf{b}_f), \quad (3.4)$$

$$\mathbf{i}_t = \sigma(\mathbf{W}_{iH}\mathbf{H}_{t-1} + \mathbf{W}_{iX}\mathbf{X}_{t-1} + \mathbf{b}_i), \quad (3.5)$$

$$\mathbf{o}_t = \sigma(\mathbf{W}_{oH}\mathbf{H}_{t-1} + \mathbf{W}_{oX}\mathbf{X}_{t-1} + \mathbf{b}_o), \quad (3.6)$$

$$\tilde{\mathbf{c}}_t = \tanh(\mathbf{W}_{cH}\mathbf{H}_{t-1} + \mathbf{W}_{cX}\mathbf{X}_{t-1} + \mathbf{b}_c), \quad (3.7)$$

$$\mathbf{c}_t = \mathbf{f}_t \times \mathbf{c}_{t-1} + \mathbf{i}_t \times \tilde{\mathbf{c}}_t, \quad (3.8)$$

$$\mathbf{H}_t = \mathbf{o}_t \times \tanh(\mathbf{c}_t). \quad (3.9)$$

### 3.1.5 GRU

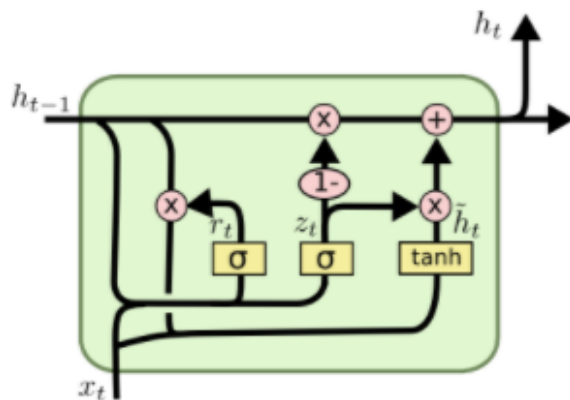


FIGURE 3.5: A GRU cell that is repeated over time (source: [18]).

A gated recurrent unit neural network is a newer, simplified version of the LSTM that deals with the short term memory problem of a vanilla recurrent neural network. It was introduced by **Cho et al.** in 2014. The LSTM is changed by merging the forget and input gate into an update gate. Also, the memory cell and hidden states are combined. The difference in performance between variations of the LSTM neural network is discussed in Section 3.1.6. The following GRU equations are as found in [23]:

$$\mathbf{z}_t = \sigma(\mathbf{W}_{zH}\mathbf{H}_{t-1} + \mathbf{W}_{zX}\mathbf{X}_{t-1} + \mathbf{b}_z), \quad (3.10)$$

$$\mathbf{r}_t = \sigma(\mathbf{W}_{rH}\mathbf{H}_{t-1} + \mathbf{W}_{rX}\mathbf{X}_{t-1} + \mathbf{b}_r), \quad (3.11)$$

$$\tilde{\mathbf{H}}_t = \tanh(\mathbf{W}_{HH}(\mathbf{r}_t \times \mathbf{H}_{t-1}) + \mathbf{W}_{HX}\mathbf{X}_t + \mathbf{b}_H), \quad (3.12)$$

$$\mathbf{H}_t = \mathbf{z}_t \times \mathbf{H}_{t-1} + (1 - \mathbf{z}_t) \times \tilde{\mathbf{H}}_t. \quad (3.13)$$

### 3.1.6 Performance of different parameter settings and variations of LSTM neural network models from literature

Paper [2] conducts an empirical evaluation of the GRU and compares it with the older LSTM. It was found that it outperformed the vanilla RNN and attained similar performance as the LSTM on the task of polyphonic music modelling and speech signal modelling. According to [18], the next step in sequence modelling is the use of attention models or grid LSTM's.

There exists a lot of variations of the LSTM neural networks. Paper [7] discusses a large-scale analysis of eight LSTM variants on the tasks of: speech recognition, handwriting recognition and polyphonic music modelling. The hyperparameters of the models were optimized using a random search method. The influence of each of the hyperparameters was assessed using the fANOVA toolbox. This toolbox is in more detail explained in [10]. It was found that none of the assessed variants could significantly outperform the conventional LSTM architecture e.g. GRU. However, it was stated that the LSTM variants in some occasions were able to simplify the calculation load and number of parameters, without the lost of performance. Next, it was found that the forget and output gate were the most crucial gates of the LSTM network. When one of the two was removed, a significant lost of performance occurred. There was also an hyperparameter search conducted with following hyperparameters:

- Amount of LSTM hidden states
- Learning rate
- Momentum term
- Standard deviation of Gaussian input noise

It was concluded that it can be assumed that there is no interaction between the different parameters. The largest interaction could be found between the learning rate and the amount of LSTM hidden states, which was still small. Therefore, parameters can be varied individually which can drastically reduce the amount of runs that had to be performed to see the effect on the model. Next, it was concluded that the learning rate was the most important parameter and could be tuned by setting it initially high e.g. to 1, and then let it decrease until the error on a validation set starts increasing. The use of a momentum term, which takes previous values of the weights into account when updating, was found to be unimportant in their setting of online gradient descent. The use of gaussian input noise to avoid overfitting was found to be not helpful.

### 3.2 Short-Term residential electrical load forecasting

In paper [20] a novel pooling-based deep recurrent neural network is proposed which collects load profiles of neighbouring houses into a pool of training inputs. Pooling of neighbouring households historical load to serve as input of a deep LSTM neural network, is proposed to increase the data volume and diversity of the training set. The goal of using a pooled training set is to avoid overfitting present when using a deep LSTM neural network. Regarding notation, LSTM is used here instead of RNN with LSTM units as done in the paper. The idea is as quoted by [20], to use the interconnected spacial information to compensate insufficient temporal information. The pool of data allows to learn the correlations between neighbouring households and the shared uncertainties coming from external factors. Pools consisting out of 10 households are used. From the pool of inputs every epoch a randomly chosen batch is fed to the LSTM network. Training is stopped when the MSE on the training set is converged. When the training ends, performance is tested for each household in the pool.

Performance of the proposed method was evaluated based on a test set of 30 days and is twofold :

1. Performance of the proposed method with respect to ARIMA, vanilla LSTM, SVR and DLSTM (without pooling)
2. The effect of the neural network depth and pooling

For the first part of the method evaluation it was concluded that the proposed DLSTM with pooling, outperforms all other methods based on the metrics RMSE, NRMSE and MAE.

The amount of which the PDLSTM outperformed the other methods can be seen in Table 3.6. The effect of the depth of the DLSTM and the pooling method is depicted in Figure 3.7. It can be seen that without the pooling method the DLSTM only benefits from extra LSTM layers till three. This is because from that point, overfitting will reduce the generalization capacity of the DLSTM. With the pooling technique, extra layers stay beneficial. It can thus be concluded that introducing

### 3.2. Short-Term residential electrical load forecasting

---

extra hidden layers is a good choice to model the non-linear relations, but this can only be done efficiently when overfitting is mitigated by the use of a pooling strategy. The LSTM with pooling used for benchmarking consisted out of five layers and thirty hidden units in each layer.

<i>Network Architecture</i>	<i>RMSE (kWh)</i>	<i>NRMSE (kWh)</i>	<i>MAE (kWh)</i>
<i>ARIMA</i>	0.5593	0.1132	0.2998
<i>RNN</i>	0.5280	0.1076	0.2913
<i>SVR</i>	0.5180	0.1048	0.2855
<i>DRNN</i>	0.4815	0.0974	0.2698
<i>PDRNN</i>	0.4505	0.0912	0.2510
<i>Improvement from DRNN to PDRNN</i>		6.45%	6.96%
<i>Improvement from ARIMA to PDRNN</i>		19.46%	16.28%

FIGURE 3.6: Comparing different methods in [20].

In [13] it is chosen for a deep LSTM approach to forecast the electricity load of a single household. A deep LSTM has multiple LSTM layers. It is first discussed that the aggregated electrical load serie shows more regularity than the load signal of an individual household. This is substantiated by making use of a density based clustering technique, where it is shown that the different daily consumptions profiles of the aggregated signal could be described by one cluster and no outliers. An outlier means that a daily consumption profile could not be assigned to a cluster. On the other hand for individual household load series, the amount of outliers can range to over 80. The amount of outliers a load signal has, is a measure of the amount of regularity of the signal. Less outliers corresponds to more regularity.

Because the household load signals are characterized by the residents daily routines, this is tried to be learned directly by the deep LSTM. Inputs that are given to the LSTM are  $k$  past half hour load values, time of the day, day of the week if it is a bank holiday. In Table 3.8 the results are shown of the LSTM method in comparison with other forecasting techniques. It can be seen that the LSTM outperforms the rest in making individual forecasts. Forecasting was performed on 69 different electrical load

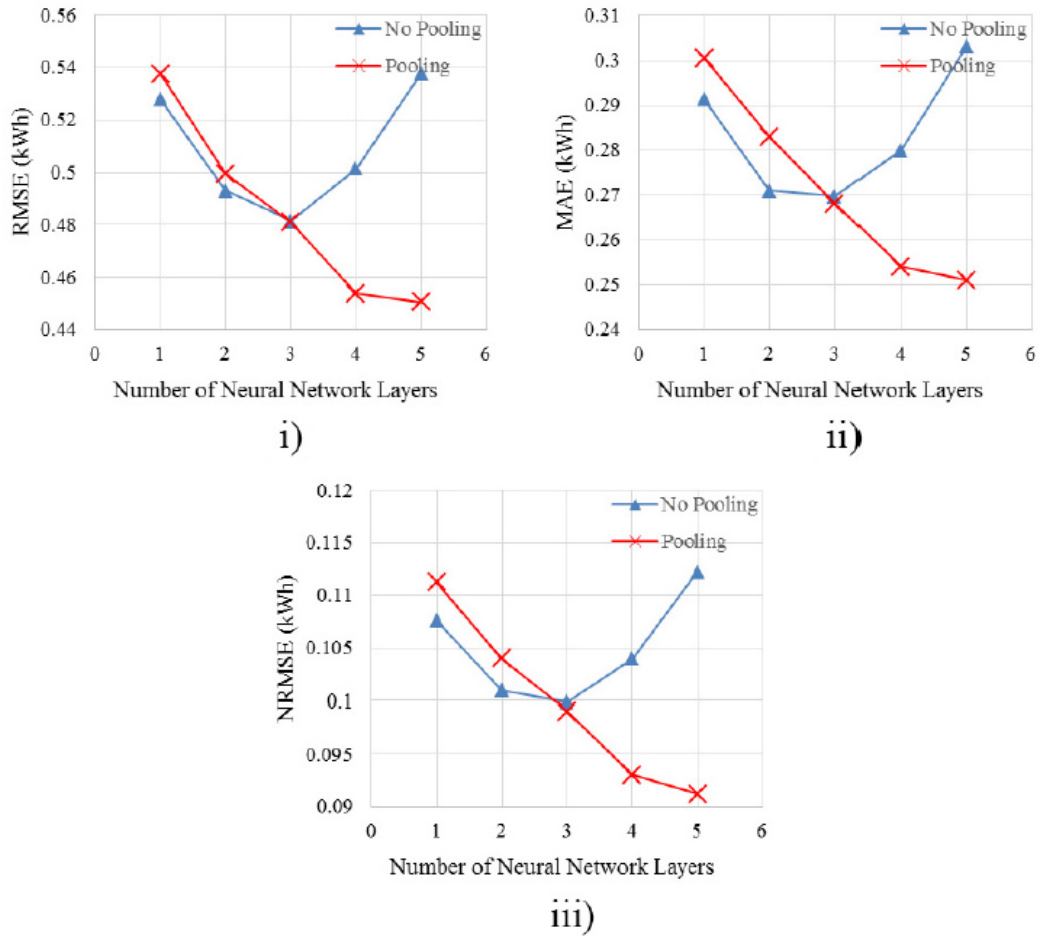


FIGURE 3.7: Influence of the number of layers and the pooling method (Source: [20]).

series coming from households in Australia. It was concluded that methods IS-HF and KNN (k-nearest neighbour), that have good performance on an aggregated time serie, perform much worse for individual households.

By making use of linear regression in function of the amount of outliers, to obtain a measure of regularity, it is shown that LSTM and BPNN-T (Back-Propagation neural network) perform similar for regular load signals e.g. an aggregated load signal. The LSTM only starts to differentiate in performance when irregularity grows and the BPNN-T is then outperformed. Things that can be improved in [13] are practical useful forecasts of an horizon of 24 hours instead of only half an hour. Also, instead of using a rule of thumb during hyperparameter tuning, it is better to perform an hyperparameter search.

### CNN-LSTM paper

In [12] a novel technique is proposed which makes use of a convolutional neural network for which the outputs are given to a LSTM neural network and next a fully

<i>Method/Scenario</i>	<i>Avg. MAPE individual forecasts</i>	<i>Avg. MAPE Aggregating forecasts</i>	<i>Avg. MAPE forecasting the aggregate</i>
LSTM/2 time steps	<b>44.39 %</b>	<b>8.18%</b>	<b>9.14%</b>
LSTM/6 time steps	<b>44.31%</b>	<b>8.39%</b>	<b>8.95%</b>
LSTM/12 time steps	<b>44.06%</b>	<b>8.64%</b>	<b>8.58%</b>
Empirical mean	136.46%	32.54%	32.54%
MAPE minimisation	<b>46.00%</b>	34.91%	27.28%
BPNN-D/1 day	80.02%	11.69%	14.50%
BPNN-D/2 days	75.28%	11.67%	14.48%
BPNN-D/3 days	74.10%	11.66%	14.42%
BPNN-T/2 time steps	49.62%	<b>8.37%</b>	9.54%
BPNN-T/6 time steps	49.04%	<b>8.29%</b>	9.55%
BPNN-T/12 time steps	49.49%	<b>8.36%</b>	9.17%
KNN/2 time steps	74.83%	15.37%	11.23%
KNN/6 time steps	71.19%	14.61%	12.10%
KNN/12 time steps	81.13%	15.23%	15.30%
ELM/2 time steps	122.90%	33.68%	Not tested
ELM/6 time steps	136.49%	35.35%	Not tested
ELM/12 time steps	123.45%	30.05%	Not tested
IS-HF	96.76%	20.43%	32.09%

FIGURE 3.8: Different approaches tried in [13] and their performance in making 29,808 predictions.

connected neural network is used to produce the outputs. The purpose of the CNN is to extract features among several variables that affect electricity consumption and to remove the noise that comes initially together with the raw inputs. The CNN is made up out of convolution layers and pooling layers and makes use of the “ReLU” activation function. The main purpose of a convolution layer is to extract features while the pooling layer reduces the number of parameters by making use of the max pooling principle. Using the max pooling principle means taking the max value of each neuron cluster of the previous layer. As discussed in paper [13] LSTM is suitable to alleviate the problem of a vanishing or exploding gradient which characterized a vanilla RNN. LSTM is able to preserve long-term memory by making use of memory states that is used in the calculation of hidden states. It is therefore suitable to remembering the irregular trend of the electrical load serie. Finally, a fully connected time-serie predicts the load forecast.

Paper [12] showed the superiority of using the CNN-LSTM with respect to only making use of a LSTM as can be seen in Table 3.9.

The inputs that were used to forecast the consumptions of the households which are located in France are: three submeters with historical loads, global intensity, voltage,

Prediction performance with time resolution change.

Method	Resolution	MSE	RMSE	MAE	MAPE
Linear Regression	Minutely	0.4046	0.6361	0.4176	74.52
	Hourly	0.4247	0.6517	0.5022	83.74
	Daily	0.2526	0.5026	0.3915	52.69
	Weekly	0.1480	0.3847	0.3199	41.33
LSTM	Minutely	0.7480	0.8649	0.6278	51.45
	Hourly	0.5145	0.7173	0.5260	44.37
	Daily	0.2406	0.4905	0.4125	38.72
	Weekly	0.1049	0.3239	0.2438	35.78
CNN-LSTM	Minutely	<b>0.3738</b>	<b>0.6114</b>	<b>0.3493</b>	<b>34.84</b>
	Hourly	<b>0.3549</b>	<b>0.5957</b>	<b>0.3317</b>	<b>32.83</b>
	Daily	<b>0.1037</b>	<b>0.3221</b>	<b>0.2569</b>	<b>31.83</b>
	Weekly	<b>0.0952</b>	<b>0.3085</b>	<b>0.2382</b>	<b>31.84</b>

FIGURE 3.9: Comparison between LSTM and CNN-LSTM. (source: [12])

global reactive power, global active power, time, day and month. Also an analysis is performed to investigate the influence of the different inputs by calculating the average class activation score over the inputs. The results are shown in Figure 3.10. It can be seen that especially Sub metering 3 has a big influence on the final forecasts. This sub meter corresponds to the electric water heater and air conditioner of the house. Explained limitations in the paper are the setting of the hyperparameters that were set by trial and error instead of using an automated method e.g. a genetic algorithm. A further limitation is the lack of household characteristics e.g. the amount of residents living in the house. It has previously been shown by C. Beckel et al. that household occupancy is one of the primarily drivers of electrical consumption in a household. In [19] a CNN-GRU is implemented and also here it is found that the addition of the CNN works beneficial in comparison to a LSTM alone.

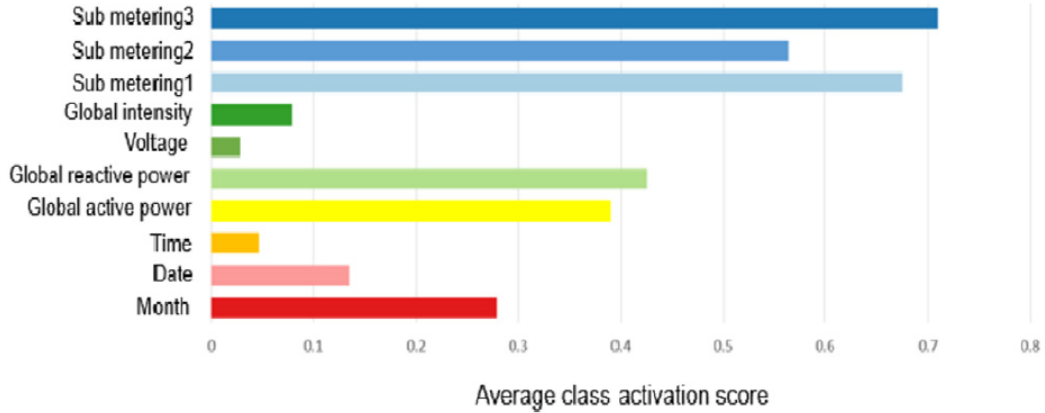


FIGURE 3.10: The importance of the different inputs based on the average class activation score. (source: [12])

### 3.3 Conclusion

In this chapter the literature study was explained that started with an introduction to neural networks. It was seen that the vanilla recurrent neural network suffered from a vanishing gradient and that this can be mitigated by using a LSTM neural network. A LSTM can longer take important aspects of the presented time series into account, which can be used during prediction. A LSTM makes use of three gates: forget gate  $\mathbf{f}_t$ , input gate  $\mathbf{i}_t$  and an output gate  $\mathbf{o}_t$ . Next, it was found that the conventional LSTM architecture couldn't be significantly outperformed by a LSTM variant e.g. GRU and it was discovered that the learning rate is one of the most important parameters to tune of the LSTM. During the literature study on short-term residential forecasting, it was found that load signals of different households can be pooled in one training set to counteract overfitting. It was seen that a deep LSTM is suitable for the task of short-term residential forecasting. Finally, it was discovered that applying a CNN on the raw data to extract features among several variables that affect electricity consumption and to remove the noise, after which the outputs are feeded to a LSTM enhances the prediction performance of the model in comparison to using LSTM alone.



# Chapter 4

## Forecasting the electricity consumption of individual households

In this chapter different forecasting techniques to perform 24 hours ahead predictions for individual household electrical consumption are discussed. The time series have a half hourly frequency, which means that 48 data points have to be estimated during each prediction of a day. The day we want to forecast is further indicated as the “desired day”. First the raw data is introduced and preprocessing steps are explained in Section 4.1. Section 4.4 presents the baseline models. These models are implemented using a straightforward approach. They serve as a benchmark for more complex models in Section 4.5 “Long Short-Term Memory” neural networks are most suitable to process time series and have therefore been chosen as the core model which is analysed with different design choices. Finally, a parameter search is conducted which consists of analysing the best parameters for optimal results.

### 4.1 Preprocessing

The available raw data is summarized by Table 2.1. Three series are selected from the file *consumption.csv* for which the important characteristics are summarized by Table 4.1. The chosen time series have the least amount of missing data and don’t contain large shifts of the mean consumption during the year. Figure 4.1 shows the electrical consumption of the three selected series. The validation set used during the parameter search consists out of the 10 last days in November. Only 10 days are selected to reduce the amount of predictions the models have to calculate. Additionally, these days don’t contain any missing values for the three series. The months January until November compose the training set and December is taken as test set.

The corresponding average temperature series are also used. They don’t contain any missing values.

#### 4. FORECASTING THE ELECTRICITY CONSUMPTION OF INDIVIDUAL HOUSEHOLDS

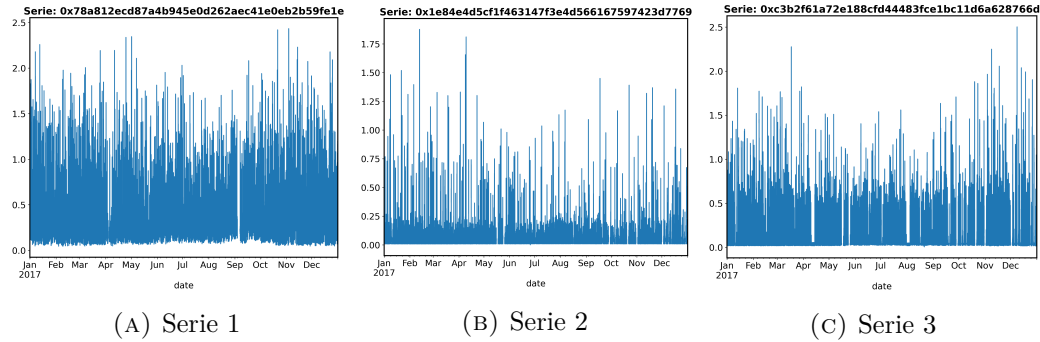


FIGURE 4.1: The electrical consumption in 2017 for the three selected series.

Characteristic	Serie 1	Serie 2	Serie 3
Mean daily consumption [kWh]	14.55	3.17	6.58
Standard deviation daily consumption [kWh]	3.21	0.99	2.57
Median daily consumption [kWh]	14.09	2.96	5.88
Maximum daily consumption [kWh]	30.08	6.60	17.15
Minimum daily consumption [kWh]	7.51	1.83	1.50
Total missing days (consumption)	4	25	26
Days in validation set (21-30 November)	10	10	10
Days in Test set (December)	31	23	23
Days in training set (Rest)	320	307	306
Mean average temperature [ $^{\circ}\text{C}$ ]	10.37	10.61	10.22
Standard deviation average temperature [ $^{\circ}\text{C}$ ]	5.09	5.20	5.01
Median average temperature [ $^{\circ}\text{C}$ ]	10.46	10.61	10.35
Maximum average temperature [ $^{\circ}\text{C}$ ]	23.99	24.51	22.95
Minimum average temperature [ $^{\circ}\text{C}$ ]	-1.07	-1.28	-1.42
Missing average temperature days	0	0	0
Amount of holidays in 2017	8	8	8

TABLE 4.1: Summarizing characteristics about the selected series.

In this chapter the series containing the electrical consumption are not aggregated as was the case in Section 2.3. Therefore, the min-max normalization is a suitable normalization method for each serie. The choice has been made to impute the missing data. A bias might be introduced by imputing the data, however it is a trade off for a larger data set. By imputing the missing values more training data is available and time jumps are avoided. As discussed earlier, missing data are always complete days. These are estimated using baseline models that will be discussed in Section 4.4 in the following order: “previous week forecast”, “previous day forecast” and “mean forecast”. When the first baseline model can’t make a prediction for the missing day i.e. the day during previous week is not available, the next baseline model is used and so on.

## 4.2 Error metrics

The metrics used to evaluate the performance of predictions are RMSE Eq. 4.1, NRMSE Eq. 4.2, MAE Eq. 4.3, MSE Eq. 4.4 and MAPE Eq. 4.5

$$RMSE = \sqrt{\frac{\sum_{t=1}^N (\hat{y}_t - y_t)^2}{N}}, \quad (4.1)$$

$$NRMSE = \frac{RMSE}{y_{max} - y_{min}}, \quad (4.2)$$

$$MAE = \frac{\sum_{t=1}^N |\hat{y}_t - y_t|}{N}, \quad (4.3)$$

$$MSE = \frac{\sum_{t=1}^N (\hat{y}_t - y_t)^2}{N}, \quad (4.4)$$

$$MAPE = \frac{\sum_{t=1}^N |\hat{y}_t - y_t| / y_t}{N}. \quad (4.5)$$

It is expected that the *MAE* penalizes outliers less severely than *MSE*, which takes the error squared. Therefore, using the *MSE* metric, more emphasis is put on predicting the peaks of the reference signal correctly with respect to *MAE*. The advantage of using RMSE and MAE is that they both have an error in kWh which is intuitive. NRMSE and MAPE take the reference signal into account. NRMSE gives a larger error, when the reference signal has a small difference between the  $y_{max}$  and  $y_{min}$ . MAPE penalizes a small MAE more severely on a small reference value than on a larger one due to the division by  $y$ .

## 4.3 Microsoft Azure cloud

The calculations executed in this chapter are performed on a virtual machine using the Microsoft Azure services. This was possible because Microsoft provides students with \$100 of free credit. Table 4.2 shows the different features of the CPU/GPU's used during this thesis.

Microsoft Azure hosts tutorials to help to transfer the calculations to the cloud. A workspace and computation cluster have to be set up before any python script can be ran. It is crucial to set up the python environment correctly on the virtual machine. This can be accomplished using a YAML file where commands are given with which packages should be installed and which channels should be used by Conda to find these packages. Conda is part of Anaconda, it is an open source package management system. It differentiates with Pip in the following points according to the Anaconda documentation:

- Conda can install packages of any language and not only Python.
- Conda makes it easy to create isolated environments containing different Python versions and packages.
- Pip installs dependencies in a serial loop while Conda fulfils all package dependencies simultaneously using a SAT-solver.

However, it is sometimes still necessary to use Pip when it is the only option to install a package. Using an isolated environment on a local machine makes it easy to transfer this environment automatically to a YAML file that is sent to the virtual machine.

Finally, it is noted that while performing the calculations a warning occurred that the TensorFlow binary was not compiled to support CPU instructions as SSE4.1 SSE4.2 AVX AVX2 AVX512F FMA. This means that the binaries in the tensorflow package are from a different machine and that the CPU used to run the calculations on this moment, is not able to use all its features. This warning was not fixed, but is given as a possible suggestion to the reader to improve calculation speeds when reusing the developed Python scripts.

#### 4.4 Baseline models

As was discussed in the introduction of the chapter, the baseline models use a straightforward approach to forecast the desired day. Therefore, they serve as a benchmark for more complex models that are explained in Section 4.5. The following baseline models are considered:

- Model 1: “1 day ago forecast”
- Model 2: “7 days ago forecast”
- Model 3: “Closest day forecast”
- Model 4: “Mean forecast”
- Model 5: “MAPE forecast”

Name	Logical cores	RAM (GB)	Storage (GB)	Cost
F4s v2 (CPU - Azure)	4	8	32	\$0.194/hour
NVIDIA Tesla K80 (GPU - Azure)	6	56	380	\$1.166/hour
i7-5500U@ 2.40 GHz (CPU - local)	4	12	32	—

TABLE 4.2: Specifications of different CPU’s and GPU used.

The models consider all the days preceding the desired day as training data. As will be seen in Section 4.5, the prediction for a day is calculated one value at a time and the total 48 values are calculated recursively. This recursively predicting does not apply to the baseline models. Here, all the 48 values are calculated at once, meaning one full day ahead. In the case of Model 5: “MAPE forecast”, the predictions are done consecutively but the values that are calculated are not used during next predictions.

#### **Model 1: “1 day ago forecast”**

This model considers the consumption values of the day preceding the desired day as the forecast for the desired day. For example, the 24 hours ahead prediction starting from Tuesday 19/12/2021 00.00 am is taken equal to the 48 consumption values that are recorded between Monday 18/12/2021 at 00:00 am and Tuesday 19/12/2021 at 00:00 am. The philosophy of the model is that the most recent consumption data serves as a good prediction. However, one can think logically and know that the most recent data is not guaranteed to behave the same. For example, as was found in Section 2.3.2 the consumption of a weekend day behaves differently than the consumption of a weekday. Therefore, violating the assumption that the most recent data is also the most adequate to use as prediction. It is expected that people have a reasonable routine and it is likely that this routine will also be present in the electricity consumption. Therefore, from a human behaviour perspective it makes more sense to use the same day of the previous week as prediction for the desired day.

#### **Model 2: “7 days ago forecast”**

This model tries to capture the human weekly routine and therefore it takes the same weekday of the previous week as the prediction for the desired day.

#### **Model 3: “Closest day forecast”**

This model looks for a past day that would be representative to serve as prediction for the desired day based on following features:

- Day of the week
- Holiday
- Average temperature

If 24 hours ahead of 19/12/2017 at 00:00 am has to be predicted, the following calendar information can be extracted from this time stamp : it is a weekday, more specifically a Tuesday and it is not a holiday. From the exogenous variable, it is known that the average temperature was 12.6°C. From the training set, which means, all the days before 19/12/2017, select all the previous Tuesdays which are not holidays, and find the day with the closest average temperature based on euclidean distance. It could be the Tuesday 10/01/2017 with an average temperature of 11.4°C for example. The consumption values of Tuesday 10/01/2017 day are chosen to serve

as prediction for the desired day, namely Tuesday 19/12/2017.

It should be noted that this method expects a good prediction of the average temperature of 19/12/2017. As can be seen in Table 4.1, no temperature values are missing for the three selected series. This table also shows that there are only 8 holidays. To increase the amount of days when the desired day is a holiday, all Sundays are considered. This is according what was found in Section 2.3.3 where Figure 2.10 shows the normalized MAE between a holiday and a Sunday is the smallest.

#### Model 4: “Mean forecast”

This model uses calendar information to group the same kind of days as was done for Model 3. For example, if the desired day is 19/12/2017, all the previous Tuesdays which are not holidays, are selected. The mean consumption of all previous Tuesdays is used as a prediction. In this model no extra Sundays are used when the desired day is a holiday.

The choice of this model is inspired by [13]. It is expected to identify frequently recurring behaviour. The model can identify trends as for example an increased consumption around 07 : 30 am and 06 : 00 pm as shown in Figure 2.7, but the performance on predicting correct peak values is expected to be lower due to the averaging of a large variation of peak sizes.

#### Model 5: “MAPE forecast”

This model solves a non-linear optimization problem for each step to be predicted. The objective function 4.6 should be minimized to obtain an estimated load  $\hat{y}$ . To obtain a 24 hour ahead prediction, 48 predictions are consecutively calculated. This model served as baseline model in [13]. The same type of days as the desired day is selected as was done in Model 3. When calculating a prediction for time  $t$  of the desired day, an empirical probability mass function is derived using all the available historic predictions of time  $t$  originating from the selected days

$$\epsilon_t(p) = \sum_{i=1}^K \zeta_t(p_i) \left| \frac{(p - p_i)}{p_i} \right|. \quad (4.6)$$

Eq. 4.6 shows the non-linear optimization with  $\epsilon_t$  the MAPE expectation for time  $t$ ,  $\zeta_t(p_i)$  an empirical probability mass function in function of the  $p_i^t$ h possible discretized consumption value and  $p$  a load value within the empirical range.  $\zeta_t(p_i)$  is calculated by making a histogram with the “Freedman-Diaconis rule” to decide the bin size. Figure B.1 shows an example of such an histogram. The amount of discretized values  $p_i$  is equal to the  $K$  bins and  $p_i$  is taken as the midpoint of two bin edges. From the count in the histogram, the value of the probability mass function for each discretized consumption value is found. The prediction value  $p$ , at time  $t$  of the desired day, is found by solving Eq. 4.7. To solve the optimization an IPOPT solver is used in a casADi software environment. A practical consideration of using this model is that the calculation load due to solving each time an optimization is higher than in the

previous models

$$\hat{y} = \operatorname{argmin}_p(\epsilon_t(p)). \quad (4.7)$$

#### 4.4.1 Results of baseline models

The performance of the baseline models on the different test sets with respect to different error metrics is given by Tables 4.3, 4.4 and 4.5. The error metrics are computed on a test set, which consists of a selected amount of days in December. More specifically, the days are selected where there are predictions available from all the different models. This is necessary because Model 1, 2 and 3 are not able to always give predictions due the presence of missing data. The models with the worst and best performance are respectively indicated with red and green.

	Closest day	1 day	7 days	mean	MAPE
Mean absolute error	0.2049	0.1954	0.1896	0.1542	0.1920
Mean squared error	0.1148	0.1090	0.1011	0.0701	0.1079
Normalized root mean squared error	0.1591	0.1550	0.1493	0.1243	0.1542
Root mean square error	0.3389	0.3302	0.3180	0.2648	0.3285
Mean absolute percentage error	0.5709	0.6163	0.5840	0.4594	0.4138

TABLE 4.3: Baseline results for Serie 1 tested on 31 days of December.

	Closest day	1 day	7 days	mean	MAPE
Mean absolute error	0.0559	0.0750	0.0693	0.0473	0.0507
Mean squared error	0.0123	0.0264	0.0188	0.0085	0.0125
Normalized root mean squared error	0.0823	0.1205	0.1017	0.0681	0.0828
Root mean square error	0.1111	0.1625	0.1373	0.0919	0.1117
Mean absolute percentage error	1.601	2.1993	2.3123	1.6657	0.7841

TABLE 4.4: Baseline results for Serie 2 tested on 12 days of December.

	Closest day	1 day	7 days	mean	MAPE
Mean absolute error	0.1267	0.1370	0.1323	0.1038	0.1130
Mean squared error	0.0824	0.0846	0.0895	0.0521	0.0743
Normalized root mean squared error	0.1453	0.1472	0.1514	0.1155	0.1380
Root mean square error	0.2871	0.2909	0.2991	0.2282	0.2726
Mean absolute percentage error	0.8609	1.3153	0.9271	0.8094	0.4792

TABLE 4.5: Baseline results for Serie 3 tested on 12 days of December.

#### 4. FORECASTING THE ELECTRICITY CONSUMPTION OF INDIVIDUAL HOUSEHOLDS

---

In the tables it can be seen that the “mean forecast” outperforms all other models on all the different error metrics except for MAPE. For all three series the “MAPE forecast”, performs best on the MAPE metric. This is a logical result because this model is optimized to reduce the MAPE. It is observed that the “closest day forecast” together with the “mean forecast” or “MAPE forecast” perform second and third best for Serie 2 and 3. “1 day ago forecast” and “7 days ago forecast” perform worst for these series. This ranking of models is not valid for Serie 1. Here, the “closest day forecast” performs overall as one of the worst models. It can thus be concluded that the performance of the models is certainly serie dependent. Because “mean forecast” performs best on all the different error metrics except MAPE and “MAPE forecast” gives the lowest MAPE, both models are included in the comparison with the more complex models of Section 4.5 in Chapter 5.

By empirical inspection it is observed that model 1, 2 and 3, who copy the consumption of another day, show more peaks in their prediction than model 4 and 5. Predictions during the test set of models 4 and 5 can be seen in Figure 4.2. A practical downside of models 1 and 2 during calculation of the predictions for the test set was that sometimes no prediction is possible due to the missing of the day one day or week ago in the reference signal.

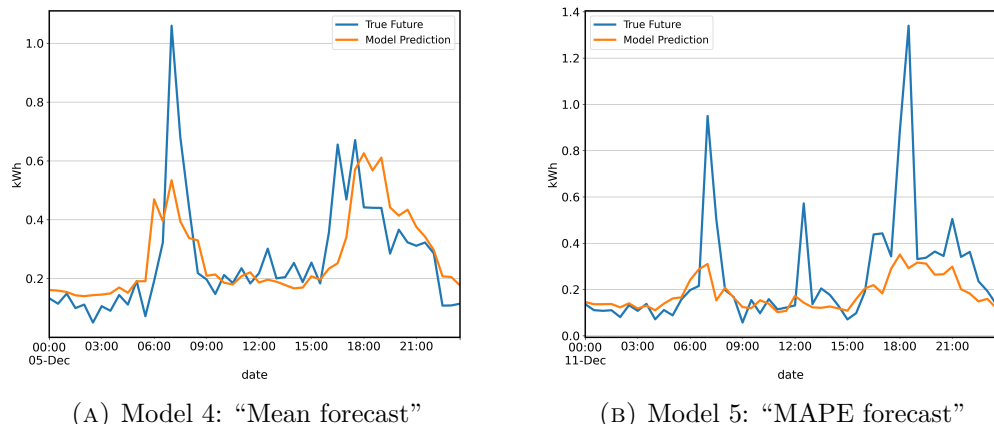


FIGURE 4.2: Daily predictions of two baseline models. (Blue: True / Orange: Prediction)

In Table 4.6 the overall performance of the baseline models on all 261 time series that contain a full year of measurements in the “consumption.csv” file, is given. The MAPE metric is not used because 99 series contain reference values of zero, which leads to a division by zero according to Eq. 4.5. Relative performance of a model on one serie is assessed by normalizing the error by division by the largest error produced by one of the models. Therefore, the error of each serie is a value between one and zero and the model that performed worst will have an error of one. Finally,

an average value is calculated over the different time series for each model. The closer the calculated value is to one, the more often this model performed worst with comparison to the other models. By applying this normalization, the NRMSE leads to the same result as RMSE. It is observed that the order of model performance based on the three metrics in Table 4.6 over all the time series is: “mean forecast”, “MAPE forecast”, “7 days ago forecast”, “1 day ago forecast” and finally “closest day forecast”. From Table 4.6 it is concluded that “mean forecast” is expected to give the best results on a randomly chosen time serie.

Error metric	Closest day	1 day	7 days	mean	MAPE
Mean absolute error	0.950	0.8298	0.8224	0.7274	0.7918
Mean squared error	0.8377	0.7771	0.7363	0.4996	0.6907
Root mean square error	0.9084	0.8621	0.8426	0.6993	0.8155

TABLE 4.6: Relative performance over all the 261 time series with a full year of measurements.

## 4.5 Implementation deep LSTM neural network

In this section deep Long short-term memory models are presented in different variations. LSTM models are specialized in time series learning as discussed in Section 3.1.4. The term “deep” refers to multiple LSTM layers that are stacked on top of each other. The goal of the developed models is to make a 24 hours ahead forecast of the electrical consumption of an individual household. The advantage of using a deep architecture is that it can learn load features hierarchically [20]. This means that load features learned in a higher layer will be the combinations of features learned in lower layers.

First, practical considerations during the implementation of the models using Keras are discussed. Keras is a neural network library in Python which can be backend by Tensorflow which is a library for a number of various tasks in machine learning. This section covers the used inputs, batch size, choice between a stateless and stateful model, initialization, measures taken to avoid overfitting and the chosen error metrics. Next, the specific LSTM models developed are explained in Section 4.5. Finally, the conducted parameter search is described in Section 4.5.5.

### 4.5.1 Practical considerations of the models in Keras

#### Inputs

The inputs to these models are normalized similarly as in [5] and [13]:

- Historic electrical consumption (min-max normalization)
- Average daily temperature (min-max normalization)

- Day of the week (one hot encoding)
- Time of the day (one hot encoding)
- Holiday (one hot encoding)

How far the model will look back into the history of electrical consumptions during a prediction, is determined by the lag value. This value corresponds to the amount of time steps that will be taken into account. The LSTM model in Keras expects a matrix  $\mathbf{X}$  as input with three dimensions: sample number, amount of time steps and amount of features. One sample of the  $\mathbf{X}$  matrix e.g.  $(1, \text{lag value}, \text{features})$ , equals a 2D matrix of dimensions  $\text{time steps} \times \text{features}$ . Every column contains a different time serie that serves as input to the model. In the first column an amount of *lag value* of previous consumption values is stored. The further down the rows of the first column, the closer time gets to the actual value that needs to be predicted. This is also the case for the temperature, but because temperature is only known on daily basis and the frequency of the values on the reference signal is one every thirty minutes, the temperature value is often the same in the second column of the 2D matrix. The values originating from the reference signal and daily average temperature serie are normalized by using a min-max normalization. Every value will now lay between zero and one.

In the next 7 columns of the 2D matrix, information is given about which day of the week it is. This is encoded using an one hot encoding. For every row one of the 7 columns which corresponds with the day of the week gets an one and the rest will be set to zero. Very similarly the information about the time of the day is indicated. There are 48 columns and for every row only one column gets an one to indicate the time of the day. Finally, this is also done to indicate if it is a holiday. In total the input matrix  $\mathbf{X}$  has 59 columns which corresponds to the amount of features. Every sample of  $\mathbf{X}$  is used for a prediction of one time step of half an hour of the desired day. To make a 24 hours ahead prediction, the total 48 values are calculated recursively. Previous predictions are used in next ones by adding them to the history of electrical consumptions. The assumption is taken that the reference signal is available until the desired day. For example, if a prediction of the electrical consumption of 19/12/2017 is desired, it is assumed that the reference signal is available till 18/12/2017 24:00.

### **Batch size**

A batch size has to be specified in the Keras fit function. The batch size determines how many samples of  $\mathbf{X}$  are feeded to the model at once and their outputs compared with their reference to define an objective function. This objective function is used to calculate the gradients for weight updates. Because every sample of  $\mathbf{X}$  outputs one prediction value, the amount of samples of  $\mathbf{X}$  correspond to the amount of predictions made.

### Stateless versus Stateful

Keras introduces a concept of stateless and stateful. As explained in Section 4.5.1 the input given to a LSTM model is a matrix with three dimensions: sample number, time steps, features. A stateless model interprets every sample of  $\mathbf{X}$  as if they have no relations with each other [6]. A stateless model is not able to see that the different samples of  $\mathbf{X}$  originate from the same time series. Therefore, the hidden and memory states are reset when a new sample of  $\mathbf{X}$  is considered during model training and prediction. When the hidden states and memory states are reset, they are again initialized to zero vectors. If there is no relation between the different samples of  $\mathbf{X}$ , it is logical to collect as many samples as possible and the input data is generated by moving a window every time one step further on the original time series as can be seen in Figure 4.3.

A stateful model doesn't reset its hidden and memory states when considering a new sample of  $\mathbf{X}$ . Because of this an additional condition is imposed to the input data that now, when all the samples of  $\mathbf{X}$  are glued behind each other, has to return the original times series sampled from. If this condition is not fulfilled, the hidden states and memory states would traverse a different serie than the original one. After one epoch during training the states are reset because the end of the original time serie has no connection with its start. During predictions, the hidden and memory states are also preserved. Therefore, seeding of the model before prediction is possible as explained in Section 4.5.4.

The advantage of using a stateful model in comparison to a stateless one, is that during training and prediction more data can be presented to the hidden and memory states before they are reset. Therefore, the capability of the LSTM of long term remembering important features of the data, is more exploited. However, a practical disadvantage of using a stateful model is that Keras expects that the batch size chosen during training, equals the one during prediction. Each prediction uses one sample of input matrix  $\mathbf{X}$  to output one prediction value. This means that the batch size during training is forced to be equal to one. It was tried to circumvent this by first training on a model with chosen batch size and then transfer the learned model weights to a new, identical model with batch size one which would be used during the prediction. However, after testing it was found that the `get_weights()` and `set_weights()` commands in Keras didn't reproduce the same prediction results. It could only be used on the same model to set the weights to the ones, a chosen amount of epochs back during training. This is useful e.g. during the manual implementation of early stopping to restore the weights that performed best. In literature it was found that setting the weights on different models is possible when using the underlying Tensorflow library, but not in Keras. In addition, a stateful model expects that the training and validation sets are divisible by the batch size. To satisfy this condition samples of the input matrix can be thrown away. As will be seen in Section 4.5.4, it was chosen to set the batch size of the developed stateful model 3 equal to one which is called "online learning" in literature. Both the previous conditions are then fulfilled.

#### 4. FORECASTING THE ELECTRICITY CONSUMPTION OF INDIVIDUAL HOUSEHOLDS

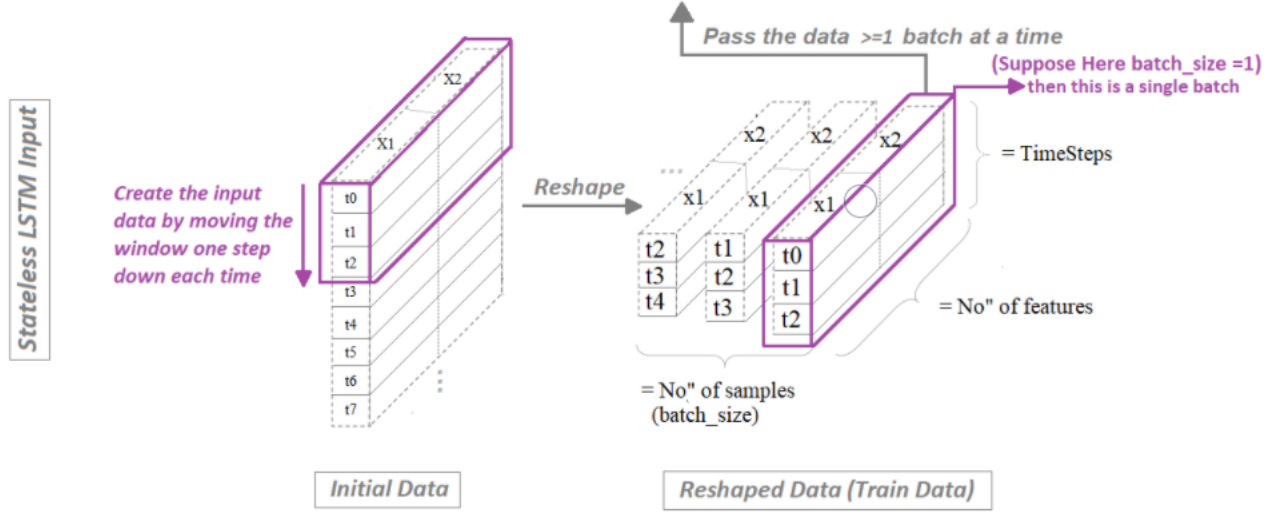


FIGURE 4.3: The generation of inputs for a stateless model (Source: [6]).

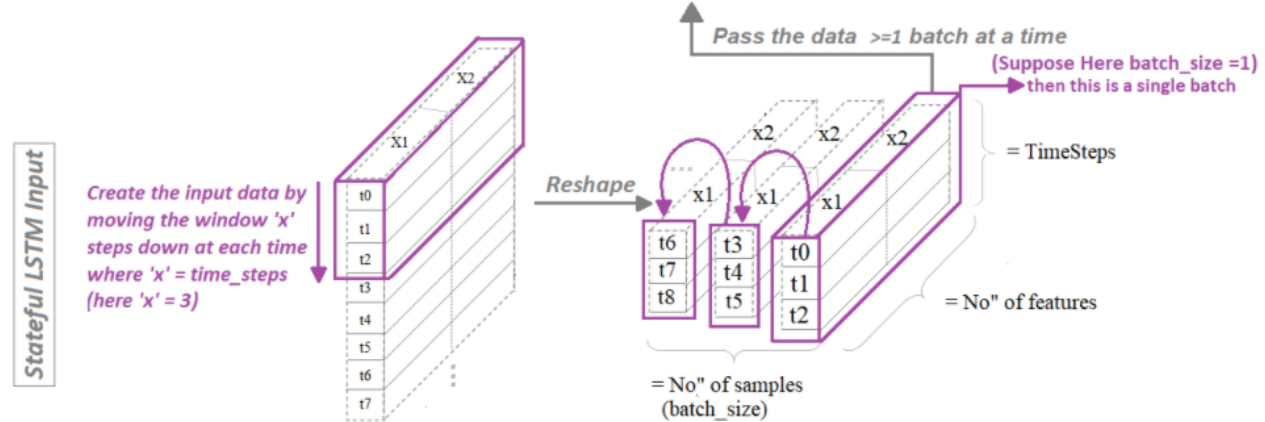


FIGURE 4.4: The generation of inputs for a stateful model (Source: [6]).

#### Initialization

The LSTM equations in Section 3.1.4 show four weight matrices  $\mathbf{W}$  with an index  $H$  and four weight matrices with an index  $X$ . These are respectively the recurrent and kernel weights and they are both initialized in a different way. A recurrent weight matrix is initialized using an orthogonal initialization and the kernel weight matrix uses a glorot uniform initialization. Both methods make use of random sampling of a distribution during the generation of the initial values. The biases  $\mathbf{b}$ , memory

states  $\mathbf{c}_t$  and hidden states  $\mathbf{H}_t$  of the LSTM equations are all initialized by arrays filled with zeros.

### Overfitting avoidance in Keras

Different ways to avoid overfitting can be applied in Keras:

- Early Stopping
- Dropout and recurrent dropout in the LSTM layer
- Dropout in the dense layers
- $l_2$  regularization on the kernel weights, recurrent weights, bias and activity.

### Error metrics

The MAE metric is used to evaluate the prediction performance on the validation set during the parameter search in Section 4.5.5. During training the MSE is used in the objective function which is used to derive weight updates.

## 4.5.2 Deep LSTM neural networks

First, the input data of the LSTM is calculated in the tailor made function *input\_output\_LSTM*. This is done before training using the GPU that is listed in Table 4.2. The inputs that are used are discussed in Section 4.5.1. Next, the models are built. Three different models are considered from which the first two are stateless models and the third is a stateful model. For the stateless models it is possible to shuffle the input data. When it is desired that before splitting the inputs of the LSTM in a training and validation set, the data is shuffled and not just the last part is taken as validation set, shuffling should be done manually before the inputs are assigned to the Keras fit function. During prediction, every model will predict one value at a time [22]. This means that 48 predictions are needed for a 24 hours ahead prediction. Each model makes use of early stopping on a validation set to avoid overfitting. The models can have multiple LSTM layers on top of each other. The hidden state vector  $\mathbf{H}_j$  serves then as input instead of  $\mathbf{X}_k$  for the layer above. The specific parameters and layout that is chosen for each of the three models is discussed in Section 4.5.5.

### Model 1: Stateless with no flatten layer

One sample of the input matrix  $\mathbf{X}$  consists of  $N$  timesteps which are fed to the LSTM layer as is shown in Figure 4.6.  $N$  equals to the chosen lag value. When the final LSTM block is reached the output of this block will be translated to a single prediction value by a conventional layer of hidden neurons (dense layer). The subseries are created by shifting the window one time step further as is explained

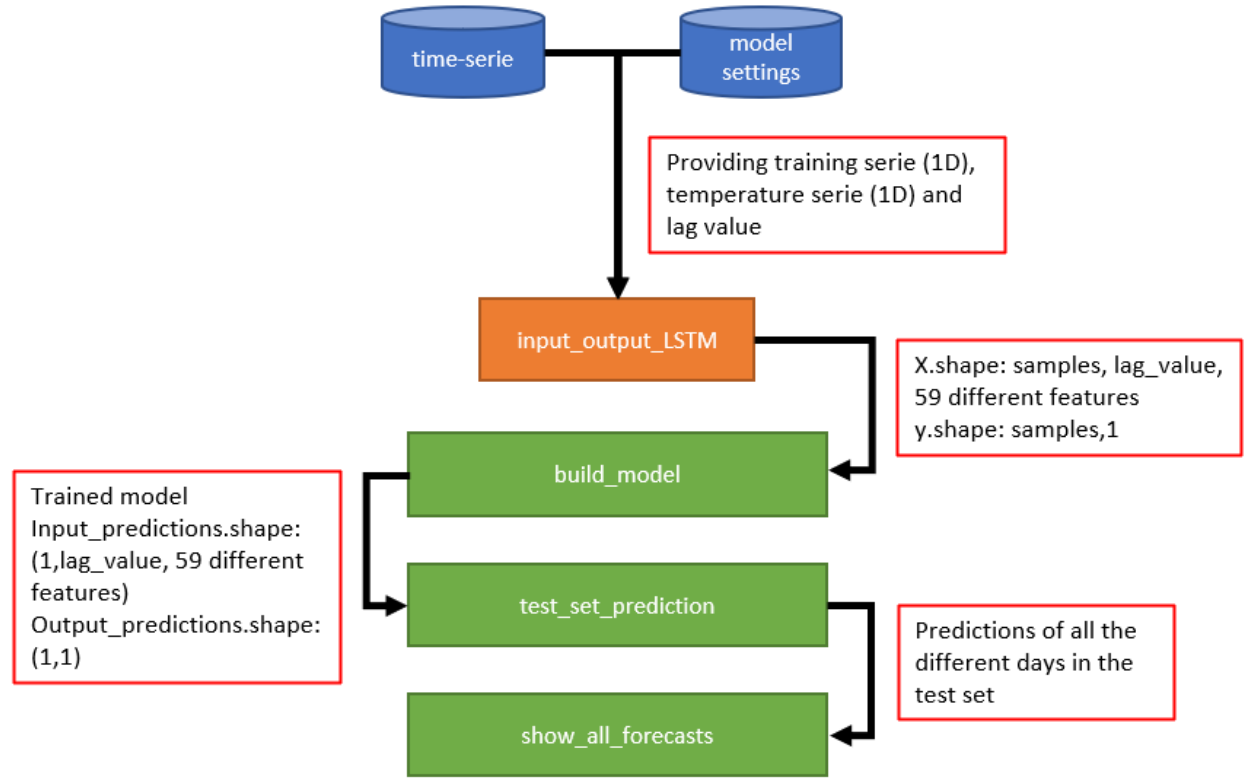


FIGURE 4.5: The flow of functions that are executed in order during the prediction process with LSTM models.

in Section 4.5.1. Because Model 1 is stateless  $C_0$  and  $H_0$  will be initialized as zero vectors. Although that Figure 4.6 gives the impression that there are multiple LSTM blocks, this only serves as a visual interpretation. There is actually only one LSTM block that is reused for every  $\mathbf{X}_k$ . This means that when the same amount of layers and hidden recurrent states are chosen, all the three models will have the same amount of trainable parameters.

#### 4.5.3 Model 2: Stateless with flatten layer

Additionally to the output of the last LSTM block also the previous outputs of the LSTM blocks are inputs to the dense layer. This model corresponds to the model depicted in [13].

#### 4.5.4 Model 3: Stateful

Where the previous two models only go through a subserie before making a prediction, this model sees the whole original time serie when making predictions. This is possible because the model looks one by one at each sample of the original time serie. For

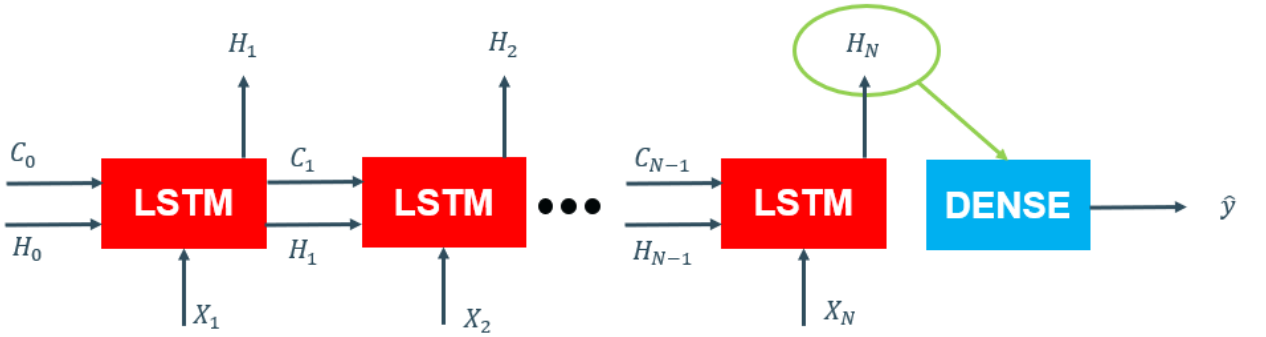


FIGURE 4.6: Model 1 - stateless model with as input a subserie of  $N$  time steps and  $C_i \in \mathbb{R}^m$ ,  $H_j \in \mathbb{R}^n$ ,  $X_k \in \mathbb{R}^{59}$ ,  $\hat{y} \in \mathbb{R}^1$ .

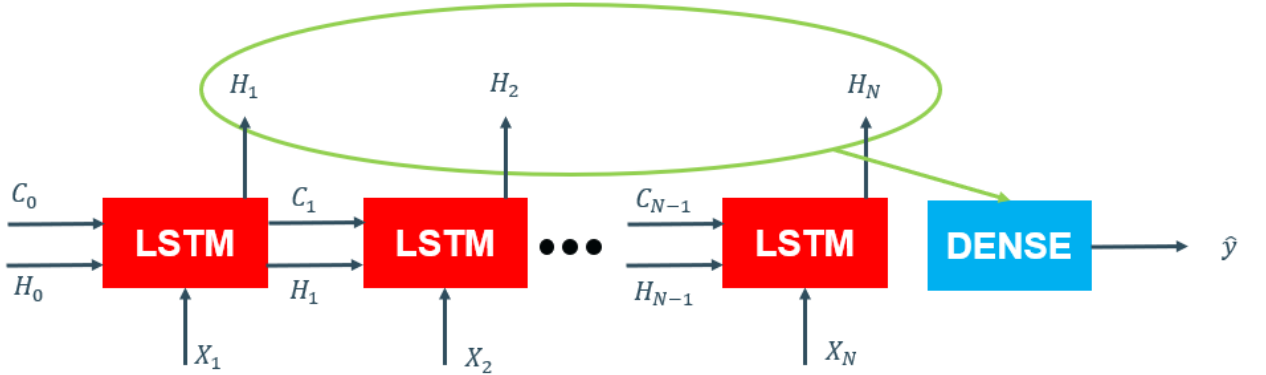


FIGURE 4.7: Model 2 - stateless model with as input a serie of  $N$  time steps and  $C_i \in \mathbb{R}^m$ ,  $H_j \in \mathbb{R}^n$ ,  $X_k \in \mathbb{R}^{59}$ ,  $\hat{y} \in \mathbb{R}^1$ .

example  $\mathbf{X}_1$  is feeded to the model and  $C_1$  and  $H_1$  come out.  $C_1$  and  $H_1$  are now again set as  $C_0$  and  $H_0$  when the next sample  $\mathbf{X}_2$  is used. This means that the model glues every subserie of one value together, which recreates the original serie. The shape of  $\mathbf{X}$  is now  $(15500, 1, 59)$  and each sample is an array. After training and before prediction of the test set or validation set, it is important that the memory states  $\mathbf{C}_i$  and hidden states  $\mathbf{H}_j$  are set “right” for prediction. Therefore, the model is first seeded, which means that all the inputs before the desired day are shown to the model. When the model then reaches the desired day, it has the chance to collect important information in the memory states and the hidden states that can be used during the prediction. During the consecutive predicting of a 24 hours ahead forecast, the model only uses previous predictions as input in comparison to Model 1 and 2, who use a serie as input of each prediction with at the end the previous predicted values.

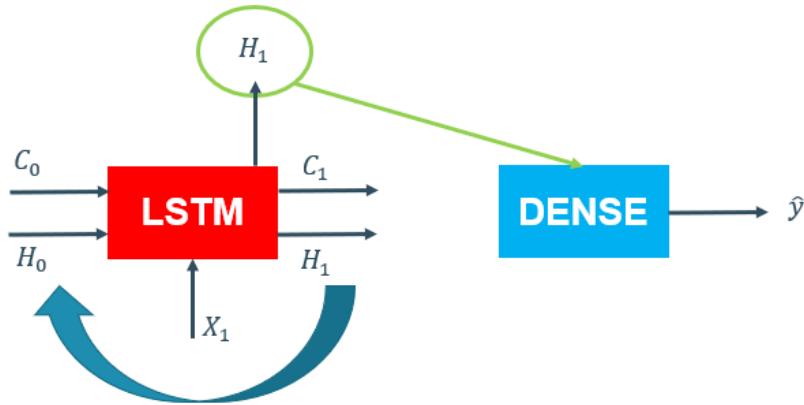


FIGURE 4.8: Model 3 - stateful model that connects single LSTM blocks and  $C_i \in \mathbb{R}^m$ ,  $H_j \in \mathbb{R}^n$ ,  $X_k \in \mathbb{R}^{59}$ ,  $\hat{y} \in \mathbb{R}^1$ .

#### 4.5.5 Parameter search

This section will show that the different LSTM models are dependent on the choice of good parameters to perform well. During a parameter search different values for the parameters are tried and the values that give the best results, are retained. Because it is not straightforward what the influence of one parameter exactly is on the model, all the different parameters are assumed to depend on each other. If all the different parameters are varied simultaneously the calculation load will rapidly blow up. To deal with this, the parameter search is conducted in three phases. The cost of this reduction in calculation load will be that dependencies between parameters are neglected. During the parameter search every combination is repeated three times to reduce the influence of the random initialization of the weights in the weight matrices. The error value that is used to decide if a combination of values behaves better or worse, is based on the MAE on the 10 last days of November, averaged over three runs. This validation set is used for all three models on all three series. Only 10 days are chosen to reduce the calculation load. An advantage of using this validation set in comparison to cross-validation, is that it can be used for all models. Cross-validation for Model 3, is not possible because it would cause interruptions in time. Inspiration for the values tried during the parameter search is found in [20].

- Phase 1: different model layouts are tried (calculation time  $\approx 10$  hours)
- Phase 2: the most complex model is chosen and regulation is added (calculation time  $\approx 6 \times 4$  hours)
- Phase 3: after comparing the previous phases, the best set of values is chosen and the learning rate is more precisely tuned (calculation time  $\approx 7$  hours)

The values tried for the different parameters are displayed in Table 4.7. A total of 24 combinations is tried during phase one and each combination is run 3 times. The

Parameter	Values
Hidden states	[20, 50]
LSTM layers	[1, 3]
Neurons dense layer	[50]
Dense layers	[1]
Lag value	[48, 96]
Number epochs	[2]
Batch size	[48]
Learning rates	[ $10^{-4}$ , $10^{-3}$ , $10^{-2}$ ]
Shuffle	[True]
Repeat	[3]

TABLE 4.7: Parameters used during phase 1 for the two stateless models.

batch size chosen is only one number to make a fair comparison between the different settings with respect to the amount of weight updates that will be performed. With a batch size of 48, there are around  $\frac{15500}{48} \approx 320$  weight updates per epoch and 640 in total. One LSTM layer is compared with three LSTM layers on top of each other in order to see a clear effect when a different amount of LSTM layers is used. Only two epochs are considered to reduce the calculation load and therefore early stopping is not used during the parameter search.

Changes to the parameters in Table 4.7 are made for model 3. In model 3 a batch size of one, a lag value of one and shuffling “False” are used. A batch size of one is chosen because then the prerequisites for a stateful model as discussed in Section 4.5.4, are fulfilled.

In phase two, the assumption is made that a more complex model is able to better capture the non-linear relations in the data and regulation is added to avoid overfitting. The values for the learning rate and lag value that were part of the lowest average MAE during phase one, are selected during phase two. Also, the amount of hidden states is taken equal to 50 and the amount of LSTM layers to 3. The regulation shown in Table 4.8, is always added one at a time. The synergy between different regularization methods is thus neglected.

Kind of regularization	Kind of dropout
regularizer on input weight matrix LSTM	dropout inputs LSTM
regularizer on recurrent weight matrix LSTM	dropout recurrent states
regularizer on DENSE layer	dropout dense layer
[ $10^{-2}$ , $10^{-3}$ , $10^{-4}$ , $10^{-5}$ ]	[0.2, 0.3, 0.4, 0.5]

TABLE 4.8: Different regularization added during phase 2.

When l2-norm regularization is added to a weight matrix, the l2-norm of the weights is added in the objective function. This means that large weight values are seen as an artificial error and the model tries to keep the weights small. The regularization parameter defines the trade off between the model focussing on reducing the error on the training set and the l2-norm of the weights. Setting a large regularization parameter will give a model that becomes less “expressive”. Therefore, the regularization parameter will contribute in the avoidance of overfitting.

The dropout layer that is used after the LSTM layer and after the dense layer sets a rate of its inputs to zero. Similar, the dropout and recurrent dropout parameters in the LSTM layer set respectively a rate of its inputs  $\mathbf{X}_k$  and  $\mathbf{H}_j$  to zero. The dropout rate values that are chosen between 0.2 and 0.5 as is advised in the original paper [21].

It was found in [7], that the learning rate is a very important parameter that has to be tuned correctly to enhance the model performance. Therefore, during phase three a range of learning rates is tried for the best model after inspection of phase one and two. The learning rate that leads to the the smallest MAE on the validation set is selected. The different learning rates that are tried are  $10^{-2}$ ,  $5 \times 10^{-3}$ ,  $2 \times 10^{-3}$ ,  $10^{-3}$ ,  $10^{-4}$  and  $10^{-5}$ . The selection of multiple learning rates of size of magnitude  $10^{-3}$ , is conform the parameter search in [20].

In order to speed up the calculations, multithreading is implemented to calculate the parameter search in parallel. For the implementation, the Python Multiprocessing library is used. It was found that one thread takes considerably longer than when the full CPU is used to calculate the same run, but still a time gain is obtained when a total of 4 runs is considered.

The importance of setting good parameters is stressed by the fact that for certain parameters the loss during training becomes “not a number”. This is because the model becomes unstable and gets a very large loss which eventually becomes a nan. When this occurs the model is tried again with different initialization of the weights, which often solves the problem. Because this increased the calculation time, for model three, nan values are also included as training errors.

### Model 1: Stateless with no flatten layer

#### Phase 1:

Table 4.9 shows phase one of the parameter search for Model 1, using the parameters listed in Table 4.7. Each value shows a percentage of improvement with respect to the worst value for one parameter for each serie during phase 1 of the parameter search. For example, when 20 hidden LSTM states  $\mathbf{H}_t$  according to the equations in Section 3.1.4 are chosen, an average improvement in MAE on the validation set of 12.08% is obtained for Serie 1 with respect to when 50 hidden LSTM states are used during all the runs of the parameter search. Because the choice of 50 hidden states gives an improvement of 0%, these values are left out.

The calculations for Model 1 were done on a local machine (see Table 4.2) for 9 hours

and 48 minutes. It is clear from Table 4.9 that when the learning rate is varied, this has the most impact on the average performance of the model for Serie 2 and 3. This result corresponds with paper [7] where it was concluded that this parameter is the most important when tuning a LSTM. Next, it can be seen that the lag value of 96 time steps didn't lead to much more improvement with respect to using a lag value of 48. A reason for this can be that the day, two days ago, is not very representative for the desired day and the hidden states and memory states of the LSTM don't collect much more valuable information to use during the prediction in comparison to a lag value of 48. It can be argued that the day a week ago would add more value, because of the human weekly routine. In comparison Model 3 traverses the whole historic signal before making predictions. It is therefore expected that the model better captures the weekly routine in the hidden states and memory states that can be used during the prediction.

An unexpected result found is that less LSTM units and only one LSTM layer in the case of Serie 1 gives raise to a lower MAE. The reason for this could be the presence of overfitting when using a too complex model. Table 4.10 gives the combination of values for the parameters that performed best during phase one. In the next phase of the parameter search, regulation is added and compared with the results in Table 4.10.

Model 1: Stateless (no flatten layer)					
Chosen parameter	Value	Serie 1	Serie 2	Serie 3	
Hidden states LSTM	20	12.08	1.24	1.48	
	50				
layers LSTM	1	9.82			
	3		4.26	5.80	
Lag value	48	4.25		0.390	
	96		2.06		
Learning rate	$10^{-2}$				
	$10^{-3}$	0.0594	17.2	10.6	
	$10^{-4}$	8.74	25.0	12.2	

TABLE 4.9: Each value in this table shows the average error when the corresponding parameter value is used, normalized by the largest error of the possible values of one parameter and finally subtracted by one. Therefore, each value shows a percentage of improvement with respect to the worst value for one parameter for each serie during phase 1 of the parameter search.

Model 1: Stateless (no flatten layer)			
Parameters	Serie 1	Serie 2	Serie 3
Hidden states LSTM	20	50	20
layers LSTM	1	3	3
Lag value	96	96	48
Learning rate	0.01	0.0001	0.0001
MAE error 1	0.133	0.0426	0.100
MAE error 2	0.135	0.0433	0.100
MAE error 3	0.138	0.0428	0.101

TABLE 4.10: The values of the parameters with the lowest average MAE on the validation set over three runs.

### Phase 2

In this section the learning rate and the lag value out Table 4.10 are combined with the most complex model with regulation. With most complex model, it is meant that 50 hidden LSTM states and 3 LSTM layers are used. A sensitivity analysis is done to look which kind of regulation has the most effect with respect to the MAE. Finally, the results of phase two are compared with Table 4.10. This approach assumes that adding regulation can nullify the use of a possible too complex model. The amount of regularization added is always the same for each of the LSTM layers. The performance is calculated as an average MAE on the 10 last days of November over three runs.

From Figure 4.9 it can be derived that:

- Serie 1: The best setting during phase one according to Table 4.10 outperformed all settings during phase two.
- Serie 2: The best setting after phase one and two is when a dropout rate of 0.2 is added on the input states of the LSTM together with 3 LSTM layers and 50 hidden states.
- Serie 3: The best setting after phase one and two is when a dropout rate of 0.4 is added on the dense layer together with 3 LSTM layers and 50 hidden states.

### Phase 3

During this phase special attention is devoted to the learning rate. As was displayed in Table 4.9 changing the learning rate could lead to significant differences in model performance. Therefore, a sensitivity analysis for the learning rate is performed on the best models after phase one and two. Figure 4.10 shows as expected a U-shape error in function of the learning rate. A learning rate that is chosen too large is vulnerable to oscillations and will not converge to a good result and a learning rate that is too small will take a very long time to attain good results and therefore

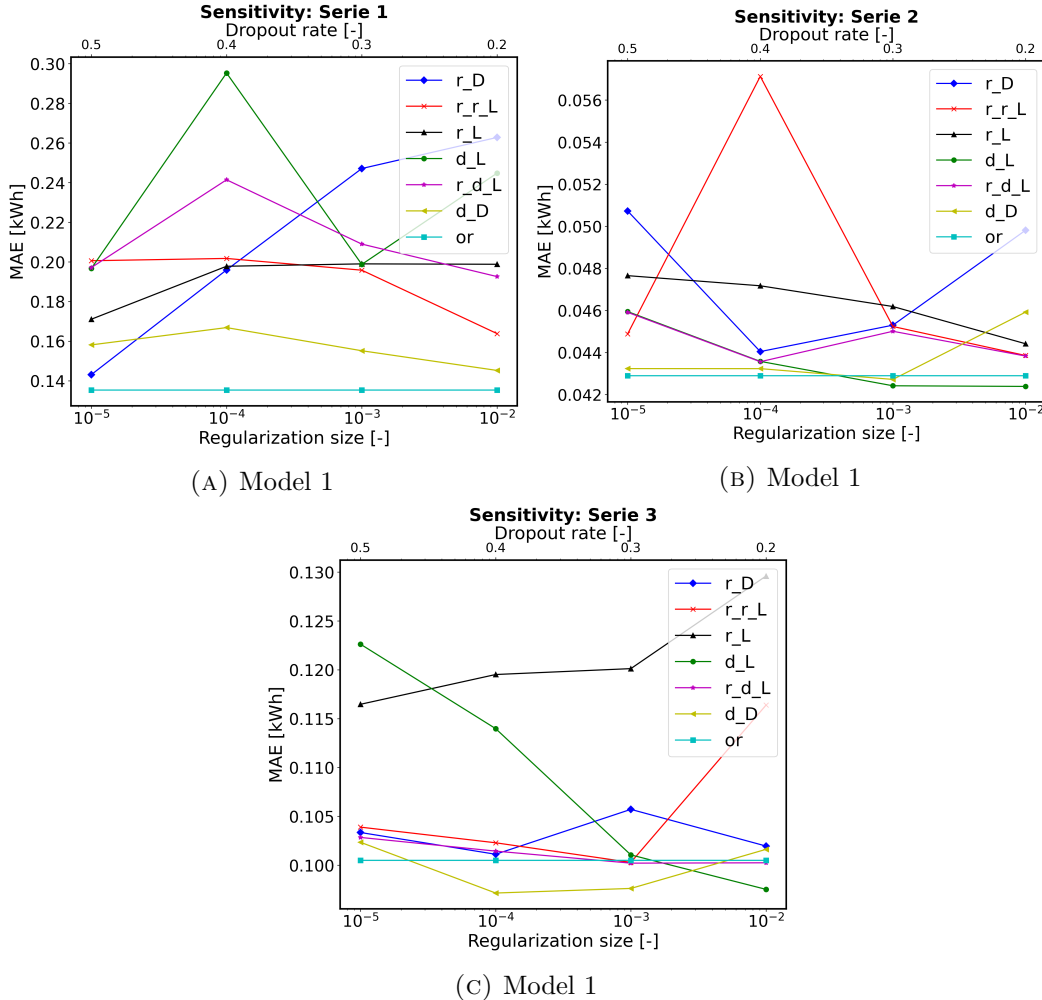


FIGURE 4.9: Results of the sensitivity analysis on the size of the regularization parameter and the dropout rate according to MAE. (Legend:  $r_D$ : regularization size of weights of DENSE layer,  $r_{r\_L}$ : regularization size of recurrent weight of LSTM,  $r_L$ : regularization size of input weights of LSTM,  $d_L$ : dropout rate of inputs LSTM,  $r_{d\_L}$ : dropout rate of hidden states LSTM,  $d_D$ : dropout rate of DENSE layer,  $or$ : best performing serie from phase one)

has an increased error when compared on a fixed amount of epochs. The resulting U-shape corresponds to what is found in [7]. The same workflow to conduct the parameter search will be followed for Model 2 and 3.

### Final model

The final parameters for model one are displayed in Table 4.11.

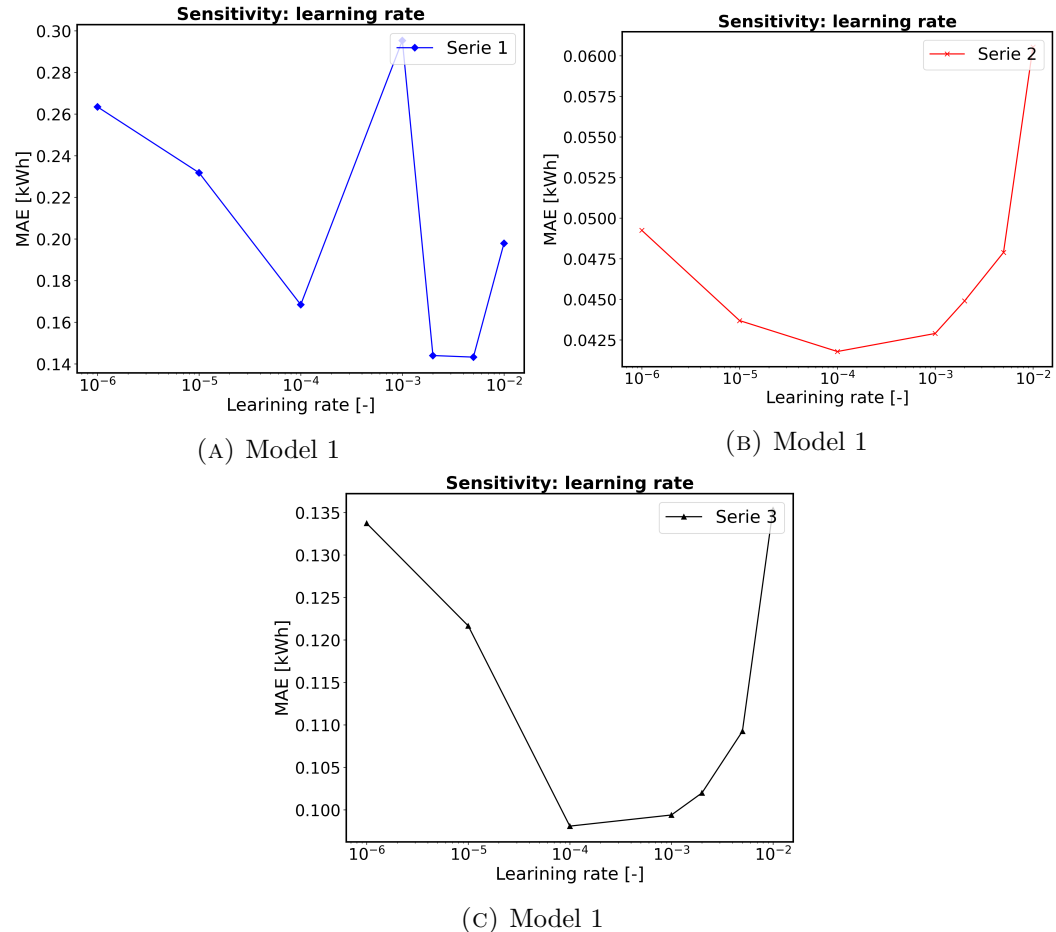


FIGURE 4.10: The MAE on the validation set in function of the learning rate size.

Model 1: Stateless (no flatten layer)			
Parameters	Serie 1	Serie 2	Serie 3
Hidden states LSTM	20	50	50
layers LSTM	1	3	3
Lag value	96	96	48
Learning rate	0.005	0.0001	0.0001
Dropout inputs LSTM	0	0.2	0
Dropout DENSE	0	0	0.4

TABLE 4.11: Final values found after the parameter search for model 1.

### Model 2: Stateless with flatten layer

#### Phase 1

From Table B.1 it can again be seen that the choice of learning rate has the potential

to give a large improvement and the use of an increased lag value of 96 didn't give a major improvement.

### Phase 2

From Figure B.2 it follows that:

- Serie 1: The best setting after phase one and two is found when a regularization parameter on the input weight matrices is added of  $10^{-5}$  together with 3 LSTM layers and 50 hidden states.
- Serie 2: The best setting after phase one and two is found when a regularization parameter on the input weight matrices is added of  $10^{-3}$  together with 3 LSTM layers and 50 hidden states.
- Serie 3: The best setting after phase one and two is when a dropout rate of 0.4 is added on the dense layer together with 3 LSTM layers and 50 hidden states.

### Phase 3

Figure B.3 shows the sensitivity of the size of the learning rate in function of the MAE. Again an U-shape is observed.

### Final model

The final parameters for Model 2 are displayed in Table 4.12.

Model 2: Stateless (no flatten layer)			
Parameters	Serie 1	Serie 2	Serie 3
Hidden states LSTM	50	50	50
layers LSTM	3	3	3
Lag value	96	48	96
Learning rate	0.002	$10^{-5}$	0.0001
Regularization on input weight matrices LSTM	$10^{-5}$	$10^{-3}$	0
Dropout DENSE	0	0	0.4

TABLE 4.12: Final values found after the parameter search for model 2.

**Model 3: Stateful model**

The model is trained by making use of a batch size of one, which means that the weights are updated by comparing each output immediately with its reference. Because this model is stateful, it is first seeded before predictions are done.

**Phase: 1**

As discussed in the beginning of Section 4.5.5, the values used during phase one of Model 3 differ from the ones in Table 4.7. As can be seen in Figure B.3 the learning rate is still an important parameter to tune. Table B.4 shows the values that give the best results after phase one.

**Phase: 2**

From Figure B.4 it follows that:

- Serie 1: The best setting during phase one as shown in Table B.4, outperformed all settings during phase two.
- Serie 2: The best setting after phase one and two is found when a regularization parameter on the hidden state weight matrices is added of  $10^{-3}$  together with 3 LSTM layers and 50 hidden states.
- Serie 3: The best setting during phase one as shown in Table B.4 outperformed all settings during phase two.

It was seen that the model, when three layers are used together with 50 hidden recurrent states, often produced a very large loss during training. If this is the case, the output of the training loss becomes not a number. Only when a regularization parameter on the hidden state weight matrices or on the input weight matrices is added the obtained performance was better. The results of the two regularizers are shown in Figure B.4.

For Serie 1 and 3 no improvement with respect to the best results of phase one was found. It is not necessarily the case that the addition of regularization parameters or dropout layers is the only cause of this bad behaviour. As could be seen in Tables B.3 and B.4 one layer performed often better than three layers, which could also contribute to the worst results obtained during phase two. Only for serie 2 the best result of phase one is outperformed.

**Phase: 3**

Figure B.5 shows the sensitivity of the size of the learning rate in function of the MAE. An U-shape is observed for Serie 1 and 3. To find a U-shape for Serie 2, even smaller learning rates have to be considered.

**Final model**

The final parameters for Model 3 are displayed in Table 4.13.

Model 3: Stateful			
Parameters	Serie 1	Serie 2	Serie 3
Hidden states LSTM	50	50	20
layers LSTM	1	3	1
Lag value	1	1	1
Learning rate	$10^{-4}$	$10^{-6}$	$10^{-4}$
Regularization on hidden states weigh matrices LSTM	0	$10^{-3}$	0

TABLE 4.13: Final values found after the parameter search for model 3.

## 4.6 Conclusion

This chapter discussed the data to conduct the electricity consumption forecast on and which models were used. First, the baseline models were discussed. It was found that the mean forecast performed best for the error metrics: MAE, MSE, NRMSE and RMSE. “MAPE forecast” performed best when the MAPE error metric was used. Both models predict the trend line and don’t predict peaks in contrary to the closest day, 1 day and 7 days models. Next, the LSTM models that were developed were discussed. This included the practical considerations of the implementation of the LSTM models in Keras and a parameter search. The parameter search was done in three phases in order to reduce calculation load. It was found that the learning rate was the parameter that contributed often the most to the model performance.



# Chapter 5

## Model evaluation

This chapter discusses the performance of the models that were introduced in Chapter 4 on the test set. As was shown in Table 4.1, the test set consists out of the days of the month December. The goal of the test set is to assess the model performance on new data and it is therefore important that the models are not trained and their parameters are not tuned using this data. Missing days in the test set are removed to avoid the influence of the estimation error of the reference signal on the model performance. In this chapter first the model selection is explained after which a discussion of the performance on the test set follows.

### 5.1 Model selection

In Chapter 4 the model parameters are tuned, but there is still a factor of random model performance due to the random initialization of the weight matrices. To reduce this influence, the model is trained 10 times and the model that performed best on a validation set using the *MAE* metric is selected. As validation set the 10 last days of November are used. Also, during training early stopping is applied wherefore an additional 10% of the training data is taken to serve as a second validation set. For a stateless model this 10% is randomly taken from the remaining training data. For a stateful model this 10% originates from the end of the training data. The patience parameter is taken as 5, which means that the validation error can increase 5 times before the model is stopped. The maximum amount of epochs that is allowed is set to 150. The parameter values obtained after tuning for the three time series can be found in Chapter 4. Table 5.1 summarizes the amount of epochs that the selected model ran. There can be a large difference in the amount of training epoch and Table 5.1 shows that Serie 2 needs often a lot of epochs. Although, it was found that for both Model 2 and 3 there is not much improvement anymore on the training and validation sets after respectively epoch 60 and epoch 20 as shown in Figure 5.1. Model 3 takes longer to predict than the other two models due to the additional seeding that is required.

## 5. MODEL EVALUATION

---

	<b>Model 1</b>	<b>Model 2</b>	<b>Model 3</b>
<b>Serie 1</b>	5	16	5
<b>Serie 2</b>	7	150	150
<b>Serie 3</b>	19	11	6

TABLE 5.1: The amount of training epochs for each selected model.

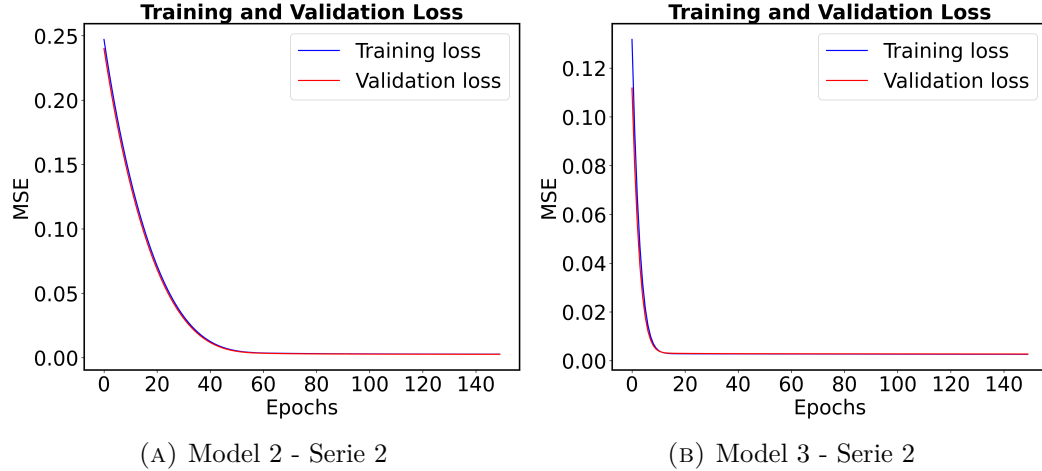


FIGURE 5.1: The evolution of the MSE on the training and validation sets.

## 5.2 Performance on the test set

In this section the results on the test set are discussed for the models that were selected in section 5.1. Also, the two best baseline models “mean forecast” and “MAPE forecast”, that were explained in Section 4.4, are included in the comparison. An advantage that the baseline models have in comparison to the LSTM neural networks is that they use the previous data till the day to forecast to make predictions while the LSTM neural networks only trains on data till November. (Seeding not taken into account) This is because it needs data for the validation set to tune parameters and implement early stopping.

The baseline models and the LSTM neural networks both belong to a different group of models, respectively to the lazy models and eager models. A lazy model only looks at the data when the query is known i.e. what day to forecast. For example a “mean forecast” looks after it knows which day to forecast to the same weekdays and takes the average. In comparison an eager model already makes generalizations on a training set before it knows which day it has to predict. This applies to the LSTM models.

Model 1 and Model 2 make use of a lag value of 48 or 96 and no seeding. When the day after a missing day(s) is predicted the inputs used during prediction could

## 5.2. Performance on the test set

---

originate entirely from an estimated reference signal for the missing day(s). If this is the case, it is expected that the error on the desired day will be larger. The estimation of the reference signal is done by substituting the missing values as described in Section 4.1. For both Serie 1 and Serie 2 there are 8 missing days in the test set.

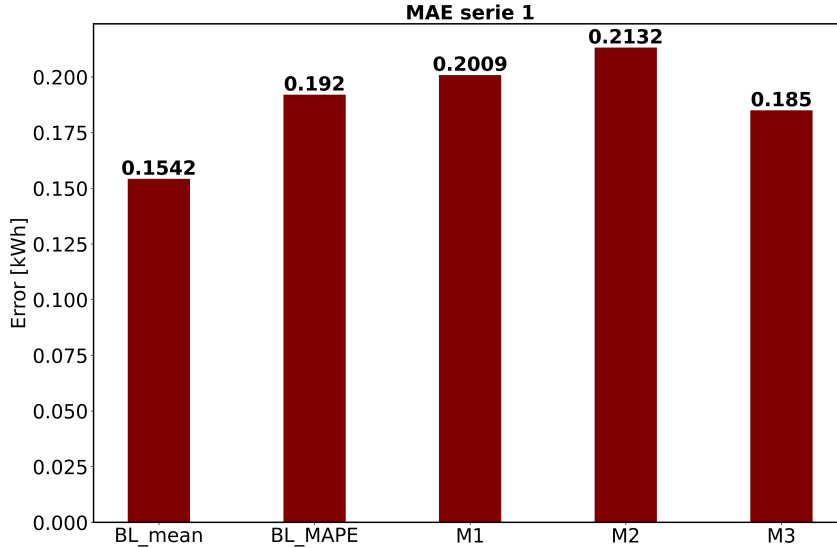


FIGURE 5.2: The MAE performance on all the days of the test set for Serie 1.

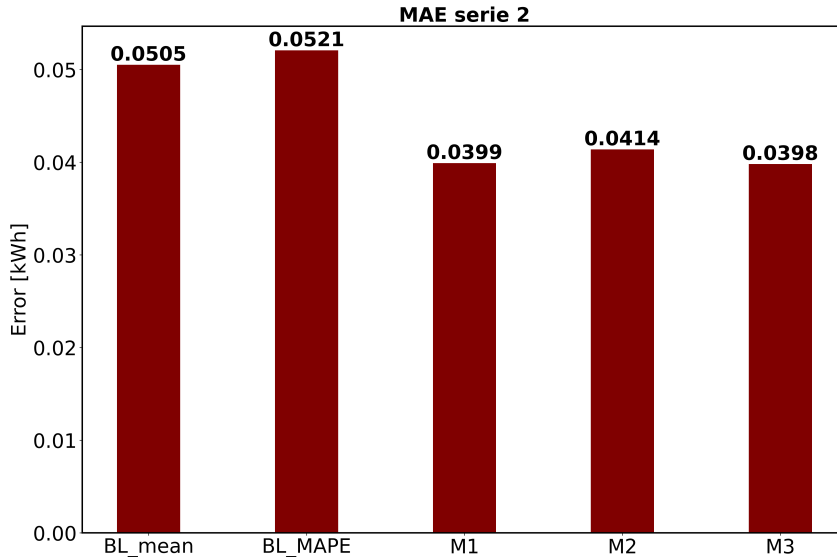


FIGURE 5.3: The MAE performance on all the days of the test set for Serie 2.

Figures 5.2, 5.3 and 5.4 give a comparison of the three LSTM models and the two baseline models. It can be seen that there is a reduction of the MAE for Series 2 and 3 for all the LSTM models and for Serie 1, Model 3 attains a smaller error than

## 5. MODEL EVALUATION

---

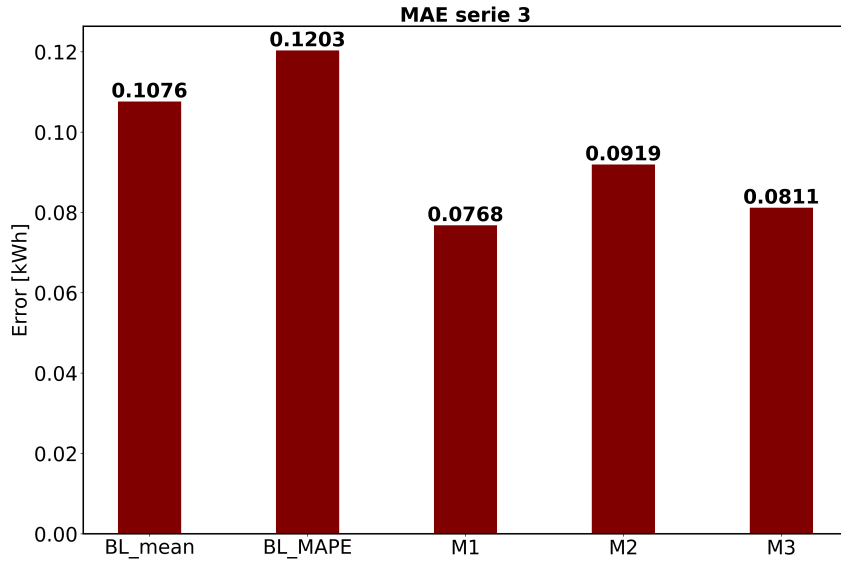


FIGURE 5.4: The MAE performance on all the days of the test set for Serie 3.

the “MAPE forecast” model. Also, it can be noticed that Model 2 for all the three series behaves slightly worse than the other two LSTM models. It is clear that the performance of the models is serie dependent.

To get more insight in how the MAE error is distributed over the test set, it is calculated for each individual day and displayed in Figures C.1, C.2 and C.3 in Appendix C. Figures C.2 and C.3 are discontinuous due to the missing days that are present in the reference signal in the month December. When the reference values of a day are not known, the day is removed from the test set to remove an additional estimation error of the reference signal during the calculation of the MAE. This is also the case for the calculation of the MAE in Figures 5.2, 5.3 and 5.4.

Next, it is noted that the MAPE for the LSTM models is much higher than for the baseline models as is shown in Table 5.2. As displayed in Figure 5.5 this is due to an overestimation of the reference signal when the values are small.

	Mean forecast	MAPE forecast	Model 1	Model 2	Model 3
Serie 1	0.46	0.41	3.07	3.37	3.27
Serie 2	1.82	0.83	3.67	3.64	3.65
Serie 3	0.80	0.48	3.30	3.44	3.21

TABLE 5.2: The MAPE for each Model and serie.

To get better insight in the actual output of the different models, Figure 5.5 shows the prediction of the different models on a chosen day in the test set.

First, it is again stressed that the “mean squared error” is chosen as metric during training of the LSTM models. Because of this, the LSTM models are more pushed towards learning the peaks of the reference signal due to the squared error. It can be seen that on the 7<sup>th</sup> of December, the peaks of Serie 1 and Serie 3 are present in the predicted signal. It was found that especially for Serie 1, the LSTM models are predicting a higher consumption than the reference signal. The shape of the reference and prediction signals are similar, but there is an offset between the two signals. A reason for the shift could be that the LSTM models are trained using the MSE metric. It is found in literature that when a least square fitting is performed on data points the curve that is fitted can be much disturbed by the presence of outliers. The disturbance resulted also in a shift of the fitted curve. Because during training the MSE is used, the peaks during the day also act as outliers that could be responsible for the model shift. A solution to solve this is to get rid of the squared error and punish more proportional by using the MAE metric instead. On the other hand it can be argued that it is better to predict a higher consumption than one that is too low, because it is better to anticipate to a worse scenario than expected.

The reader is reminded that there is no regulation added for Model 1: Serie 1 and Model 3: Serie 1 and 3. When regularization is added this is clearly visible in Figure 5.5 because without regulation the predicted signal is much more choppy. A clear example can be seen for Model 2 and 3 in serie 3. These two models both show a small bump in the predicted signal before the larger peak. Model 2 where a form of regularization is added shows a very smooth bump while in Model 3 without regularization, the bump is much more choppy.

It can be seen that the “mean forecast” is able to identify the two peaks in Serie 1 and the large peak in Serie 3, but as is expected from a mean, this peak is smaller due to averaging. The “mean forecast” method however suffers less from the offset than the LSTM models in Serie 1.

As expected the “MAPE forecast” will focus on correctly predicting the low values in the reference signal because these will get in the denominator of the MAPE metric according to Eq. 4.5. It can be seen that the peaks will be ignored when this method is applied.

### 5.3 Conclusion

In this chapter the performance of the developed models is assessed. Firstly, the model selection was discussed and it was explained that the models obtained after the parameter search are ran ten times with different initialized weight matrices. The one that performed best on the validation was selected. The number of epochs that the models trained was low, except for model 2 and 3 on Serie 2.

## 5. MODEL EVALUATION

---

Secondly, the performance on the test set is discussed for the LSTM models and two baseline models using bar plots that displayed the MAE on the test set for each serie. It was concluded that there is a reduction for all the three LSTM models in comparison to both the baseline models for Serie 2 and 3. Also, Model 2 always performed worse based on MAE than the other LSTM models and it can be concluded that the flattening layer didn't have much effect.

7 December is chosen for which all the predicted signals are grouped for the different models. From this figure is was clear that the LSTM models are able to identify peaks of the reference signal and they have the same overall shape. Predicting the peaks correctly is an important, practical feature e.g. to anticipate electrical peak consumption demands. It was also noticed that the predictions are often an overestimation of the reference signal. Especially for Serie 1, the shape of the reference and prediction signals are similar, but there is an offset between the two signals. The offset could possibly be reduced with another choice of error metric during training. However, it can be a serie dependent effect due to the fact that only for Serie 1 there is a large offset at the start. It can be argued that in practice it is better to overestimate, than underestimate. Because of the overestimation on small values, it was found that the MAPE of the three LSTM neural networks performed worse than the baseline models. Also, the influence of adding regularization could be seen which leads to more smooth signals.

The “mean forecast” baseline model was not able to predict the peaks in the reference signal as good as the LSTM models, but it has a lower offset error in Serie 1. The “MAPE forecast” is focussed on predicting all the small values correct to minimize the MAPE, but ignores all the peaks of the reference signal.

### 5.3. Conclusion

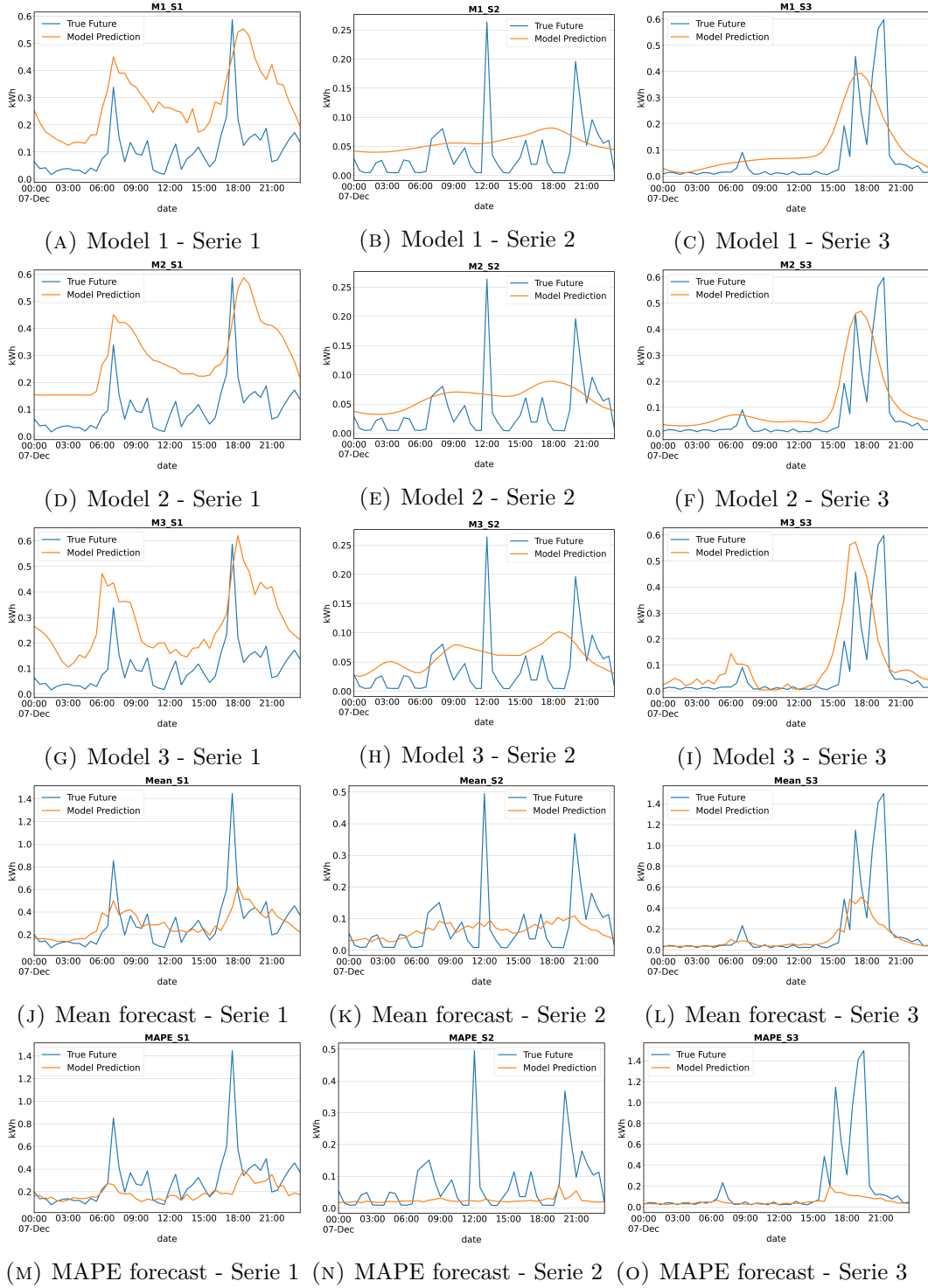


FIGURE 5.5: The prediction results of the different models on 7th December. (True values: blue/ Prediction: orange)



# Chapter 6

## Conclusion

This master thesis focussed on the implementation of deep LSTM neural networks to make 24 hours ahead predictions of the electrical consumption of individual households. The task of forecasting the electricity consumption of an individual household was seen to be of a significant complexity due to the high uncertainty and volatility in the load signal. This is because the load signal is directly influenced by the decisions made by the residents. The main contribution made with this thesis is showing that by only using the past electrical consumption behaviour, daily average temperature values and calendar data, it is possible with LSTM neural networks to outperform baseline models on 24 hours ahead forecasting, learn a non-linear relation between the inputs and amount of electrical consumption and predict peaks. This work aimed at implementing different versions of the LSTM neural network and to compare and investigate them.

The first part of this research elaborated the exploratory data analysis. It started with the description of the used dataset that originates from the IEEE-CIS technical challenge on energy prediction from smart data. Preprocessing on the series with a full year of measurements is carried out. Two methods to impute missing data are compared and it was found that the Average Neighbours methods was more suitable for estimating the missing data than the Mean method available in the Scikit-learn library. Further, consumption series with zero days and shifts in the rolling mean were identified and normalization was done using the total yearly consumption. Next followed a data analysis on an aggregated load signal. Seasonality was investigated and it could be seen that the daily consumption profile showed a morning peak (07:30 am), an evening peak (06:00 pm) and a peak after midnight due to the use of heat storage systems. The consumption profiles of weekdays and weekend days are compared and it is observed that the morning peak is higher for a weekend day and decreases less. The influence of bank holidays is investigated and it was learned that a bank holiday behaves most similar to a Sunday. Also, there was a negative correlation between the temperature and the amount of electrical consumption. Finally, different household attributes were examined and it was seen that the order of dwelling types that are expected to consume more electricity is: Flat < Bungalow < Semi detached

## 6. CONCLUSION

---

< Terraced < Detached. When there are more bedrooms in an housing unit, the consumption is also expected to be higher.

In Chapter 3 the conducted literature study is elaborated. First an introduction was given to neural networks and it was discussed that a vanishing gradient and overfitting are challenges for the vanilla recurrent neural network. A LSTM neural network can be used to mitigate the effect of a vanishing gradient and early stopping, adding the l2-norm of the weights in the objective function and dropout layers can be applied to mitigate overfitting. Next, it is discovered that the learning rate is a very important parameter to tune in a LSTM and different variants of a LSTM e.g. GRU can't significantly outperform the conventional LSTM architecture. The second part of the literature study discussed the state of the art short-term residential electrical load forecasting. First a pooling method was introduced that combined the load signals of neighbouring households in a pool of training data. Making use of pooling reduced the effect of overfitting. It was concluded that a deep LSTM is the most suitable model for short-term residential load forecasting with respect to ARIMA and SVR, and more LSTM layers can be beneficial. Further, a CNN on the raw data can extract features among several variables that effect electricity consumption and remove noise that comes initially together with the raw inputs. The use of a CNN-LSTM gave improved results with respect to a LSTM alone. Finally, it was found that especially an electric water heater and air conditioner had a big influence on the electrical consumption.

In Chapter 4, the development of baseline models and the LSTM neural networks is explained for the three consumption series with the least amount of missing data. The baseline model performing best on all error metrics except MAPE was the “mean forecast” and the baseline model performing best on the MAPE metric was the “MAPE forecast”. Both baseline models predict the trend line and don't accurately forecast peaks. Next, the three implemented LSTM models were discussed. Two of the three LSTM models developed were stateless with Model 2 having an additional flattening layer in comparison to Model 1. Model 3 is a stateful model, which makes use of seeding before it makes predictions. A parameter search is conducted where tuning the learning rate often contributed most to model performance.

In Chapter 5, the models that were retrieved were evaluated on a test set consisting out of 30 days. The three LSTM models outperformed both the baseline models for Serie 2 and 3 based on the MAE metric. The flattening layer didn't lead to much improvement because the second model always performed slightly worse than Model 1 and 3 based on the MAE. All three LSTM models are able to predict peaks with a higher precision than the baseline models. The predictions of the LSTM neural networks are often an overestimation of the reference signal. Especially for Serie 1, the shape of the reference and prediction signals are similar, but there is an large offset between the two signals at the start. The offset could possibly be reduced with another choice of error metric during training. However, it can be a serie dependent effect because the large offset at the start only occurred for Serie

---

1. Because of the overestimation on small values, it was found that the MAPE of the LSTM neural networks was worse than the baseline models. It can be argued that in practice it is better to overestimate, than underestimate. Also, the influence of adding regularization could be seen which leads to more smooth signals. The “mean forecast” baseline model was not able to predict the peaks in the reference signal as good as the LSTM models, but it has a lower offset error in Serie 1. The “MAPE forecast” is focussed on predicting all the small consumption values correct to minimize the MAPE, but ignores all the peaks of the reference signal.

The practical usefulness of the LSTM neural networks is the ability to better monitor the demand side of the low voltage grid. Scheduling of maintenance work on the grid can be optimized, which needs detailed forecasting of the consumption series of only a small amount of households. Expenses can be saved by implementing customized updates to the network. Individual household predictions can be used as part of a congestion prediction, which means predicting when the low voltage grid can't handle the demand anymore. Especially, predicting the peaks in the household electrical consumption is in that case important. If an accurate congestion prediction can be made, reliability of the network can be increased and the risk for blackouts and brownouts is decreased. Because the thesis is developed together with the STADIUS Research Group at the KU Leuven, it is in line with their research and it can be used to build further on.

In this last paragraph, suggestions for future work is made. In Chapter 4 a parameter search is conducted where parameter values are manually chosen. In order to use an automated approach, which can lead to better results, a genetic algorithm can be developed with as objective function the performance of the candidate model on a validation set. Also, a more extensive, manual parameter search, where the synergy between different parameters is not neglected as was the case in Section 4.5.5, can be tried. The LSTM neural network is a black box model and it is not immediately clear which inputs contribute most to good results. Research can be conducted to find which inputs contribute most to the results of the model. The effect of pooling neighbouring households as was described in [20] can be investigated. When spatial information about the households is absent, clustering could be done based on the exogenous variables e.g. temperature together with the assumption that two households with similar exogenous series are located close to each other. The final suggestion of future work is the use of a CNN-LSTM as discussed in Chapter 3, where a CNN is used to remove noise from the inputs and extract features from the raw data that serve as inputs to a LSTM.



# **Appendices**



## Appendix A

# Different household attributes

Attribute	Filled places
Dwelling type (5 cat.)	1702
# Occupants (max 4)	74
# Bedrooms (max 5)	1859
Heating fuel (4 cat.)	78
Hot water fuel (3 cat.)	76
Boiler age (2 cat.)	74
Loft insulation (2 cat.)	75
Wall insulation (5 cat.)	75
Heating temperature (4 cat.)	74
Efficient lighting percentage (4 cat.)	73
Dishwasher (0,1,2)	76
Freezer (0,1,2)	70
Fridge freezer (0,1,2)	70
Refrigerator (0,1,2)	73
Tumble Dryer (0,1,2)	76
Washing machine (0,1,2)	76
Game console (0,1,2,3)	72
Laptop (0,1,2,3,4)	70
Pc (0,1,2,3)	70
Router (0,1,2)	69
Set top box (0,1,2,3)	70
Tablet (0,1,2,3,4)	70
Tv (0,1,2,3,4)	75

TABLE A.1: Amount of response on the voluntary questionnaires.



## Appendix B

# Forecasting the electricity consumption of individual households - extra

In this appendix extra information and Figures are added that are not necessary to understand the work discussed in Chapter 4.

### B.1 Baseline models

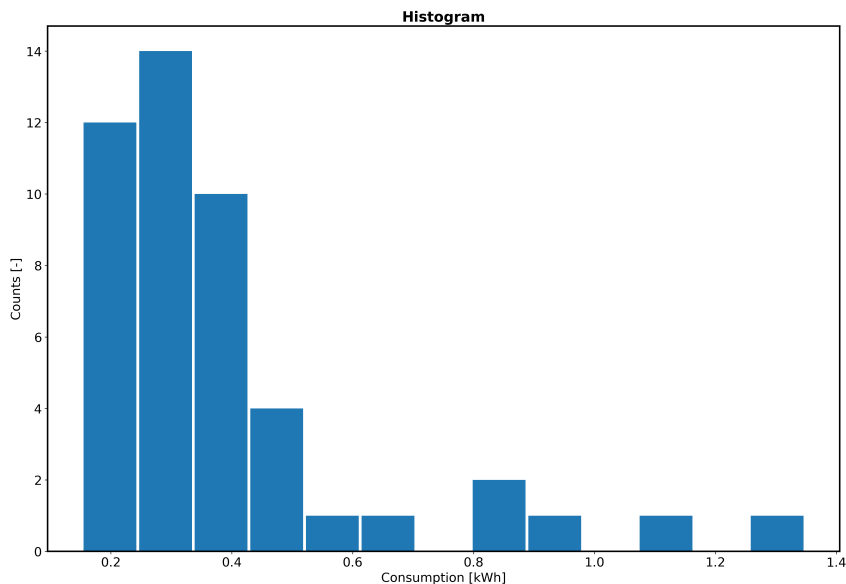


FIGURE B.1: An example histogram of the consumption in [kWh] versus count [-] used during MAPE forecast.

## B.2 Parameter Search

### B.2.1 Model 2

Model 2: Stateless (flatten layer)					
Chosen parameter	Value	Serie 1	Serie 2	Serie 3	
Hidden states LSTM	20	0.446	0.0622		
	50			0.319	
layers LSTM	1				
	3	21.3	10.60	9.98	
Lag value	48	7.51	2.84		
	96			1.76	
Learning rate	$10^{-2}$				
	$10^{-3}$	23.4	2.51	13.2	
	$10^{-4}$	43.0	12.8	17.9	

TABLE B.1: Each value in this table shows the average error when the corresponding parameter value is used, normalized by the largest error of the possible values of one parameter and finally subtracted by one. Therefore, each value shows a percentage of improvement with respect to the worst value for one parameter for each serie during phase 1 of the parameter search.

Model 2: Stateless (flatten layer)			
Parameters	Serie 1	Serie 2	Serie 3
Hidden states LSTM	20	50	50
layers LSTM	3	3	3
Lag value	96	48	96
Learning rate	0.001	0.0001	0.001
MAE error 1	0.137	0.0426	0.0973
MAE error 2	0.139	0.0430	0.107
MAE error 3	0.136	0.0424	0.100

TABLE B.2: The values of the parameters with the lowest average MAE on the validation set over three runs.

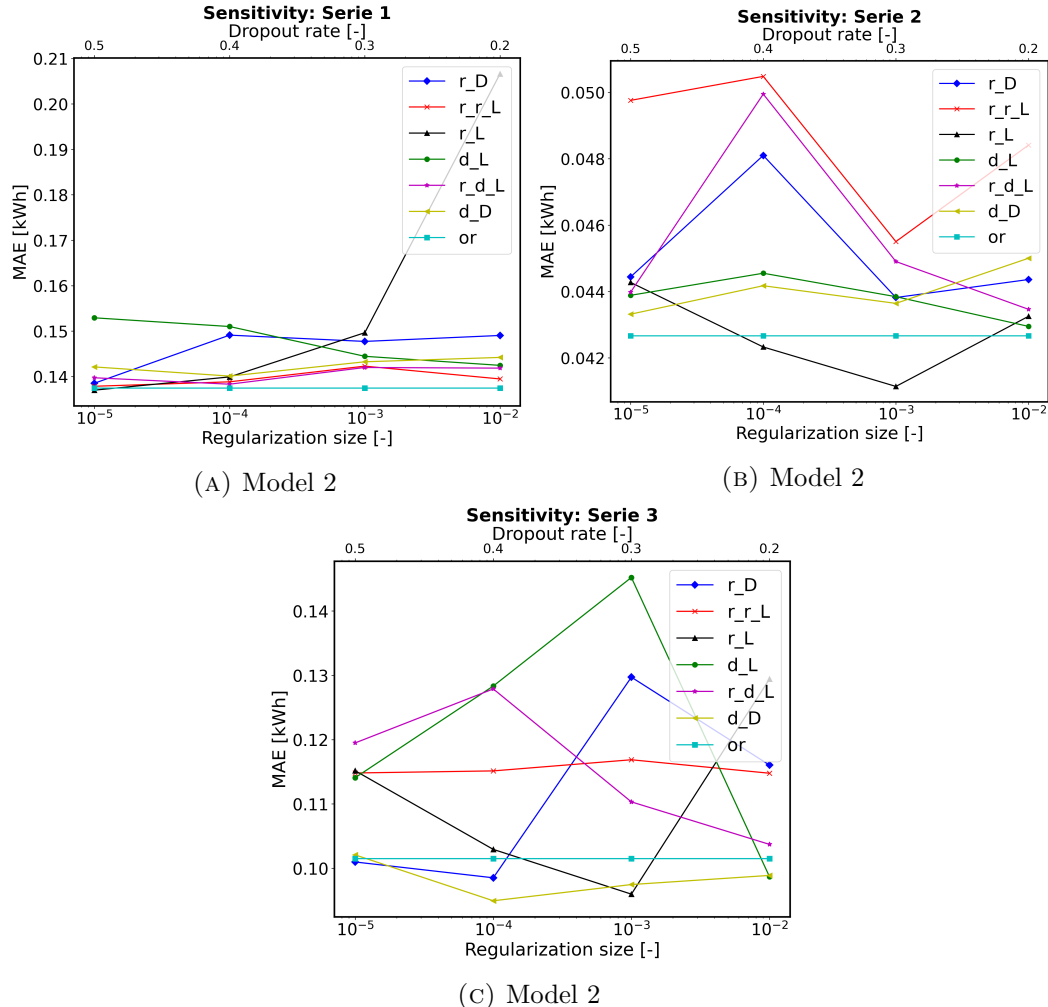


FIGURE B.2: Results of the sensitivity analysis on the size of the regularization parameter and the dropout rate according to MAE.(Legend:  $r\_D$ : regularization size of weights of DENSE layer,  $r\_r\_L$ : regularization size of recurrent weight of LSTM,  $r\_L$ : regularization size of input weights of LSTM,  $d\_L$ : dropout rate of inputs LSTM,  $r\_d\_L$ : dropout rate of hidden states LSTM,  $d\_D$ : dropout rate of DENSE layer, *or*: best performing serie from phase one)

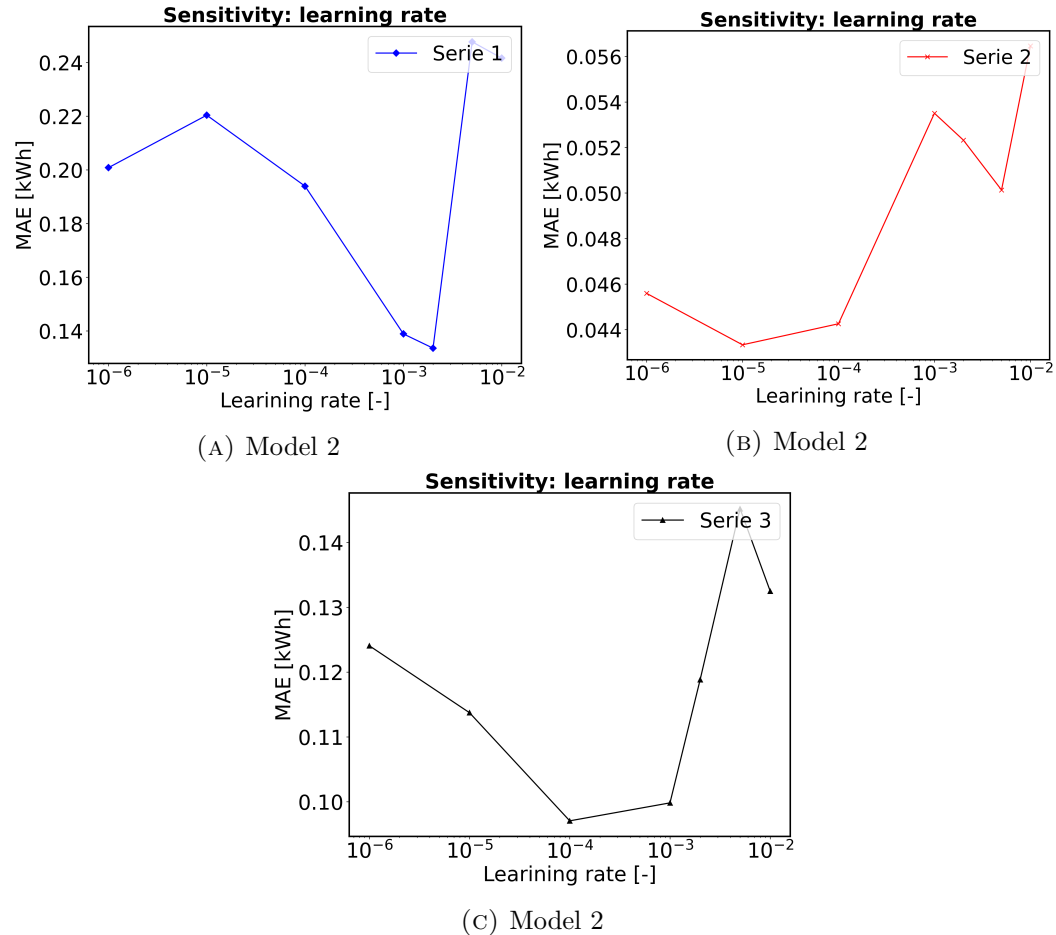


FIGURE B.3: The evaluation of the error on the validation set in function of the learning rate size.

### B.2.2 Model 3

Model 3: Stateful (1 time step)				
Chosen parameter	Value	Serie 1	Serie 2	Serie 3
Hidden states LSTM	20	6.66		0.55
	50		0.51	
layers LSTM	1	30.00	1.52	7.42
	3			
Learning rate	$10^{-2}$			
	$10^{-3}$	17.72	0.0	0.0
	$10^{-4}$	27.28	2.28	11.13

TABLE B.3: Each value in this table shows the average error when the corresponding parameter value is used, normalized by the largest error of the possible values of one parameter and finally subtracted by one. Therefore, each value shows a percentage of improvement with respect to the worst value for one parameter for each serie during phase 1 of the parameter search.

Model 3: Stateful (1 time step)			
Parameters	Serie 1	Serie 2	Serie 3
Hidden states LSTM	50	50	20
layers LSTM	1	1	1
Learning rate	0.0001	0.0001	0.0001
MAE error 1	0.132	0.0522	0.109
MAE error 2	0.130	0.0613	0.111
MAE error 3	0.138	0.0570	0.112

TABLE B.4: The values of the parameters with the lowest average MAE on the validation set over three runs.

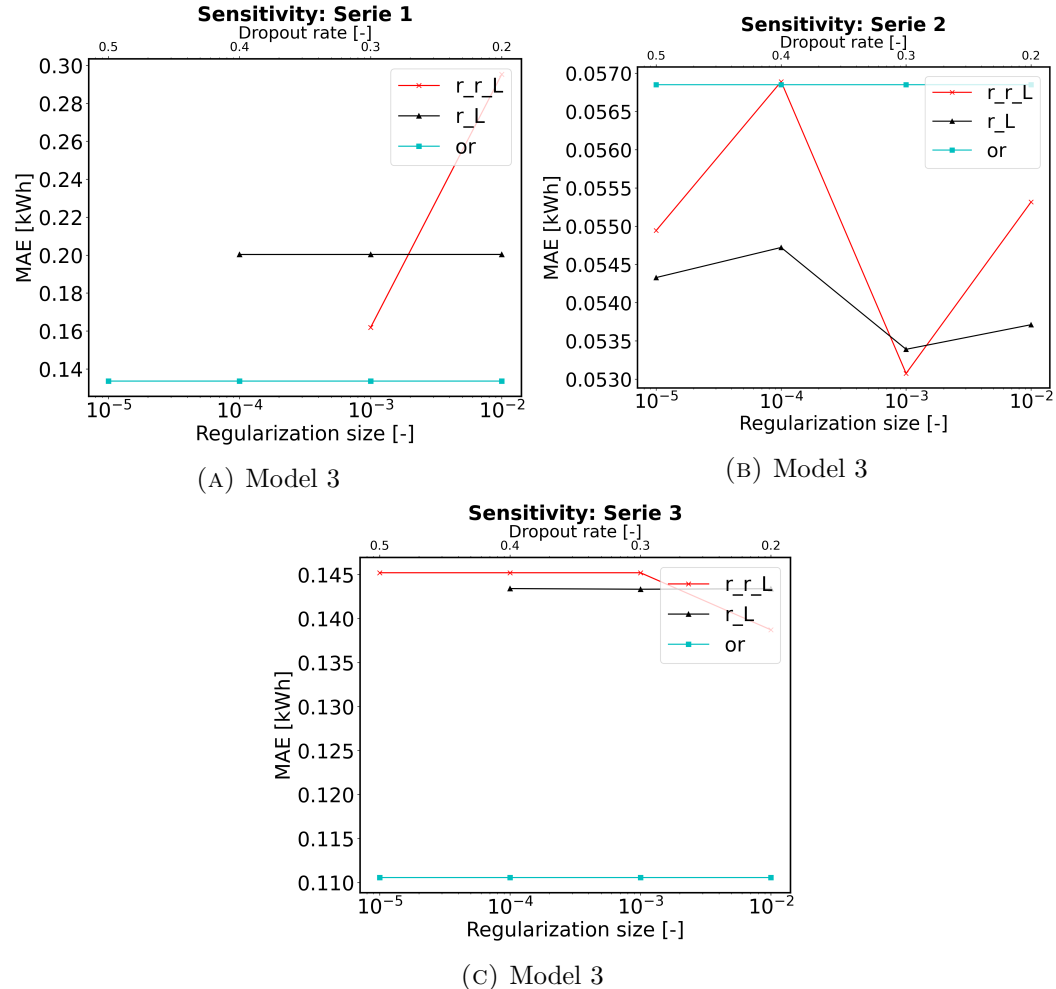


FIGURE B.4: Results of the sensitivity analysis on the size of regulation parameter and the dropout rate with respect to the mean absolute error.(Legend:  $r\_r\_L$ : regularization size of recurrent weight of LSTM,  $r\_L$ : regularization size of input weights of LSTM and  $or$ : best performing serie from phase one)

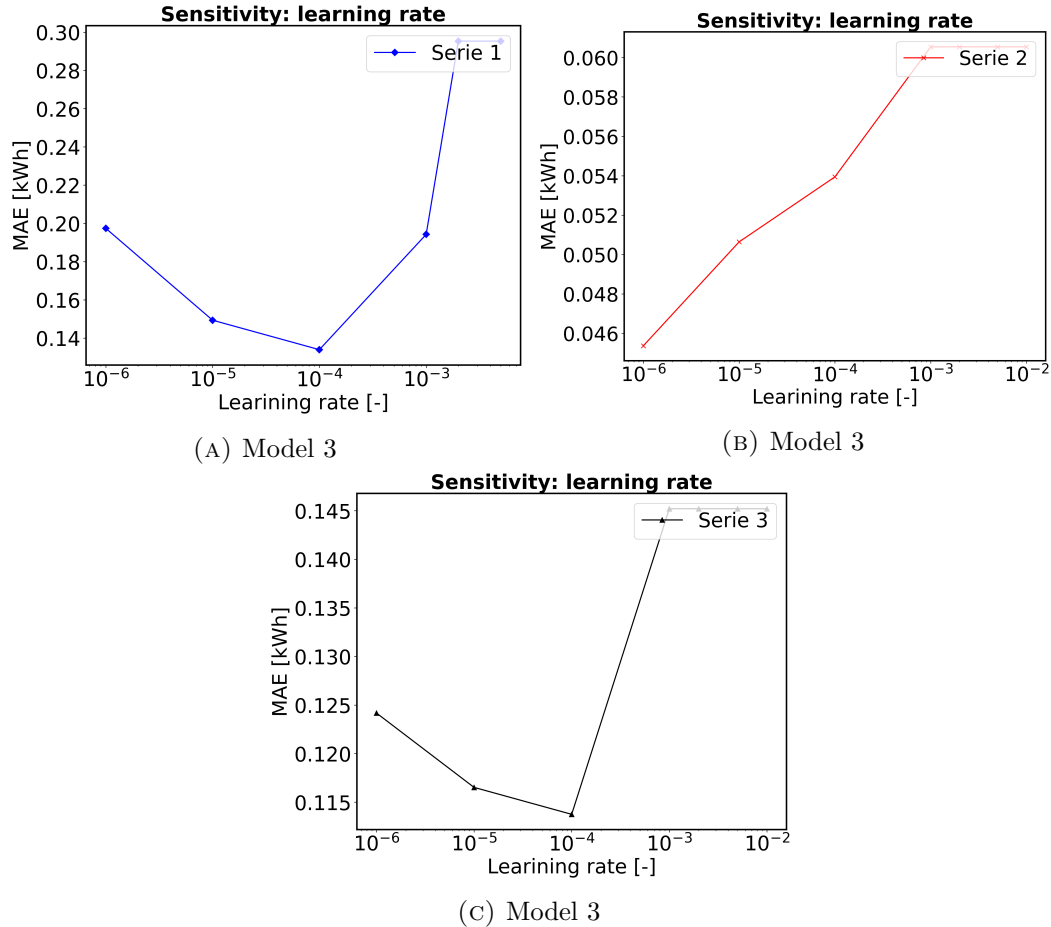


FIGURE B.5: The evaluation of the error on the validation set in function of the learning rate size.



## Appendix C

### Model evaluation - extra

#### C.1 Results on the testset

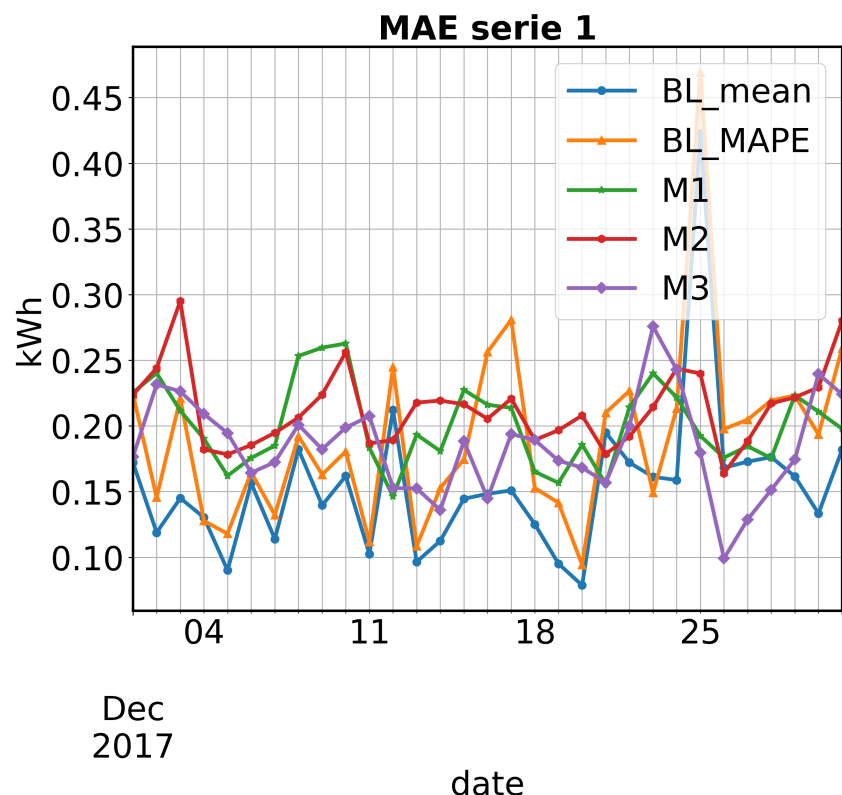


FIGURE C.1: The MAE performance for the different days in the test set for Serie 1.

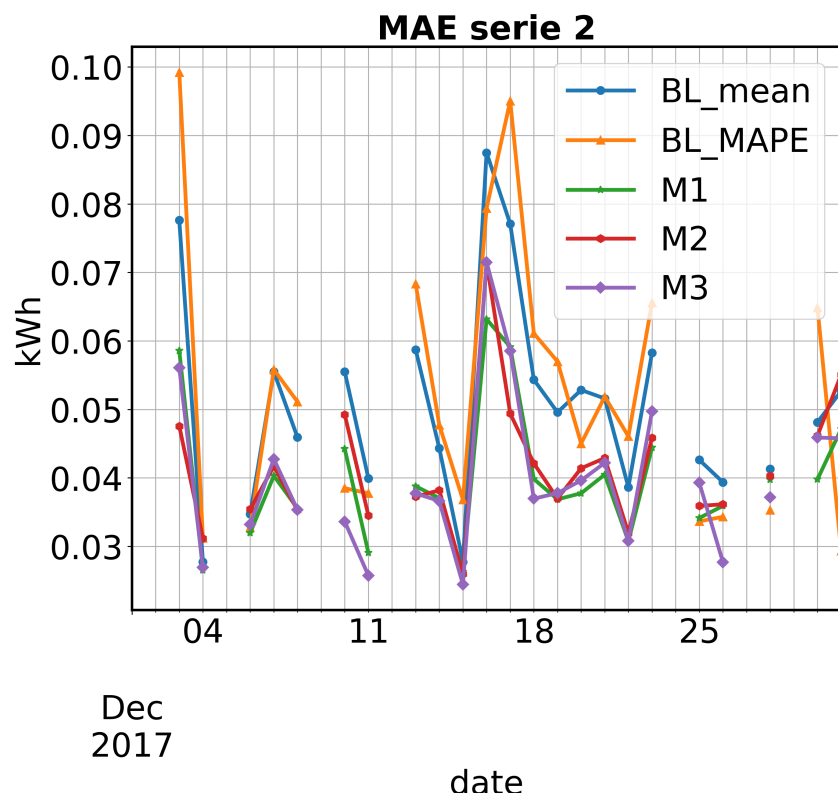


FIGURE C.2: The MAE performance for the different days in the test set for Serie 2.

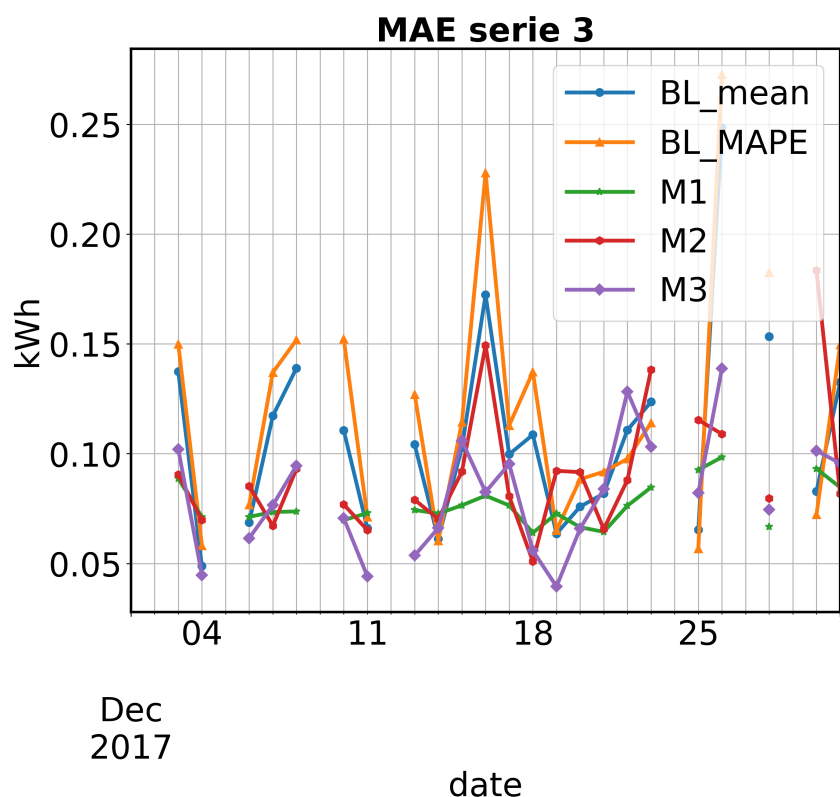


FIGURE C.3: The MAE performance for the different days in the test set for Serie 3.



# Bibliography

- [1] W. Charytoniuk, M. S. Chen, and P. Van Olinda. Nonparametric regression based short-term load forecasting. *IEEE Power Engineering Review*, 17(11):56, 1997.
- [2] J. Chung, C. Gulcehre, K. Cho, and Y. Bengio. Empirical Evaluation of Gated Recurrent Neural Networks on Sequence Modeling. pages 1–9, 2014.
- [3] E. Contaxi, C. Delkis, S. Kavatza, and C. Vournas. The effect of humidity in a weather-sensitive peak load forecasting model. *2006 IEEE PES Power Systems Conference and Exposition, PSCE 2006 - Proceedings*, pages 1528–1534, 2006.
- [4] S. S. S. R. Depuru, L. Wang, V. Devabhaktuni, and N. Gudi. Smart meters for power grid - Challenges, issues, advantages and status. *2011 IEEE/PES Power Systems Conference and Exposition, PSCE 2011*, pages 1–7, 2011.
- [5] M. Espinoza, J. Suykens, R. Belmans, and B. De Moor. Electric Load Forecasting. *IEEE control systems magazine*, (October 2007):43–57, 2007.
- [6] M. Fneish. Keras\_LSTM\_Diagram: Understanding Keras Recurrent Nets' structure and data flow in a single diagram.
- [7] K. Greff, R. K. Srivastava, J. Koutnik, B. R. Steunebrink, and J. Schmidhuber. LSTM: A Search Space Odyssey. *IEEE Transactions on Neural Networks and Learning Systems*, 28(10):2222–2232, 2017.
- [8] B. Hammer. On the approximation capability of recurrent neural networks. *Neurocomputing*, 31(1-4):107–123, mar 2000.
- [9] B. A. Hoverstad, A. Tidemann, H. Langseth, and P. Ozturk. Short-Term Load Forecasting With Seasonal Decomposition Using Evolution for Parameter Tuning. *IEEE Transactions on Smart Grid*, 6(4):1904–1913, 2015.
- [10] F. Hutter, H. Hoos, and K. Leyton-Brown. An efficient approach for assessing hyperparameter importance. *31st International Conference on Machine Learning, ICML 2014*, 2:1130–1144, 2014.
- [11] F. Javed, N. Arshad, F. Wallin, I. Vassileva, and E. Dahlquist. Forecasting for demand response in smart grids: An analysis on use of anthropologic and

## BIBLIOGRAPHY

---

- structural data and short term multiple loads forecasting. *Applied Energy*, 96:150–160, 2012.
- [12] T. Y. Kim and S. B. Cho. Predicting residential energy consumption using CNN-LSTM neural networks. *Energy*, 182:72–81, 2019.
  - [13] W. Kong, Z. Y. Dong, Y. Jia, D. J. Hill, Y. Xu, and Y. Zhang. Short-Term Residential Load Forecasting Based on LSTM Recurrent Neural Network. *IEEE Transactions on Smart Grid*, 10(1):841–851, 2019.
  - [14] J. Lago. A ratios and clustering based approach to forecast electricity consumption, 2020.
  - [15] J. Lemmens, B. Macharis, R. Gys, and D. Vonken. Data-Driven Asset Management With the Ngin Analytics Platform : Assessing Ev and Pv Impact on the Flemish Lv Grid. (June):3–6, 2019.
  - [16] S. Narjes Fallah, R. Chand Deo, M. Shojafar, M. Conti, and S. Shamshirband. Computational Intelligence Approaches for Energy Load Forecasting in Smart Energy Management Grids: State of the Art, Future Challenges, and Research Directions. 11:596, 2018.
  - [17] M. A. Nielsen. Neural Networks and Deep Learning, 2015.
  - [18] C. Olah. Understanding LSTM Networks.
  - [19] M. Sajjad, Z. A. Khan, A. Ullah, T. Hussain, W. Ullah, M. Y. Lee, and S. W. Baik. A Novel CNN-GRU-Based Hybrid Approach for Short-Term Residential Load Forecasting. *IEEE Access*, 8:143759–143768, 2020.
  - [20] H. Shi, M. Xu, and R. Li. Deep Learning for Household Load Forecasting-A Novel Pooling Deep RNN. *IEEE Transactions on Smart Grid*, 9(5):5271–5280, 2018.
  - [21] N. Srivastave, G. Hinton, A. Krizhevsky, I. Sutskever, and R. Salakhutdinov. Dropout: A Simple Way to Prevent Neural Networks from Overfitting Nitish. *Joernal of Machine Learning Research* 15, 2014.
  - [22] J. Suykens. Recurrent neural networks - ANN lecture. 0, 2021.
  - [23] J. Teuwen and N. Moriakov. *Convolutional neural networks*. Elsevier Inc., 2019.
  - [24] M. Zhang, Aston Lipton, Zachary Li and A. Smola. *Dive Into Deep Learning*, volume 17. 2020.